AD_____

Award Number: DAMD17-03-1-0066

TITLE: Biochemical Markers of Brain Injury: An Integrated Proteomics-Based Approach

PRINCIPAL INVESTIGATOR: Ronald L. Hayes, Ph.D.

CONTRACTING ORGANIZATION: University of Florida
Gainesville, Florida 32611

REPORT DATE: February 2005

TYPE OF REPORT: Annual

PREPARED FOR: U.S. Army Medical Research and Materiel Command
Fort Detrick, Maryland 21702-5012

REPORT DOCUMENTATION PAGE

Form Approved
OMB No. 074-0188

1. AGENCY USE ONLY (Leave blank)	2. REPORT DATE	3. REPORT TYPE AND DATES COVERED
	February 2005	Annual (1 Feb 04 - 31 Jan 05)

4. TITLE AND SUBTITLE
Biochemical Markers of Brain Injury: An Integrated Proteomics-Based Approach

5. FUNDING NUMBERS
DAMD17-03-1-0066

6. AUTHOR(S)
Ronald L. Hayes, Ph.D.

7. PERFORMING ORGANIZATION NAME(S) AND ADDRESS(ES)
University of Florida
Gainesville, Florida 32611

E-Mail: hayes@mbi.ufl.edu

8. PERFORMING ORGANIZATION REPORT NUMBER

9. SPONSORING / MONITORING AGENCY NAME(S) AND ADDRESS(ES)
U.S. Army Medical Research and Materiel Command
Fort Detrick, Maryland 21702-5012

10. SPONSORING / MONITORING AGENCY REPORT NUMBER

11. SUPPLEMENTARY NOTES
Original contains color plates. All DTIC reproductions will be in black and white.

12a. DISTRIBUTION / AVAILABILITY STATEMENT
Approved for Public Release; Distribution Unlimited

12b. DISTRIBUTION CODE

13. ABSTRACT (Maximum 200 Words)

Background: Brain injury poses a major problem to military care, accounting for 25% of all combat casualties and is the leading cause of death among wounded soldiers reaching Echelon I medical treatment. Incidence of brain injury and resultant long-term disabilities caused by traumatic insults and ischemic events is significantly greater in the civilian population. No clinically useful diagnostic tests exist for traumatic or ischemic brain injury to provide physicians with quantifiable neurochemical markers to help determine the seriousness of the injury, the anatomical and cellular pathology of the injury and to guide implementation of appropriate triage and medical management.

Study Design: SOW 1 employs integrated proteomics-based technologies to identify specific proteins or peptide fragments in brain released into CSF and/or blood of rats following experimental traumatic brain injury or focal cerebral ischemia. Technologies include mass spectroscopy, 2-D gel electrophoresis, phage display of single chain antibodies and antibody chips. SOW 2 employs antibody chips to determine which proteins or peptide fragments released into CSF following injury are reliably associated with different injury magnitudes and predict changes in histopathological, behavioral and electrophysiological outcome measures. SOW 3 develops ELISA-based assays capable of detecting biomarkers in blood.

Relevance: Development of "objective triage" capabilities for combat medics and/or Echelon I providers would represent a major "fieldable" breakthrough in the medical management of combat related head trauma.

14. SUBJECT TERMS
Traumatic brain injury, ischemia, biomarkers, proteomics

15. NUMBER OF PAGES
94

16. PRICE CODE

17. SECURITY CLASSIFICATION OF REPORT	18. SECURITY CLASSIFICATION OF THIS PAGE	19. SECURITY CLASSIFICATION OF ABSTRACT	20. LIMITATION OF ABSTRACT
Unclassified	Unclassified	Unclassified	Unlimited

Table of Contents

INTRODUCTION

Recent studies have highlighted the fact that traumatic brain injury (TBI) is one of the most frequent causes of mortality and morbidity on the modern battlefield. More than half of combat casualties in Iraq suffer from TBI. Forty percent of battlefield fatalities in Viet Nam were due to head wounds. It has also been reported that of patients arriving alive at military field hospitals, 20% with severe brain wounds die before surgery was performed, and 80% receive neurosurgical treatment with a 10% surgical mortality rate. Penetrating head injury alone accounts for 25% of all war time casualties and approximately 40% of these injuries are fatal.

Thus, the current proposal focuses on development of non-invasive diagnostics of TBI that ultimately will be useful in a battlefield environment. The research has been divided into 3 SOWs. The SOWs are as follows:

SOW 1: To employ integrated proteomics-based technologies to identify specific proteins or peptide fragments in brain released into CSF and/or blood of rats following experimental traumatic brain injury (TBI) or focal cerebral ischemia (middle cerebral artery occlusion: MCAO).

(A) Conduct concurrent studies employing mass spectrometry (HPLC MALDI-TOF protein profiling's Isotope-coded affinity tags-ICAT), 2D-gel electrophoresis, and phage display of single chain antibodies to detect proteins or peptide fragments in brain and CSF after TBI or MCAO.
(B) Employing injury-related proteins or peptide fragments identified in SOW 1-A, construct and validate the sensitivity of an antibody chip. Validation of the chip would on focus studies in CSF but would also explore chip utility for blood analyses.

SOW 2: Employing the antibody chip developed in SOW 1-B, determine which protein or peptide fragments released into CSF following TBI or MCAO are reliably associated with different injury magnitudes and predict changes in histopathological, behavioral and electrophysiological outcome measures.

(A) CSF will be sampled at multiple time points following injury to determine the optimal sampling time(s) predictive of injury magnitudes. If feasible based on data from SOW 1-B, limited studies will be conducted employing blood samples. (Months 25-30).
(B) Using the same injury magnitudes and data on release of protein or peptide fragments derived from the antibody chips employed in SOW 2-A, identify which sampling time(s) and which protein or peptide fragments released into CSF are optimally predictive of histopathological behavioral or electrophysiological assessments of outcome following TBI or MCAO. EEG analyses of electrophysiological alterations will be conducted following TBI and ischemia. Histopathology will be assessed by hematoxylin and eosin (H&E) staining for TBI and triphenyltetrazolium chloride (TTC) staining for MCAO. Behavioral assessments will include Morris water maze and Rotorod assessments following TBI and neurological examinations and forelimb sensorimotor assessments following MCAO.

SOW 3:
(A) Develop highly sensitive, quantitative ELISA-based assays capable of detecting blood levels of protein or peptide fragments determined to be optimally predictive of injury magnitude and outcome in SOW 2.
(B) Conduct preliminary validation of the utility of ELISA based assays employing blood samples taken following brain injury.

BODY

We have conducted extensive studies of the utility of CSF levels of αII-spectrin breakdown product levels as markers of TBI. These extensive studies represent systematic efforts to conduct preclinical assessments of the ultimate clinical utility of these biomarkers in humans **(Ringger et al., J**

Neurotrauma, 2004, included with report). Currently, there is no definitive diagnostic test for TBI to help physicians determine the seriousness of injury or the extent of cellular pathology. Calpain cleaves αII-spectrin into breakdown products (SBDP) after TBI and ischemia. Mean levels of both ipsilateral cortex (IC) and cerebral spinal fluid (CSF) SBDP at 2, 6 and 24 h after 2 levels of controlled cortical impact IC SBDP levels are significantly higher after severe (1.6 mm) injury than mild (1.0 mm) injury over time. The correlation between CSF SBDP levels and lesion size from T2-weighted magnetic resonance images 24 hrs after TBI as well as correlation of tau and S100B was assessed. Mean levels of CSF SBDP (r – 0.833) significantly correlated with lesion size while levels of CSF S100B did not (r – 0.188). Although levels of CSF and IC SBDP and lesion size are all significantly higher after 1.6 mm than 1.0 mm injury, the correlation between CSF SBDP and lesion size was not significant following the removal of controls from the analysis. This indicates CSF SBDP is a reliable marker of the presence or absence of injury. Furthermore, larger lesion sizes 24 hrs after TBI were negatively correlated with motor performance on days 1-5 after TBI (r = -0.708). Based on these data, evaluation of CSF SBDP levels as a biomarker of TBI is warranted in clinical studies.

An important component of the proposal was to develop proteomics based platforms for discovery of novel biomarkers of TBI. We have recently outlined our proteomics-based strategy and its successful application **(Wang, et al., International Review of Neurobiology, 2004, included with report)**. With the completion of human and rat genomes, the next major technological challenge facing the biomedical community is the deciphering of the human proteome. Study of the proteome has been aided by recent advances in protein separation, protein identification/quantification, and bioinformatics. Although the application of proteomics technologies in brain injury research is still in its infancy, enormous insights can be achieved from such endeavors. There are approximately 30,000-40,000 hypothetical protein products transcribable from the human genome (Aebersold and Watts, 2002; Grant & Blackstock, 2001; Grant & Husi, 2001; Hanash, 2003; Hochstrasser et al., 2002; Service, 2001; Smith, 2000). Yet, the proteome is extremely complex. Even in a single cell type the set of proteins that are expressed, as well as their steady state levels, depend o time and the specific state of the cells in response to environmental stimuli or challenges. In addition, cellular proteins are almost constantly subjected to various forms of post-translational modifications (PTMs), including phosphorylation/dephosphorylation by different kinases and phosphotases, proteolysis, or processing by different protease families, acetylation, glycosylation, and cross linking by transglutaminases or conjugation to small protein tags such as ubiquitin or SUMO (similar to ubiquitin modifier: Janssen, 2003, Schafer et al., 2003; Schwartz and Hochstrasser, 2003). Because of these challenges, one often has to focus on a specific subproteome. The case in point is neuroproteomics, or the study of nervous system proteomes. The importance of neuroproteomics studies is that they will help elucidate the poorly understood biochemical mechanisms or pathway that currently underlie various psychiatric, neurological and neurodegenerative diseases.

We have made important methodological advances to facilitate rapid discovery of putative protein biomarkers of TBI **(Haskins et al., J Neurotrauma, In Press, included with report)**. We report the rapid discovery of putative protein biomarkers of traumatic brain injury (TBI) by SDS-PAGE-capillary liquid chromatography-tandem mass spectrometry (SDS-PAGE-Capillary LC-MS^2). Ipsilateral hippocampus (IH) samples were collected from naïve rats and rats subjected to controlled cortical impact (a rodent model of TBI). Protein database searching with 15,558 uninterpreted MS^2 spectra, collected in 3 days via data-dependent Capillary LC-MS^2 of pooled samples separated by SDS-PAGE, identified more than 306 unique proteins. Differential proteomic analysis revealed differences in protein sequence coverage for 170 mammalian proteins (57 proteins in naïve only, 74 protein in injured only, and 39 proteins in both), suggesting that some of these proteins are putative biomarkers of TBI. Confidence in our results was obtained by the presence of several known biomarkers of TBI, (including αII-spectrin, brain creatine kinase, and neuron-specific enolase) in our data set. Sequence-specific discovery of putative protein biomarkers (by data-dependent Capillary LC-MS^2) and preliminary validation of selected biomarkers (by targeted Capillary LC-MS^2), show that SDS-PAGE prior to *in vitro* proteolysis and Capillary LC-MS^2 is a promising strategy for the rapid discovery of putative protein biomarkers

associated with a specific pathophysiological state (i.e., TBI) without *a priori* knowledge of the molecules involved.

We have importantly expanded our search for biochemical markers of acute CNS injury. Consistent with our focus on examining proteolytic mechanisms of damage, we have examined the role of cathepsin B mRNA and protein expression following contusion spinal cord injury **(RC Ellis et al., J Neurochem., 2004, included with report)**. These studies lay the foundation for future research in TBI. We provide the first data that cathepsin B (Cath B), a lysosomal cysteine protease, is upregulated following contusion spinal cord injury (SCI). Following T12 laminectomy and moderate contusion, Cath B mRNA and protein expression profiles were examined from 2 to 168 hrs post-injury in rats using real-time PCR and immunoblots, respectively. Contusion injury significantly increased mRNA Cath B in the injury site and adjacent segments over sham injury levels. While the largest mRNA Cath B induction (20-fold over naïve) was seen in the injury site, the caudal segment routinely yielded mRNA Cath B levels greater than 10-fold over naïve. Interestingly, sham injury animals also experienced mRNA induction at several time points at the injury site and in segments rostral and caudal to the injury site. Contusion injury also significantly elevated levels of Cath B proenzyme protein (37 kDa) over sham injury in the injury site (48, 72 and 168 hrs post-injury). Furthermore, significant protein increases of single and double chain Cath B (both active forms) occurred at the injury site at 72 and 168 hrs post-injury. Similar significant increases in Cath B protein levels were seen in areas adjacent to the injury site. The induction of Cath B mRNA and protein expression following contusion injury is previously undescribed and suggests that Cath B may potentially be involved in the secondary injury cascade, perhaps for as long as 1 week post-injury.

KEY RESEARCH ACCOMPLISHMENTS

- We have provided the first systematic preclinical confirmation of a biochemical marker of TBI confirming that such markers can be reliably associated with varying magnitudes of injury including lesion volume.

- We have published the first characterization of a comprehensive and successful proteomics-based platform to discover novel biomarkers of TBI.
- We have made significant advances in methodologies facilitating rapid discovery of potential protein biomarkers of TBI.

- We have expanded our effort to identify new proteolytic markers of TBI incorporating studies of cathepsins in addition to ongoing studies of calpain proteolysis.

REPORTABLE OUTCOMES

Publications

NC Ringger, BE O'Steen, JG Brabham, X Siler, J Pineda, KKW Wang, **RL Hayes**. A novel marker for traumatic brain injury: CSF αII-spectrin breakdown product levels. J Neurotrauma, 21(10) 1443-1456, 2004.

Wang KKW, Ottens AK, Haskins WE, Liu MC, Kobeissy F, Denslow ND, Chen S, **Hayes RL**. Proteomics studies of traumatic brain injury in International Review of Neurobiology, Vol. 62, Human Brain Proteome. Neubold EL, Ed. Elsevier, New York, 2004, pp 215-340.

William Haskins, Firas H. Kobeissy, Regina A. Wolper, Andrew K. Ottens, Jason W. Kitlen, Scott H McClung, Barbara E. O'Steen, Marjorie M. Chow, Jose A. Pineda, Nancy D. Denslow, **Ronald L. Hayes**, Kevin KW Wang. Rapid discovery of putative protein biomarkers of traumatic brain injury by SDS-

PAGE-capillary liquid chromatography-tandem mass spectrometry. (J Neurotrauma, In Press).

Rebecca C. Ellis, J. Nicole Earnhardt, **Ronald L. Hayes**, Kevin K.W. Wang and Douglas K. Anderson. Cathepsin B mRNA and protein expression following contusion spinal cord injury. J. Neurochem, 88:689-697, 2004.

Abstracts

Ronald L. Hayes & Andrew K. Ottens. Developing proteomics-based platforms to study brain injury: Challenges in data analysis and interpretation. Applied Math Seminar, UF Department of Mathematics, Apr. 2004.

Angileri FF, Aguennouz M. Germano A, Toscano A, deDivitis O, Glusa M, Lewis SB, Wang KKW, Papa L, Pike BR, Newcomb-Fernandez JK, Hayes RL, Pineda J, Vita G, d'Avella D, Tomasello F. Detection of αII-spectrin and breakdown products in humans after severe traumatic brain injury. Society for Academic Emergency Medicine, May 2004.

Andrew K Ottens, Firas H Kobeissy, Zhiqun Zhang, Erin Golden, Regina Wolper, Su-Shing Chen, Ming Chen Liu, Ronald L Hayes, Kevin KW Wang. The bioinformatic challenge in brain injury neuroproteomics. Bioinformatics Workshop, 2004.

S Sadasivan, RC Ellis, W O'Steen, MC Liu, RL Hayes, D Anderson, KKW Wang. Concurrent proteolysis of axonal αII-spectrin and myelin basic protein following spinal cord injury. 10th Annual Kentucky Spinal Cord & Head Injury Research Symposium, June 2004.

Kevin KW Wang, Nancy D Denslow & Ronald L Hayes. Applying proteomics in brain injury studies. International Neurotrauma Symposium (INTS), September 2004.

JA Pineda, JM Aikman BE O'Steen, EA Johnson, KK Wang, J Flint and RL Hayes. αII-spectrin and severity of injury after controlled cortical impact in the immature rat brain. INTS, Sept. 2004.

Jitendra R Dave, Changping Yao, Anthony J Williams, XiChun M Lu, Ren Wu Chen, Rebecca Whipple, Rebecca Connors, Kevin KW Wang, Ronald L Hayes and Frank C Tortella. Penetrating brain injury in the rat: VII proteomics-based identification of protein expression. INTS., Sept. 2004.

AK Ottens, EC Golden, MC Liu, R Wolper, ND Denslow, RL Hayes, KKW Wang. Quantitative degradomic mass spectrometry approach to monitoring myelin basic protein proteolysis resulting from TBI. SFN, Oct. 2004.

FH Kobeissy, AK Ottens, R Wolper, ZQ Zhang, RL Hayes, ND Denslow, KKW Wang. Utilizing an innovative and powerful multidimensional separation scheme for neuroproteomics analysis. SFN, Oct. 2004.

Wenrong Zheng, Ming Cheng Liu, Ronald L Hayes, Kevin KW Wang. Simultaneous breakdown of αII- and βII-spectrin by calpain and caspase-3 in rat cerebrocortical culture under oncotic, apoptotic and excitotoxic challenges. SFN, Oct. 2004.

Ming Cheng Liu, Wenrong Zheng, B O'Steen, Ronald L Hayes and Kevin KW Wang. Degradation of βII-spectrin in rat brain after traumatic brain injury. SFN, Oct. 2004.

SL Janssen, RL Hayes, MS Gold, KKW Wang. αII-spectrin and βII-spectrin breakdown in PC12 cells after alcohol treatment. SFN, Oct. 2004.

Wenrong Zheng, Ming Cheng Liu, Ronald L Hayes, Kevin KW Wang. Simultaneous breakdown of αII- and βII-spectrin by calpain and caspase-3 in rat cerebrocortical culture under oncotic, apoptotic and excitotoxic challenges. NNS, Oct. 2004.

Ming Cheng Liu, Wenrong Zheng, B O'Steen, Ronald L Hayes and Kevin KW Wang. Degradation of βII-spectrin in rat brain after traumatic brain injury. NNS, Oct. 2004.

SI Svetlov, KKW Wang, RL Hayes. Oligomerization of cannabinoid receptors as a pathogenic marker of TBI. NNS, Oct. 2004.

Oral Presentations

Award Recipient and Invited Speaker, Lance Award Ceremony, Charlotte, NC
Conference Attendee, Critical Care Congress, Orlando, FL
Invited Attendee, CHI's Utilizing Biomarkers in Diagnostic Research conference, San Francisco, CA
Invited Speaker, Applied Math Seminar, Dept. of Mathematics, UF-Gainesville
Invited Participant, Molecular Diagnostics Conference, CHI sponsored, San Francisco, CA
Invited Speaker, Grand Rounds, Univ of Mississippi Dept Neurosurgery, Jackson, MS
Invited Speaker & Poster Presentation, DoD Peer Review Medical Research Program Meeting, San Juan, Puerto Rico
Invited Speaker, Brain Injuries Conference, Tampa, FL
Invited Speaker, Kentucky Spinal Cord & Head Injury Research Symposium, Lexington, KY
Invited Speaker, ROSE 20th Annual Seminar, Minneapolis, MN
Invited Speaker, Combine ATACCC & NATO Meetings, St. Petersburg, FL
Invited Speaker, ACRM-ASNR Joint Conference, Ponte Vedra, FL
Attendee, Congress of Neurological Surgeons, San Francisco, CA
Attendee, National Neurotrauma Society Annual Meeting, San Diego, CA

CONCLUSIONS

In summary, we continue to make significant progress in our second year of funding. We have confirmed that a prototypical biomarker, αII-spectrin breakdown products, are a reliable index of injury magnitude and potentially outcome. We have also published the development of an effective integrated proteomics-based platform to study biomarkers of acute CNS injury such as TBI and ischemia. We have significantly enhanced this discovery platform by developing novel techniques to facilitate rapid discovery of new protein biomarkers of TBI. finally, our research has historically integrated a "degradomics" approach focusing on detecting breakdown products of calpain proteolysis. Having confirmed that this approach is successful, we are now expanding our research to examine the potential utility of developing biomarkers of other proteases such as cathepsins.

JOURNAL OF NEUROTRAUMA
Volume 21, Number 10, 2004

Pp. 1443–1456

A Novel Marker for Traumatic Brain Injury: CSF αII-Spectrin Breakdown Product Levels

N.C. RINGGER,[1,4] B.E. O'STEEN,[1,4] J.G. BRABHAM,[1] X. SILVER,[5] J. PINEDA,[3,4] K.K.W. WANG,[1,2,4] and R.L. HAYES[1,2,4]

ABSTRACT

Currently, there is no definitive diagnostic test for traumatic brain injury (TBI) to help physicians determine the seriousness of injury or the extent of cellular pathology. Calpain cleaves αII-spectrin into breakdown products (SBDP) after TBI and ischemia. Mean levels of both ipsilateral cortex (IC) and cerebral spinal fluid (CSF) SBDP at 2, 6, and 24 h after two levels of controlled cortical impact (1.0 mm and 1.6 mm of cortical deformation) in rats were significantly elevated by injury. CSF and IC SBDP levels were significantly higher after severe (1.6 mm) injury than mild (1.0 mm) injury over time. The correlation between CSF SBDP levels and lesion size from T2-weighted magnetic resonance images 24 hours after TBI as well as correlation of tau and S100β was assessed. Mean levels of CSF SBDP ($r = 0.833$) and tau ($r = 0.693$) significantly correlated with lesion size while levels of CSF S100β did not ($r = 0.188$). Although levels of CSF and IC SBDP and lesion size are all significantly higher after 1.6 mm than 1.0 mm injury, the correlation between CSF SBDP and lesion size was not significant following the removal of controls from the analysis. This indicates CSF SBDP is a reliable marker of the presence or absence of injury. Furthermore, larger lesion sizes 24 h after TBI were negatively correlated with motor performance on days 1–5 after TBI ($r = -0.708$). Based on these data, evaluation of CSF SBDP levels as a biomarker of TBI is warranted in clinical studies.

Key words: biomarker; CSF; injury magnitude; lesion size; spectrin; S100β; tau

AU1

INTRODUCTION

THE DIFFICULTY of diagnosis and prediction of outcome after acute traumatic brain injury (TBI) is associated with the limitations of clinical assessment and neuroimaging (Zink, 2001). Sedatives may be used to treat patients with TBI that exhibit confusion, agitation, or non-compliance with accompanying increased brain metabolism (Mirski et al., 1995). Treatment with anticonvulsant or sedative drugs may confound information obtained from a clinical neuropsychological examination (Mirski et al., 1995). Many mild head trauma patients with a Glasgow Coma Scale (GCS) between 13 and 15 may have coincidental intoxication with drugs and alcohol that may also confound clinical neuropsychological examinations (Kelly, 1995). Head injuries may also be overlooked

[1]Department of Neuroscience, [2]Department of Psychiatry, [3]Department of Pediatrics, [4]Center for Traumatic Brain Injuries, and [5]Advanced Magnetic Resonance Imaging and Spectroscopy (AMRIS) Facility, Evelyn F. and William L. McKnight Brain Institute, University of Florida, Gainesville, Florida.

in multi-trauma patients (Buduhan and McRitchie, 2000). Clinical indicators may not predict significant intracranial trauma (Harad and Kerstein, 1992). Neurologic damage from TBI, stroke or perinatal asphyxia may precede changes seen by modern neuroimagining techniques. Although mild traumatic injury may cause long term disabilities, mild trauma may not be seen acutely with radiologic or magnetic resonance imaging (MRI). Computed tomography (CT) scanning is the quickest and most available neuroimaging, yet has low sensitivity for diffuse brain damage. In a critical care patient, cost, availability, and the time to acquire images limits use of the more sensitive measures of MRI and single photon emission CT scans. Single photon emission CT scans detect regional changes of blood flow but not necessarily structural damage. Furthermore, MRI and CT often do not predict outcome (Kido et al., 1992; Kurth et al., 1994; Wilson et al., 1995; Hanlon et al., 1999). Thus there is a need for a biochemical marker of neuronal injury to improve diagnosis and prediction of outcome after TBI.

An ideal biomarker would incorporate several properties. A good biomarker would diagnose neurologic damage before neuro-radiographic signs are evident. A biomarker of acute neuronal injury would provide a measure of injury magnitude and predict neuropsychological outcome. The biomarker would also serve as an indicator of the pathogenesis of cell death including secondary cell death and indicate a target for treatment. With earlier recognition, the window for therapeutic intervention could be extended. Furthermore, a good biomarker would allow for longitudinal monitoring of the effectiveness of therapy. A biomarker with these characteristics could be used as a surrogate marker and lower the cost of clinical trials. An ideal biomarker should also be specific to the central nervous system and provide a sensitive and specific test of neuronal injury.

Earlier biomarkers such as neuron-specific enolase, lactate dehydrogenase, or creatine kinase are not been specific to the CNS and failed to reflect pathophysiology, lesion size and outcome of the injury further reinforcing the need for research into better CNS trauma indicators (Ingebrigtsen and Romner, 2002). S100β, a low molecular weight calcium-binding protein released from astrocytes, has been examined in numerous TBI studies. Serum levels of S100β have been correlated with contusion volume (Raabe et al., 1998; Herrmann et al., 2000); injury severity (Herrmann et al., 2000); neuropsychological dysfunction (Herrmann et al., 2001); GCS on admission (Elting et al., 2000); and outcome measures such as the Glasgow Outcome Score (GOS) (McKeating et al., 1998; Elting et al., 2000; Jackson et al., 2000; Raabe and Seifert, 2000; Rothoerl et al., 2000). S100β appears to be a valuable indicator of brain lesion but it is not specific to the CNS. Importantly in multitrauma patients without head injuries, S100β reached high serum levels after bone fractures and thoracic contusion (Anderson et al., 2001). Another biomarker that is being examined as an indicator of brain injury is tau (Zemlan et al., 1999). Tau is a microtubule associated protein that is expressed predominantly in axon of neurons and implicated in microtubule stability, axon elongation and axon transport (Garcia and Cleveland, 2001). In severe TBI patients, increased CSF levels of cleaved tau were found to be significant predictors of intracranial pressure and GOS at discharge (Zemlan et al., 2002), but in recent studies, CSF total tau levels did not correlate with GOS in patients with severe TBI (Franz et al., 2003) nor did serum cleaved tau levels correlate with outcome measures (Chatfield et al., 2002).

αII-spectin in the CNS is primarily localized to axons and to the presynaptic terminal of neurons (Riederer et al., 1986). In acute neuronal injury, αII-spectin, a cytoskeletal protein, is a substrate for the calcium activated cysteine proteases, calpain (calpain-1 and -2) and caspase-3. After acute neuronal injury, calcium influx initiates a cytotoxic cascade of proteases, phospholipases, kinases and phosphatases including activation of calpain and caspases which results in necrotic and apoptotic cell death respectively. Calpain and caspase-3 both cleave the 280-kDa parent band of αII-spectrin into a 150-kDa breakdown product (SBDP150). Calpain and caspase-3 cleave signature breakdown products of 145 (SBDP145) and 120 kDa (SBDP120), respectively, *in vivo* and *in vitro* (Nath et al., 1996; Wang et al., 1998; Wang, 2000). Both the calpain-mediated SBDP 145 and SBDP 150 increased acutely in the injured cortex whereas the caspase-3 mediated SBDP 120 was absent in an unilateral controlled cortical impact (CCI) model of TBI (Pike et al., 1998). This may reflect a more prominent role of oncosis than apoptosis in the cortex in our CCI model.

αII-spectrin breakdown products (SBDP) have been used as an indicator of calpain activity in models of TBI (Newcomb et al., 1997) and ischemia (Saido et al., 1993; Roberts-Lewis et al., 1994; Bartus et al., 1998) In our laboratory, levels of SBDP have recently been found to increase in rat CSF after experimental controlled cortical impact TBI (Pike et al., 2001) and middle cerebral artery occlusion (Pike et al., 2004). In this study we extend this work by systematically comparing CSF SBDP to their counterpart in injured cortex, to injury magnitude, to CSF tau and S100â and to lesion volume (accessed by MRI). This study subjects a marker of CNS injury to rigorous preclinical examination. Based on the data we have obtained, we propose that CSF SBDP levels are a promising biomarker of injury and further study is warranted in clinical TBI.

MATERIALS AND METHODS

Animals

Three groups of adult male (280–300 g) Sprague-Dawley rats (Harlan; Indianapolis, IN) were used. For study 1, CSF was withdrawn from one group of 90 rats that were sacrificed 2, 6, and 24 h after TBI. At each time point of 2, 6, and 24 h, 9 rats received mild (1.0 mm of cortical deformation) injury, 9 rats received severe (1.6 mm of cortical deformation) injury, 8 rats received a craniotomy but no cortical deformation and 4 rats remained naive (no craniotomy or cortical deformation). For study 2, a second group of rats were sequentially scanned by MRI, subjected to CSF withdrawal, and were sacrificed at 24 h following TBI. Of the second group, 9 rats each received severe (1.6 mm) injury, mild (1.0 mm) injury or craniotomy surgery and 8 rats remained naive. One rat with severe injury was removed from the study because the CSF sample contained blood that could potentially dilute out the concentration of the marker in the CSF and introduce blood-born markers. For study 3, 35 rats were administered a rotarod test on days 1–5 after TBI and scanned by MRI at 24 h and 28 days after TBI. Of the third group of rats, 10 rats each received severe (1.6 mm) injury, mild (1.0 mm) injury or a craniotomy, and 5 rats remained naive.

Surgical Preparation and Controlled Cortical Impact Traumatic Brain Injury

As previously described (Dixon et al., 1991; Pike et al., 2001), a cortical impact injury device was used to produce TBI. Adult male rats were initially anesthetized with 4% isoflurane in a carrier gas of 1:1 O_2/N_2 (4 min) followed by maintenance anesthesia of 2.5% isoflurane in the same carrier gas. Core body temperature was maintained at 37 ± 1°C by placing an adjustable temperature controlled heating pad beneath the rats. Animals were mounted in a stereotactic frame in a prone position and secured by ear and incisor bars. A midline cranial incision was made, the soft tissues were reflected and a unilateral (ipsilateral to site of impact) craniotomy (7 mm diameter) was performed adjacent to the central suture, midway between bregma and lambda. The dura mater was kept intact over the cortex. Brain trauma in rats was produced by impacting the right cortex (ipsilateral cortex) with a 5 mm diameter aluminum impactor tip (housed in a pneumatic cylinder) at a velocity of 3.5 m/sec with a 150-msec dwell time (compression duration). Compression depth was set at 1.0 mm (mild), or 1.6 mm (severe). Velocity was controlled by adjusting the pressure (compressed N_2) supplied to the pneumatic cylinder. Velocity and dwell time were measured by a linear velocity displacement transducer (Lucas Shaevitz™ model 500 HR; Detroit, MI) that produces an analogue signal by a storage-trace oscilloscope (BK Precision, model 2522B; Placentia, CA). Animals underwent identical craniotomy procedures but did not receive cortical compression. Naive rats did not undergo surgery or injury. Appropriate pre- and post-injury management was maintained to insure that all guidelines set forth by the University of Florida Institutional Animal Care and Use Committee and the National Institutes of Health guidelines detailed in the *Guide for the Care and Use of Laboratory Animals* were complied with.

CSF Withdrawal

Under anesthesia, the rat was secured in the same stereotactic frame as used in surgery. The neck was flexed to optimize exposure of the atlanto-occipital space. A mid-line incision was made over the superficial cervical muscles. A 25-gauge needle attached to polyethylene tubing was inserted into the atlanto-occipital space and CSF was gently withdrawn. CSF was immediately spun at 9,000*g* for 5 min at 4°C to remove any red blood cells from the cortical impact or from the tap. CSF was frozen at −80°C until examined.

Tissue Lysis

Cortical tissues were collected from naive animals or at 2, 6, and 24 h after craniotomy or TBI. At the appropriate post-injury time-points, the animals were anesthetized with 4% isoflurane in a carrier gas of 1:1 O_2/N_2O (4 min) and subsequently sacrificed by decapitation. Ipsilateral (to the impact site) cortex samples were rapidly dissected and snap-frozen in liquid nitrogen. Tissue samples were stored at −80°C until further processing. Frozen samples were thawed and homogenized in a glass tube with a Teflon dounce pestle in 15 volumes of ice-cold detergent-free buffer (50 mM Tris-HCl, pH 7.4, 1 mM EDTA, 2 mM EGTA, 0.33 M sucrose, 1 mM DTT) containing a broad-range protease inhibitor cocktail (Roche Molecular Biochemicals, no. 1-836-145) and sonicated. Homogenized samples were then centrifuged at 9000*g* for 5 min at 4°C. The supernatant was stored at −80°C until immunoblot analysis.

Immunoblotting

Prior to sodium dodecyl sulfate–polyacrylamide gel electrophoresis (SDS-PAGE), protein content was assayed by the Micro BCA method (Pierce, Rockford, IL) using albumin standards. For each sample, 40 μg of protein from cortical tissue or 40 μg of protein from CSF samples were added to 2 × loading buffer containing 0.2 M Tris (pH 6.8), 400 mM 2-mercapto-ethanol, 8% SDS,

0.04% Bromophenol Blue, and 40% glycerol. The amount of protein for CSF samples was optimized to identify SBDP after both mild (1.0 mm) and severe (1.6 mm) injury. The optimal amount of protein to see the 145/150 band after mild injury resulted in an amount of protein after severe (1.6 mm) injury that sometimes would make the 145 and 150 bands indistinguishable. Semi-quantitation by densitometry was used to evaluate the 145–150-kDa band together thus the blurring of the 145/150 band was not a problem. The 145–150-kDa spectrin breakdown product represents primarily calpain initiated cleavage of spectrin in our model. Consistent with a previous report that CCI in our laboratory does not produce prominent caspase-3 levels (Pike et al., 1998), caspase-3–mediated SBDP 120 was inconsistent after severe (1.6 mm) injury and absent after mild (1.0 mm) injury and was not analyzed in this set of experiments. Semi-quantitation by densitometry evaluated both the 145–150-kDa band together thus the blurring was not a problem. Samples were heated at 96°C for 10 min and then centrifuged for 1 min at 10,000*g*. Samples were resolved in a vertical electrophoresis chamber for 70 min at 150 V. A 6.5% percent stacking acrylamide gel or a 4–20% Tris-Glycine gel (Invitrogen Life Technologies, Carlsbad, CA) were used. Separated proteins were either laterally transferred as a wet transfer to a nitrocellulose membrane (0.45 μM) using a transfer buffer consisting of glycine (192 mM) and tris (25 mM), (pH 8.3) with 10% methanol at a constant voltage of 100V for 70 min at 4°C or were horizontally transferred as a semi-dry transfer to an Immobilon-P polyvinylidene fluoride (PVDF) membrane (Millipore, Bedford, MA) using 39 mM glycine, 48 mM Tris, and 5% methanol at 20 V for 2 h at room temperature. All gels were stained with coomassie blue to confirm equal loading of protein on the gel. Selected blots were also stained with Panceau red (Sigma, St. Louis, MO) to confirm transfer and that equal amounts of protein were loaded in each lane. Blots were blocked for one hour in 5% non-fat milk in TBST (20 mM Tris, 0.15 M NaCl, and 0.005% Tween-20). Following overnight incubation with the primary antibody, anti-α-spectrin monoclonal antibody (1:10,000 dilution for cortex and 1:5,000 dilution for CSF; Affiniti Research Products, UK) and 1% non-fat milk/TBST at 4°C temperature, the blots were incubated with goat anti-mouse secondary antibody (1:1000 for cortex and 1:5000 for CSF; Biorad) and 3% non-fat milk/TBST for 1 h. Blots were then washed for 1 h in TBST. Enhanced chemiluminescence reagents (ECL and ECL-Plus, Amersham) were used to visualize immunolabeling of cortical tissue and CSF, respectively, and developed on Kodak BioMax Light Film (Kodak). Semi-quantitative evaluation of protein levels was conducting using computer-assisted one-dimensional densitometric scanning (ImageJ, version 1.29, NIH). Data were acquired as integrated densitometric values from similarly exposed films.

ELISA

CSF S100β levels were measured using a rat specific ELISA kit, Nexus D_x™ Rat S100 Test Kit from SynX (Toronto, Ontario, Canada) and CSF tau was measured using a kit,Innotest™ hTau Antigen from Innogenetics, Inc. (Alpharetta, GA). The sensitivities of the S100β and tau ELISA kits were 0.02 ng/mL and 75 pg/mL, respectively.

T2-Weighted Magnetic Resonance Imaging

Animals were scanned in the Advanced Magnetic Resonance Imaging and Spectroscopy (AMRIS) facility located in the McKnight Brain Institute of the University of Florida. Animals undergoing these imaging sessions were anesthetized using isoflurane (maintenance anesthesia of 1.5–2.5% isoflurane in 1 L/min 100% O_2 continuously delivered via a nose cone). Ophthalmic lubricant was used to prevent drying of the eyes during anesthesia. Anesthetized rats were placed on a custom Plexiglas cradle constructed to support the rat comfortably in the supine position. Oxygen saturation was monitored using a pulse oxymeter positioned on the left hind limb. Body temperature was monitored using a rectal flouroptic probe and maintained using warm air. A 4.7-Tesla magnet (Oxford Instruments) and Bruker Avance Console (Bruker, Germany) and a custom built 3.3-cm (inner diameter) quadrature birdcage coil were used for all image acquisitions. T2-weighted images were acquired at 24 h and 28 days after TBI. Twelve contiguous 1.25-mm coronal slices were acquired with the following parameters: a field of view = 3.6 × 3.6 cm^2, repetition time (TR) = 2.1 seconds, echo time (TE) = 81 msec, matrix = 256 × 256 points per dimension (140 μm in plane). Areas of hypo-intensity on MRI were associated with hemorrhage or mechanical disruption and areas of hyper-intensity were associated with edema (Albensi et al., 2000). Lesion size was drawn using ParaVision Image Analysis tools (Bruker, Germany) similar to the methodology in (Neumann-Haefelin et al., 2000). The area of each lesion in each coronal slice was multiplied by the slice thickness and then added to calculate the total lesion size.

Neurological Functional Evaluation

Motor behavior was assessed in the sub-acute period after TBI by a blinded observer using a Rota-rod (Ugo Basile, Comerio, Italy; Hamm et al., 1994). Rats were placed on a Rota-rod, a rotating rod, which was set to

slowly accelerate from 4 to 40 rpm within 5 min. The Rota-rod requires the rat to walk as the revolving rod accelerates and maintain balance. The trial lasted until the rat fell off and tripped a plate that recorded the time or until the rat had stayed on the rod for 300 sec was reached. Rats underwent conditioning of two trials a day for three days prior to TBI. After TBI, the rats were tested for two trials a day on days 1–5. The average of the latency in seconds of the two trials was recorded.

Statistical Analysis

Means and standard errors of the means were calculated from individual rat densitometric values of the 145–150-kDa SBDP combined as one value. Two-way ANOVA was used to examine main effects and interaction effects of time and injury magnitude. One-way ANOVA with contrast to do pair-wise comparisons was used to determine significance between levels of SBDP and between lesion sizes of the corresponding experimental groups. Regression analysis was performed with lesion size as the outcome variable and CSF markers (SBDP, tau, S100â) as the predictor variable. Pearson correlations were calculated and tested using the asymptotic Z-test. Correlations were calculated in the individual animal between CSF SBDP levels and lesion size. The analysis of the correlations included animals in all groups (naive, craniotomy, 1.0 mm and 1.6 mm injury) unless stated otherwise. Repeated measures ANOVA (4 groups × 5 time points) were performed to determine individual group differences over the five time points on the Rota-rod test.

RESULTS

Injury Magnitude Is Associated with Increased Levels of SBDP in the Cortex and CSF after TBI

SBDP were measured by Western blot from the CSF and ipsilateral cortex (IC) at 2, 6, and 24 h after two magnitudes of TBI. Naive rats and rats that had undergone a craniotomy served as controls for this study. The two response variables, SBDP in the CSF and SBDP in the IC were analyzed via ANOVA with terms for injury magnitude, time, and the interaction of time and injury magnitude.

The results indicated there was no interaction effect ($p = 0.88$) or time effect ($p = 0.12$) on IC SBDP levels. The analysis also indicated that injury magnitude significantly increased the level of cortical SBDP ($p \leq 0.0001$). Mean levels of IC SBDP after severe (1.6 mm) injury were significantly higher than the mean levels of IC SBDP after mild (1.0 mm) injury ($p < 0.05$). Mean levels of IC SBDP after both severe (1.6 mm) and mild (1.0 mm) injury were significantly greater than mean levels of SBDP after craniotomy or in naive controls ($p < 0.0001$). Mean levels of IC SBDP did not differ between naive and after craniotomy. Representative gels show that levels of SBDP increased with injury magnitude in the ipsilateral cortex and the CSF (Fig. 1A). Levels of SBDP (both 145 and 150 kDa are densitometrically quantified together) were highest after 1.6-mm injury in the IC and CSF at all time points (Fig. 1B). F1

After severe (1.6 mm) injury, the mean levels of IC SBDP were 116.4 ± 8.9, 135.9 ± 14.1, and 135.6 ± 17.7 and after mild (1.0 mm) injury, the mean levels of IC SBDP reached 78.1 ± 9.9, 110.1 ± 19.4, and 102.8 ± 17.2 at 2, 6, and 24 h, respectively. After craniotomy, the mean levels of IC SBDP reached 22.6 ± 9.1, 40.9 ± 18.2, and 11.8 ± 4.6 at 2, 6, and 24 h, respectively. In naive rats, the mean levels of IC SBDP were 4.4 ± 1.6, 15.4 7.0, and 4.4 ± 6.5 at 2, 6, and 24 h, respectively.

There was no interaction effect ($p = 0.39$) or time effect ($p = 0.13$) on CSF SBDP levels. The analysis also indicated that injury magnitude significantly increased the levels of CSF SBDP ($p \leq 0.0001$). Mean levels of CSF SBDP after severe (1.6 mm) injury were significantly higher than the mean levels of CSF SBDP after mild (1.0 mm) injury ($p = 0.0001$). Mean levels of CSF SBDP after both severe (1.6 mm) and mild (1.0 mm) injury were significantly greater than mean levels of CSF SBDP after craniotomy or in naive controls ($p < 0.0001$). Mean levels of CSF SBDP did not differ between naive and after craniotomy.

After 1.6 mm injury, the mean levels of CSF SBDP were 153.4 ± 11.3, 114.4 ± 19.1, and 91.2 ± 23.8 and after 1.0 mm injury, the mean CSF SBDP were 82.2 ± 17.3, 71.4 ± 17.3, and 64.3 ± 17.2 at 2, 6, and 24 h, respectively. After craniotomy, the mean levels of CSF SBDP reached 7.8 ± 2.7, 19.1 ± 6.0, and 10.3 ± 5.3 at 2, 6, and 24 h, respectively. In naive rats, the mean levels of CSF SBDP were 1.0 ± 0.7, 5.7 ± 3.4, and 3.0 ± 1.4 at 2, 6, and 24 h, respectively.

The Relationship of CSF SBDP Levels with Lesion Size at 24 h Post-Injury

CSF extraction to measure SBDP and T2-weighted imaging to measure lesion size was performed in the same groups of rats at 24 h after TBI. Representative T2-weighted images of a naive rat and a rat 24 h after craniotomy, mild (1.0 mm) injury and severe (1.6 mm) injury are shown in Figure 2A. Severe (1.6 mm) injury resulted in disruption of normal architecture and swelling of the ipsilateral cortex (arrow in Fig. 2A). Less disrup- F2

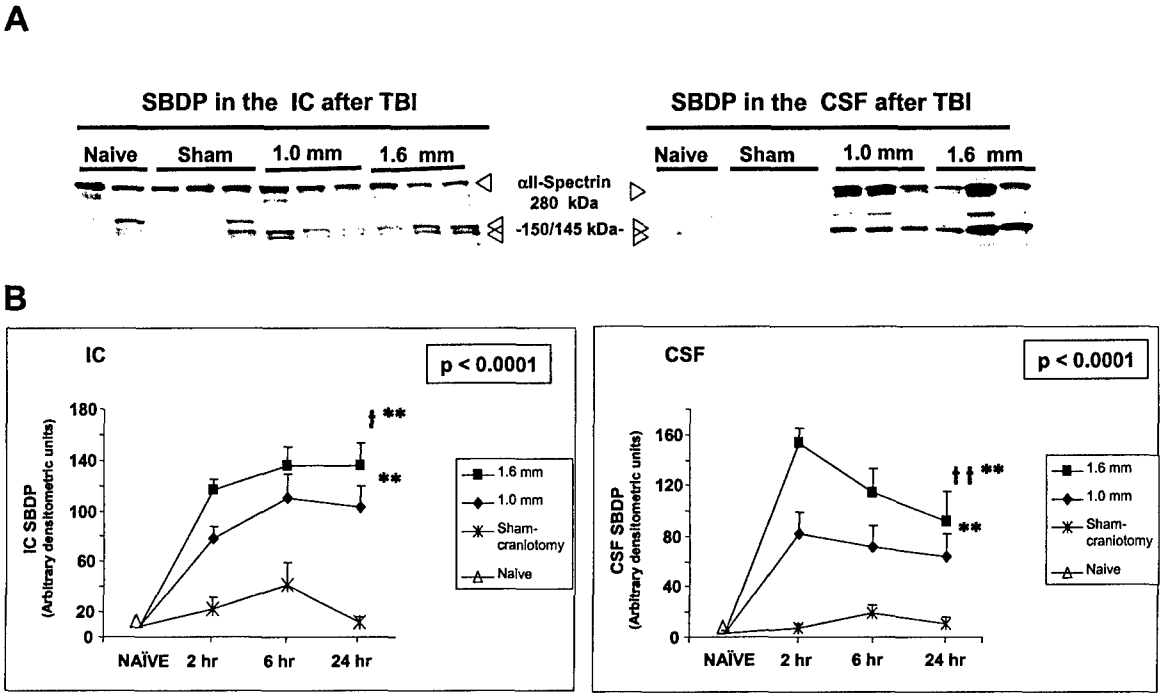

FIG. 1. Injury magnitude increases levels of SBDP in the ipsilateral cortex (IC) and CSF. (**A**) A representative Western blot of αII-spectrin and SBDP in the IC (left) and CSF (right) at 24 and 2 h, respectively, after TBI. Samples were collected after severe (1.6 mm) injury, mild (1.0 mm) injury, sham-craniotomy or from naive rats. Higher levels of SBDP are seen after severe (1.6 mm) injury than after mild (1.0) injury. Minimal SBDP is seen in the IC or CSF of naive rats or after sham-craniotomy in rats. (**B**) SBDP levels (145–150-kDa fragments) in the IC (left panel) and CSF (right panel) after sham-craniotomy, mild (1.0 mm) injury and severe (1.6 mm) injury at 2, 6, and 24 h were quantified using computer-assisted densitometric analysis (ImageJ, version 1.29×, NIH, USA). Values from naive animals were averaged as a separate time point. At each time point of 2, 6, and 24 h, 9 rats received severe (1.6 mm) injury, 9 rats received mild (1.0 mm) injury, 8 rats received a sham-cra-niotomy and 4 rats remained naive. An ANOVA was performed followed by contrast with pair-wise comparisons. Data is presented as the mean plus standard error. Standard error bars on the shams are present but not easily visable. Injury magnitude significantly increased mean levels of IC and CSF SBDP over time ($p < 0.0001$). Mean levels of SBDP after severe (1.6 mm) injury were significantly higher from the mean levels of SBDP after mild (1.0 mm) injury ($^{\dagger\dagger}p = 0.0001$ and $^{\dagger}p < 0.05$, respectively, for CSF and IC levels of SBDP). Mean levels of IC and CSF SBDP after both severe (1.6 mm) and mild (1.0 mm) injury were significantly greater than mean levels of SBDP after sham-craniotomy or in naive controls ($^{**}p < 0.0001$). Mean levels of CSF and IC SBDP did not differ between naive and sham.

FIG. 2. Lesion size on T2 weighted images increases with injury magnitude 24 h after TBI. (**A**) Representative serial T2-weighted magnetic resonance images of a naive rat and a rat 24 h after sham-craniotomy, mild (1.0 mm) and severe (1.6 mm) injury are shown. Twelve contiguous coronal 1.25 mm slices were acquired with the following parameters: a field of view = 3.6×3.6 cm^2, repetition time (TR) = 2100 sec, echo time (TE) = 81 msec, matrix = 256×256 points per dimension (140 μm in plane). Four of the 12 coronal slices for each rat are shown. Severe (1.6 mm) injury resulted in disruption of normal architecture and swelling of the ipsilateral cortex (arrow). Less disruption of normal architecture is noted after mild (1.0 mm) injury (arrowhead). Sham-craniotomy resulted in varying amounts of hyper-intensity in the ipsilateral cortex (arrowhead). (**B**) Lesion size was drawn using ParaVision Image Analysis tools (Bruker, Germany) similar to the methodology in (Neumann-Haefelin et al., 2000). The area of each lesion in each coronal slice was multiplied by the slice thickness and then added to calculate the total lesion size. One-way ANOVA with contrast to do pair-wise comparisons was used to determine difference between lesion sizes of the treatment groups. Nine rats each received severe (1.6 mm) injury, mild (1.0 mm) injury or sham surgery and 8 rats remained naive. The lesion after severe (1.6 mm) injury is significantly greater than the lesion size after mild (1.0 mm) injury ($^{\#\#}p \leq 0.001$) and both are significantly greater than after sham-craniotomy ($^{\dagger\dagger}p \leq 0.001$) or naive animals ($^{**}p \leq 0.001$) Sham injury is greater than the absense of a lesion in naive animals ($^{*}p < 0.05$).

tion of normal architecture is noted after mild (1.0 mm) injury (arrowhead in Fig. 2A). Craniotomy resulted in varying amounts of hyper-intensity in the ipsilateral cortex (arrowhead in Fig. 2A). Average lesion size was 0.044 $cm^3 \pm 0.00058$ after craniotomy, 0.100 $cm^3 \pm 0.010$ after 1.0 mm injury, and 0.166 $cm^3 \pm 0.016$ after 1.6 mm injury (Fig. 2B). Mean lesion size was significantly different between 1.6 mm and 1.0 mm injury groups and

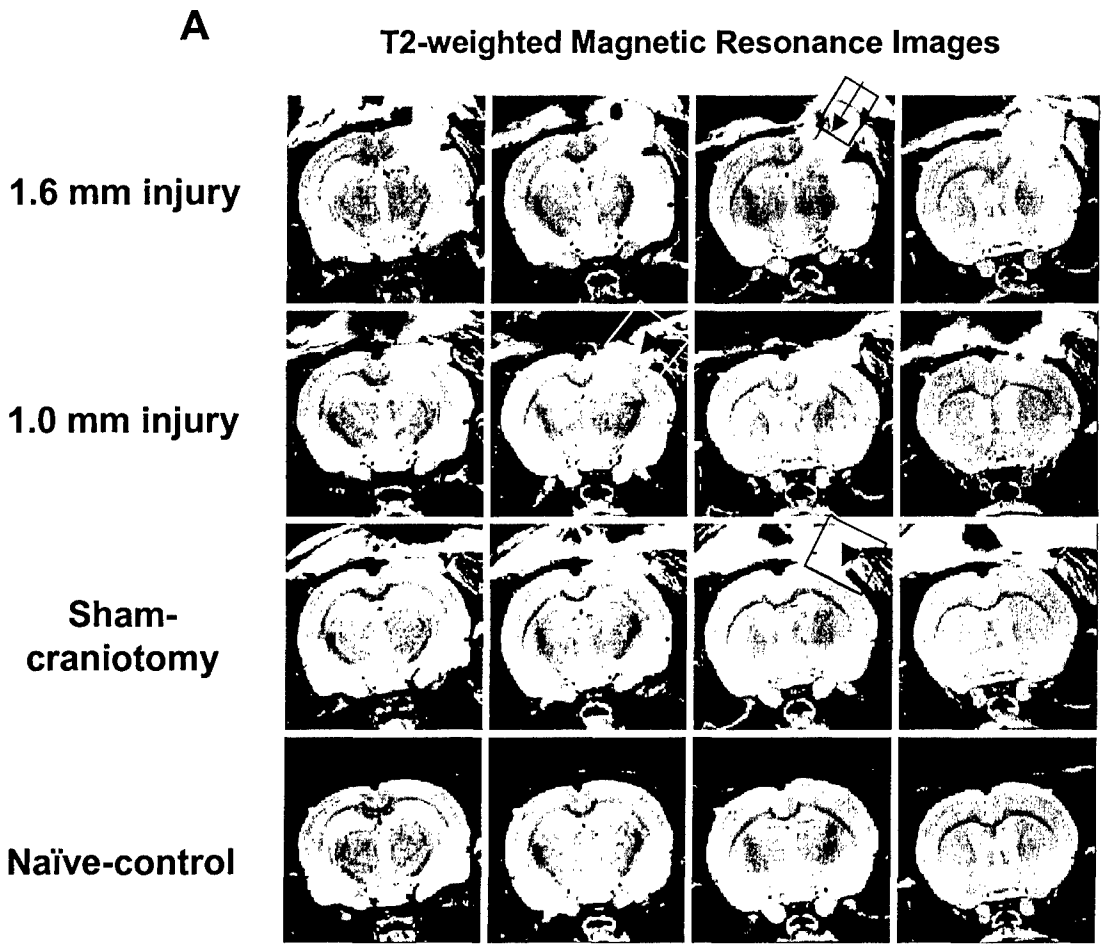

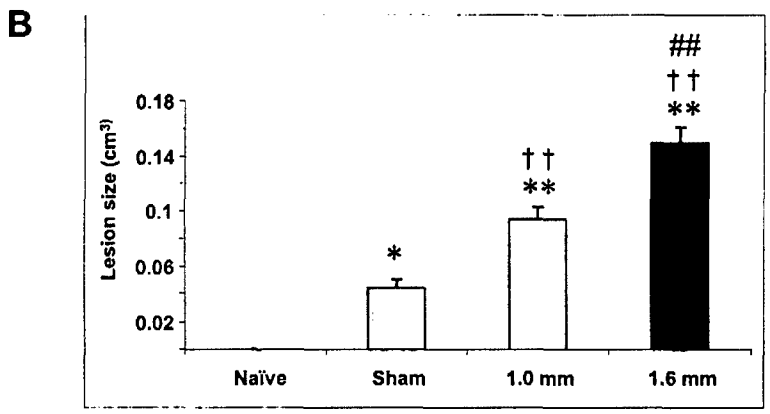

between both injury groups and after craniotomy ($p \leq 0.001$; Fig. 2B). Mean levels of CSF SBDP significantly correlated with lesion size ($r = 0.833$, $p < 0.0001$) when including all 4 groups (1.6 mm and 1.0 mm injury, craniotomy, and naive rats) (Fig. 3A). This correlation was not significant if craniotomy and sham rats were not considered in the analysis. To explore the ability of SBDP to predict lesion size, a regression analysis was run with lesion size as the outcome variable and CSF SBDP as the predictor variable from individual rats from all 4 groups. The regression weight for CSF SBDP was estimated to be 1059.86, and the parameter estimate of the intercept was 10.707. The regression analysis revealed CSF SBDP contributed significantly to predicting lesion volume ($p < 0.0001$).

Levels of CSF tau significantly correlated with lesion size ($r = 0.693$, $p < 0.0001$) (Fig. 3B) as levels of CSF S100β did not ($r = 0.188$) (Fig. 3C). The regression weight for CSF tau was estimated to be 0.00001258, and the parameter estimate of the intercept was 0.03485. CSF levels of tau significantly contributed to the prediction of lesion volume ($p < 0.0001$). Neither CSF tau or CSF S100β were correlated if just the 1.6-mm and 1.0-mm injured rats were used for analysis.

A regression analysis was performed to determine which marker or combination of markers (SBDP, tau and S100β) best predicted lesion size. A full regression model indicated the only significant variable was SBDP ($p < 0.0001$). S100β was eliminated from the model and the regression re-run looking at SBDP and tau as predictors of lesion size. CSF SBDP was again the only significant predictor of lesion size ($p < 0.0001$). CSF SBDP and CSF tau are significantly correlated ($r = 0.750$, $p < 0.0001$) and CSF SBDP has a higher correlation with CSF tau than CSF tau's correlation with lesion size.

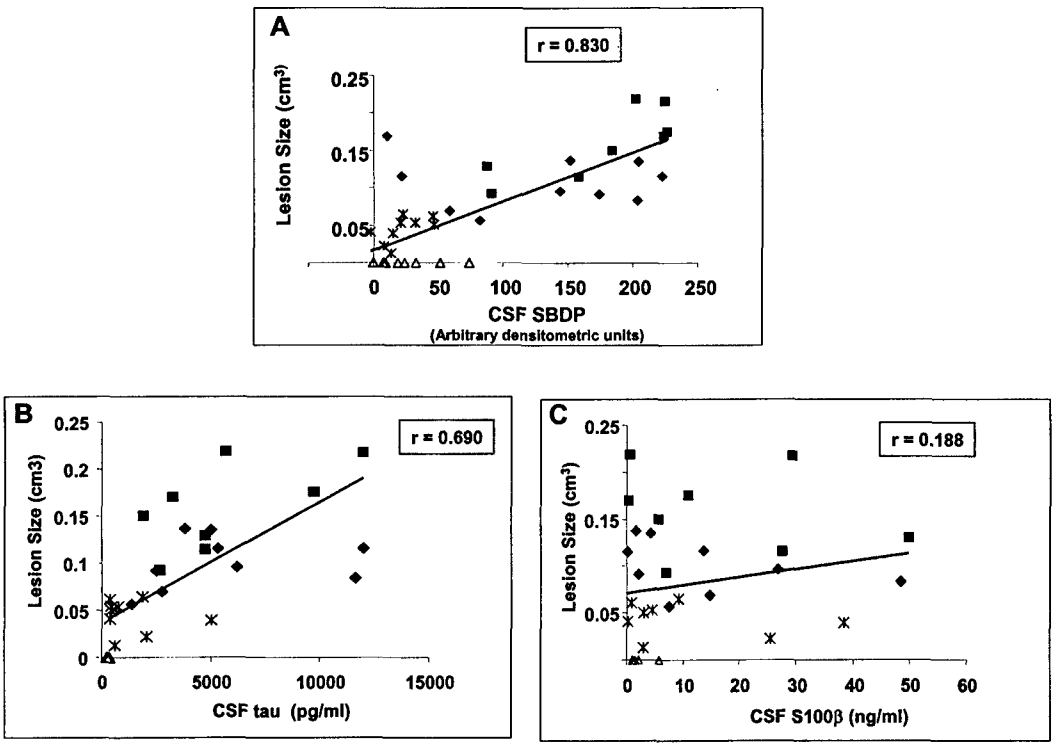

FIG. 3. The relationship of levels of CSF SBDP and tau with lesion size 24 h after TBI. Regression analysis was performed with lesion size as the out-come variable and levels of CSF markers (SBDP, tau, S100β) 24 h after TBI as the predictor variable. (**A**) Levels of CSF SBDP correlate with lesion size after TBI ($r = 0.83$, $p \leq 0.0001$). A linear regression equation showed that CSF SBDP significantly contributed to prediction of lesion size ($p \leq 0.0001$). (**B**) Levels of CSF tau correlate with lesion size after TBI ($r = 0.690$, $p < 0.001$). A linear regression equation showed that CSF tau significantly contributed to prediction of lesion size ($p \leq 0.0001$). The correlation with CSF SBDP and tau was not significant if craniotomy and sham rats were not considered in the analysis. (**C**) Levels of CSF S100β did not correlate with lesion size ($r = 0.188$). ■, rats after 1.6 mm injury; ◆, rats after 1.0 mm injury, ✳, rats after sham-craniotomy; △, naive rats.

Injury Magnitude Is Associated with Decreased Performance on the Rota-Rod Test and Increased Lesion Size

Because CSF SBDP correlated with lesion size at 24 hours, we looked at the relationship between lesion size and motor performance. Motor performance was assessed in the same (study 3) rats that lesion size was measured at 24 h and 28 days (Fig. 4A). Similar to 24 h, at 28 days lesion size varied with injury magnitude. Lesion size at 24 h in the individual animal was significantly correlated with lesion size at 28 days ($r = 0.881$, $p < 0.0001$). Assessment of Rota-rod performance prior to treatment revealed no significant differences between groups. Injury magnitude had a significant effect on Rota-rod performance ($p < 0.0001$). Mean Rota-rod scores were significantly lower after 1.6-mm injury at all time points (1–5 days after TBI) compared to mild (1.0 mm) injury, craniotomy, or naive rats ($p \leq 0.05$). After 1.0-mm injury, mean Rota-rod scores were significantly lower than in naive rats ($p < 0.01$) and showed a trend toward being lower than after craniotomy (Fig. 4A). Naive rats averaged close to a perfect score of 300 sec at all time points. Naive rats had significantly higher scores than rats after craniotomy ($p < 0.05$). Furthermore, larger lesion sizes were associated with decreased performance on the Rota-rod (Fig. 4B). In the individual rat, the average of the 5 days of Rota-rod scores correlated negatively with lesion size at 24 h ($r = -0.708$; $p < 0.0001$).

DISCUSSION

This paper examined the relationship between IC and CSF levels of SBDP and injury magnitude and outcome measures. The results show that SBDP levels in both CSF and IC SBDP increase with injury magnitude. Although both IC and CSF levels of SBDP increased, they did not parallel each other. Levels of CSF SBDP peaked at 2 h and decreased over time, while IC levels of SBDP slowly increased over the first 6 h after TBI. The correlation between lesion size and CSF levels of SBDP supported CSF SBDP as an indicator of injury. Correlational analysis of relationships between lesion size and CSF levels of SBDP indicated that CSF SBDP is a reliable marker of the presence or absence of injury but failed to be a reliable marker of injury magnitude. Although both CSF and IC SBDP levels and lesion size were significantly higher after 1.6-mm injury than after 1.0-mm injury, the correlation between CSF SBDP and lesion size was not significant following the removal of the control groups (naive and craniotomy) from the analysis. Further study is needed to show if CSF SBDP levels are a useful predictor of outcome such as lesion size.

Factors that affect brain derived protein levels in the CSF after injury have not been extensively explored and are likely to affect the variability of CSF SBDP levels and correlations with CSF SBDP. Petzold et al. (2003) suggest the main determinants of brain tissue proteins in the CSF are the extent of the primary lesion, the total pathological severity causing imbalance of brain home-

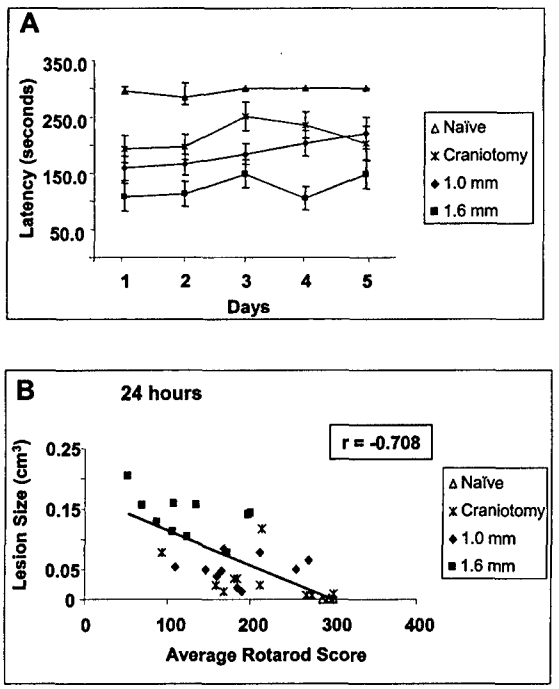

FIG. 4. Performance on the Rota-rod test decreases with increased injury magnitude and lesion size. (**A**) Rats were placed on a rotating rod, which slowly accelerated from 4 to 40 rpm within 5 min on days 1–5 after TBI. The rats were tested for two trials a day and the average of the latency in seconds of the two trials was recorded. Repeated measures ANOVA (4 groups × 5 time points) were performed to determine individual group differences over the five time points on the Rota-rod test. Of the third group of rats, 10 rats each received severe (1.6 mm) injury, mild (1.0 mm) injury or sham surgery and 5 rats remained naive. Data is presented as the mean ± SE. Injury magnitude significantly effected rotarod performance ($p < 0.0001$). Severely (1.6 mm) injured rats performed significantly worse on days 1–5 after TBI on the Rota-rod test than mildly (1.0 mm) injured rats or the sham-craniotomy group ($p < 0.05$ and $p < 0.01$, respectively). Both severe and mild injured groups performed significantly worse than the naive rats ($p < 0.01$). (**B**) Rotarod scores were averaged for the 5 days of testing for each individual rat. The average performance on the Rota-rod test was negatively correlated with lesion size at 24 h after TBI in the individual rat ($r = -0.708$; $p < 0.0001$). ■, rats after 1.6 mm injury; ◆, rats after 1.0 mm injury, ✳, rats after sham-craniotomy; △, naive rats.

ostasis, and the onset and duration of the brain injury. The CCI model that we have used in these studies has some inherent variability in impact force that affects lesion size, lesion severity and the location of pathology. Injured cells in the subarachnoid space can directly release protein into the CSF while protein from cells in the parenchyma must be transported to the CSF by flow of interstitial fluid or edema (Hans et al., 1999). The molecular flux/CSF flow theory suggests that changes in diffusion across the blood-brain and brain-CSF barriers are primarily predicated on CSF flow (Reiber and Peter, 2001; Reiber, 2003). If CSF flow rate is decreased after injury, then ventricular concentration of brain derived proteins is increased (Reiber, 2003). Variation of lesion impact might also cause variation in CSF flow rate and in the distance of brain-derived proteins from the CSF. As more is learned about factors effecting CSF levels of brain-derived proteins, the ability of CSF SBDP and other biomarkers to predict outcome may improve.

Hans et al. (1999) conducted one of the first studies to rigorously analyze a potential biomarker examining distribution and upregulation of mRNA and protein levels of IL-6 in tissue, and bioactivity of IL-6 in CSF and serum in a model of TBI. Similar to previous work in our lab examining mRNA of calpain-1 and calpain-2 (Ringger et al., 2004), IL-6 mRNA was upregulated after injury. Similar to our study, CSF levels of IL-6 peaked within 2–4 h after injury (Hans et al., 1999). IL-6 protein as seen on immunohistochemistry increased by 1 hour and persisted for 24 h, similar to the increase in IC SBDP on western blots at 2, 6, and 24 h after TBI. Hans et al. (1999) suggested that the increased tissue protein immunoreactivity reflected the increased IL-6 activity in the CSF. CSF levels of IL-6 were higher than serum levels between 2 and 8 h after injury. The CSF levels of IL-6 appear higher within 8 h of injury than in the CSF of sham animals, however the paper did not address this important question statistically.

Increased levels of calcium after TBI have been observed in several models (Fineman et al., 1993; Nadler et al., 1995; Verweij et al., 1997; Xiong et al., 1997). After TBI, calcium initiates a cytotoxic cascade of proteases including calpain which breaks down the cytoskeletal protein, spectrin. Higher levels of injury magnitude increased mRNA levels of calpain-1 and calpain-2 in the injured cortex and hippocampus (Ringger et al., 2004). Similar to our study, varying injury magnitude by depth or by velocity of impact, significantly effected lesion size (Goodman et al., 1994). Injury magnitude also significantly increased peak intracranial pressure and hippocampal neuron loss in similar models of TBI (Cherian et al., 1994; Goodman et al., 1994). Temporal increases in intracellular calcium were correlated with injury magnitude after lateral fluid percussion model of TBI in rats (Fineman et al., 1993). The corresponding increase in calcium after more severe TBI in the Fineman study may explain the association between injury magnitude and SBDP levels in the IC and CSF in our study.

In the acute time period following TBI, both CSF and IC SBDP significantly increased with injury magnitude. Calpain-mediated SBDP have been extensively examined and shown to increase in *in vivo* and *in vitro* models of neuronal injury (Bartus et al., 1995; Nath et al., 1996; Saatman et al., 1996a; Newcomb et al., 1997). Recently, it has been shown that CSF SBDP increased in models of TBI (Pike et al., 2001) and ischemia (Pike et al., 2004). The increased levels of SBDP150/145 are primarily associated with calpain activation in our CCI model. Although caspase-3 may also cleave spectrin to SBPD150, similar to prior work in our laboratory (Pike et al., 1998), the caspase-3 signature SBDP120 was not significant in our CCI model, suggesting a much less relevant role of caspase-3 in the production of SBDP in this model. Calpain inhibitors have been neuroprotective in models of TBI (Saatman et al., 1996a,b; Buki et al., 2003), ischemia (Bartus et al., 1994; Hong et al., 1994; Markgraf et al., 1998), and spinal cord injury (Banik et al., 1998). The ability of CSF levels of SBDP to reflect increased IC SBDP levels after acute neuronal injury may provide a therapeutic target for treatment of TBI and an effective way to monitor treatment of TBI if CSF is available.

CSF cleaved tau levels were significant predictors of outcome measures (intracranial pressure and GOS at discharge; Zemlan et al., 2002) supporting the finding of a significant correlation between CSF tau and lesion size in our study. On the other hand, Franz et al. (2003) showed that CSF levels of total tau did not correlate with injury severity (initial GCS) nor with outcome (GOS). The wide range of tau levels in that study was thought to be due to distance of the white matter lesion from the ventricles. Lesion variability is less in a model of CCI than in a clinical study of TBI.

An advantage of a serum biomarker is that it can be measured by less invasive methods than CSF biomarkers. The disadvantage of serum markers is that measurable serum levels of brain tissue proteins must cross the blood–brain and the CSF–blood barriers. Use of serum tau as a biomarker has produced conflicting results. Initial examination of serum cleaved tau indicated that the presence of serum cleaved tau increased the odds of the presence of an intracranial injury and a greater chance of a poor out-come (Shaw et al., 2002). Later work indicated serum cleaved tau levels did not correlate with outcome measures (Chatfield et al., 2002). After acute stroke, total tau increased in the CSF (Hesse

et al., 2001) and serum (Bitsch et al., 2002), and serum tau levels correlated to lesion size and severity. Serum tau levels, however, increased in less than 50% of stroke patients during the first 5 days after stroke (Bitsch et al., 2002).

Analysis of S100β has primarily been from the serum in clinical studies. Two clinical studies of serum levels of S100β revealed a correlation with contusion volume (Raabe et al., 1998; Herrmann et al., 2000), while in a study of mild TBI, serum S100β levels did not correlate with MRI or CT scans (Herrmann et al., 1999). S100β may be released from damaged glial cells, and this variable may not change consistently with lesion volume.

Importantly in multi-trauma patients without head injuries, S100β reached high serum levels after bone fractures and thoracic contusion and also increased after burns and minor bruising (Anderson et al., 2001). Numerous studies examined the use of S100β to mark cerebral damage after cardio-pulmonary bypass surgery (Ali et al., 2000), but S100β was found to be released from the mediastinum of cardiopulmonary bypass patients (Anderson et al., 2001). After stroke, higher serum S100β levels were associated with larger infarcts and more severe neuropsychological deficits (Aurell et al., 1991; Abraha et al., 1997; Buttner et al., 1997). Yet despite these promising correlations, Hill et al. (2000) found only 32% of stroke patients had elevated serum S100β on admission similar to serum tau levels (Bitsch et al., 2002). Early identification of stroke is necessary for optimal treatment within three hours.

The utility of SBDP as a serum marker has not been examined in clinical cases or models of stroke or TBI to the author's knowledge. Our study did not examine serum SBDP levels but further work will be important to establish if SBDP crosses the blood–brain and blood–CSF barrier and reflects SBDP levels in the CSF and brain. áII-spectrin is not found in red blood cells (Pike et al., 2001) although it is found in very low levels in other organs systems (Pike, Flint, Wang, and Hayes, unpublished data). The utility of SBDP as a marker would also benefit from knowledge of serum levels of SBDP in multi-trauma patients without head injuries and acutely after stroke.

Changes in high resolution MRI have been shown to correlate well with histology in a lateral fluid percussion model (Albensi et al., 2000) and a closed head injury model (Assaf et al., 1997) of TBI. Areas of hypo-intensity on MRI were associated with hemorrhage or mechanical disruption and areas of hyper-intensity were associated with edema (Albensi et al., 2000). At 24 h after rats underwent craniotomy, varying amounts of hyper-intensity were noted, most likely due to edema associated with the changes in cranial pressures. In the closed head injury model, areas of hyper-intensity decreased between 2 and 7 days after TBI likely representing resolution of edema (Assaf et al., 1997). Similarly in our study, the overall size of the lesion decreased between 24 h and 28 days, although a significant correlation was maintained between lesion size in individual rats at the two time points.

This study examined *in vivo* lesion size and the correlation to neuromotor function. Higher levels of injury magnitude significantly increased lesion size and decreased motor performance. In a stroke model, lesion size from T2-weighted images at 2 and 7 days after ischemia was significantly correlated with an average of individual neurological score (Palmer et al., 2001). Similarly in our study, the larger the lesion size, the worse the performance on the motor function test. Because lesion size at 24 h was highly correlated with lesion size at 28 days and significantly negatively correlated with motor performance, it is suggestive that acute levels of SBDP might correlate with both acute motor performance and chronic lesion size. Because withdrawal of CSF is a terminal procedure in our laboratory at this time, the correlation is only speculative.

In conclusion, the results of this study show that levels of SBDP in the IC and CSF are significantly higher after 1.6-mm injury than after 1.0-mm injury paralleling the significant difference in lesion size. We further showed that 24 hours after TBI, increased levels of CSF SBDP indicate the presence of a lesion. These studies strongly support the further study of CSF SBDP as a marker of CNS injury, and warrant evaluation of SBDP as a serum marker. Further examination may elucidate whether CSF or serum SBDP levels are predictors of outcome such as lesion size, GOS or neurological dysfunction. The contribution of this work is a foundation for future studies assessing the utility of this marker in human brain injury.

ACKNOWLEDGMENTS

We would like to acknowledge support of DAMD17-03-1-0066, DAMD17-01-1-0765, DAMD17-99-1-9565; NIH grants R01 NS39091, R01 NS40182. The authors would also like to thank Dr. Gary Stevens for his statistical contribution to this work. Drs. Kevin Wang and Ronald L. Hayes are inventors of technology to use alpha-spectrin as a brain injury biomarker discussed in this publication, Journal of Neurotrauma and hold equity in Banyan Biomarkers, a company commercializing the technology. Drs. Wang and Hayes may benefit from this technology by receiving royalties and equity growth.

REFERENCES

ABRAHA, H.D., BUTTERWORTH, R.J., BATH, P.M., WASSIF, W.S., GARTHWAITE, J., and SHERWOOD, R.A. (1997). Serum S-100 protein, relationship to clinical outcome in acute stroke. Ann. Clin. Biochem. **34,** 546–550.

ALBENSI, B.C., KNOBLACH, S.M., CHEW, B.G., O'REILLY, M.P., FADEN, A.I., and PEKAR, J.J. (2000). Diffusion and high resolution MRI of traumatic brain injury in rats: time course and correlation with histology. Exp. Neurol. **162,** 61–72.

ALI, M.S., HARMER, M., and VAUGHAN, R. (2000). Serum S100 protein as a marker of cerebral damage during cardiac surgery. Br. J. Anaesth. **85,** 287–298.

ANDERSON, R.E., HANSSON, L.O., NILSSON, O., DIJLAI-MERZOUG, R., and SETTERGREN, G. (2001). High serum S100B levels for trauma patients without head injuries. Neurosurgery **48,** 1255–1260.

ASSAF, Y., BEIT-YANNAI, E., SHOHAMI, E., BERMAN, E., and COHEN, Y. (1997). Diffusion- and T2-weighted MRI of closed-head injury in rats: a time course study and correlation with histology. Magn. Reson. Imaging **15,** 77–85.

AURELL, A., ROSENGREN, L.E., KARLSSON, B., OLSSON, J.E., ZBORNIKOVA, V., and HAGLID, K.G. (1991). Determination of S-100 and glial fibrillary acidic protein concentrations in cerebrospinal fluid after brain infarction. Stroke **22,** 1254–1258.

BANIK, N.L., SHIELDS, D.C., RAY, S., et al. (1998). Role of calpain in spinal cord injury: effects of calpain and free radical inhibitors. Ann. NY Acad. Sci. **844,** 131–137.

BARTUS, R.T., DEAN, R.L., MENNERICK, S., EVELETH, D., and LYNCH, G. (1998). Temporal ordering of pathogenic events following transient global ischemia. Brain Res. **790,** 1–13.

BARTUS, R.T., ELLIOTT, P.J., HAYWARD, N.J., et al. (1995). Calpain as a novel target for treating acute neurodegenerative disorders. Neurol. Res. **17,** 249–258.

BARTUS, R.T., HAYWARD, N.J., ELLIOTT, P.J., et al. (1994). Calpain inhibitor AK295 protects neurons from focal brain ischemia. Effects of postocclusion intra-arterial administration. Stroke **25,** 2265–2270.

BITSCH, A., HORN, C., KEMMLING, Y., et al. (2002). Serum tau protein level as a marker of axonal damage in acute ischemic stroke. Eur. Neurol. **47,** 45–51.

BUDUHAN, G., and McRITCHIE, D.I. (2000). Missed injuries in patients with multiple trauma. J. Trauma **49,** 600–605.

BUKI, A., FARKAS, O., DOCZI, T., and POVLISHOCK, J.T. (2003). Preinjury administration of the calpain inhibitor MDL-28170 attenuates traumatically induced axonal injury. J. Neurotrauma **20,** 261–268.

BUTTNER, T., WEYERS, S., POSTERT, T., SPRENGELMEYER, R., and KUHN, W. (1997). S-100 protein: serum marker of focal brain damage after ischemic territorial MCA infarction. Stroke **28,** 1961–1965.

CHATFIELD, D.A., ZEMLAN, F.P., DAY, D.J., and MENON, D.K. (2002). Discordant temporal patterns of S100beta and cleaved tau protein elevation after head injury: a pilot study. Br. J. Neurosurg. **16,** 471–476.

CHERIAN, L., ROBERTSON, C.S., CONTANT, C.F., JR., and BRYAN, R.M., JR. (1994). Lateral cortical impact injury in rats: cerebrovascular effects of varying depth of cortical deformation and impact velocity. J. Neurotrauma **11,** 573–585.

DIXON, C.E., CLIFTON, G.L., LIGHTHALL, J.W., YAGHMAI, A.A., and HAYES, R.L. (1991). A controlled cortical impact model of traumatic brain injury in the rat. J. Neurosci. Methods **39,** 253–262.

ELTING, J.W., DE JAGER, A.E., TEELKEN, A.W., et al. (2000). Comparison of serum S-100 protein levels following stroke and traumatic brain injury. J. Neurol. Sci. **181,** 104–110.

FINEMAN, I., HOVDA, D.A., SMITH, M., YOSHINO, A., and BECKER, D.P. (1993). Concussive brain injury is associated with a prolonged accumulation of calcium: a ^{45}Ca autoradiographic study. Brain Res. **624,** 94–102.

FRANZ, G., BEER, R., KAMPFL, A., et al. (2003). Amyloid beta 1–42 and tau in cerebrospinal fluid after severe traumatic brain injury. Neurology **60,** 1457–1461.

GARCIA, M.L., and CLEVELAND, D.W. (2001). Going new places using an old MAP: tau, microtubules and human neurodegenerative disease. Curr. Opin. Cell Biol. **13,** 41–48.

GOODMAN, J.C., CHERIAN, L., BRYAN, R.M., JR., and ROBERTSON, C.S. (1994). Lateral cortical impact injury in rats: pathologic effects of varying cortical compression and impact velocity. J. Neurotrauma **11,** 587–597.

HAMM, R.J., PIKE, B.R., O'DELL, D.M., LYETH, B.G., and JENKINS, L.W. (1994). The rotarod test: an evaluation of its effectiveness in assessing motor deficits following traumatic brain injury. J. Neurotrauma **11,** 187–196.

HANLON, R.E., DEMERY, J.A., MARTINOVICH, Z., and KELLY, J.P. (1999). Effects of acute injury characteristics on neurophysical status and vocational outcome following mild traumatic brain injury. Brain Inj. **13,** 873–887.

HANS, V.H., KOSSMANN, T., LENZLINGER, P.M., et al. (1999). Experimental axonal injury triggers interleukin-6 mRNA, protein synthesis and release into cerebrospinal fluid. J. Cereb. Blood Flow Metab. **19,** 184–194.

HARAD, F.T., and KERSTEIN, M.D. (1992). Inadequacy of bedside clinical indicators in identifying significant intracranial injury in trauma patients. J. Trauma **32,** 359–363.

HERRMANN, M., CURIO, N., JOST, S., et al. (2001). Release of biochemical markers of damage to neuronal and glial brain tissue is associated with short- and long-term neuropsychological outcome after traumatic brain injury. J. Neurol. Neurosurg. Psychiatry **70,** 95–100.

HERRMANN, M., EBERT, A.D., TOBER, D., HANN, J., and HUTH, C. (1999). A contrastive analysis of release patterns of biochemical markers of brain damage after coronary artery bypass grafting and valve replacement and their association with the neurobehavioral outcome after cardiac surgery. Eur. J. Cardiothorac Surg. **16,** 513–518.

HERRMANN, M., JOST, S., KUTZ, S., et al. (2000). Temporal profile of release of neurobiochemical markers of brain damage after traumatic brain injury is associated with intracranial pathology as demonstrated in cranial computerized tomography. J. Neurotrauma **17,** 113–122.

HESSE, C., ROSENGREN, L., ANDREASEN, N., et al. (2001). Transient increase in total tau but not phospho-tau in human cerebrospinal fluid after acute stroke. Neurosci. Lett. **297,** 187–190.

HILL, M.D., JACKOWSKI, G., BAYER, N., LAWRENCE, M., and JAESCHKE, R. (2000). Biochemical markers in acute ischemic stroke. CMAJ **162,** 1139–1140.

HONG, S.C., GOTO, Y., LANZINO, G., SOLEAU, S., KASSELL, N.F., and LEE, K.S. (1994). Neuroprotection with a calpain inhibitor in a model of focal cerebral ischemia. Stroke **25,** 663–669.

INGEBRIGTSEN, T., and ROMNER, B. (2002). Biochemical serum markers of traumatic brain injury. J. Trauma **52,** 798–808.

JACKSON, R.G., SAMRA, G.S., RADCLIFFE, J., CLARK, G.H., and PRICE, C.P. (2000). The early fall in levels of S-100 beta in traumatic brain injury. Clin. Chem. Lab. Med. **38,** 1165–1167.

KELLY, D.F. (1995). Alcohol and head injury: an issue revisited. J. Neurotrauma **12,** 883–890.

KIDO, D.K., COX, C., HAMILL, R.W., ROTHENBERG, B.M., and WOOLF, P.D. (1992). Traumatic brain injuries: predictive usefulness of CT. Radiology **182,** 777–781.

KURTH, S.M., BIGLER, E.D., and BLATTER, D.D. (1994). Neuropsychological outcome and quantitative image analysis of acute haemorrhage in traumatic brain injury: preliminary findings. Brain Inj. **8,** 489–500.

MARKGRAF, C.G., VELAYO, N.L., JOHNSON, M.P., et al. (1998). Six-hour window of opportunity for calpain inhibition in focal cerebral ischemia in rats. Stroke **29,** 152–158.

MCKEATING, E.G., ANDREWS, P.J., and MASCIA, L. (1998). Relationship of neuron specific enolase and protein S-100 concentrations in systemic and jugular venous serum to injury severity and outcome after traumatic brain injury. Acta Neurochir. Suppl. (Wien) **71,** 117–119.

MIRSKI, M.A., MUFFELMAN, B., ULATOWSKI, J.A., and HANLEY, D.F. (1995). Sedation for the critically ill neurologic patient. Crit. Care Med. **23,** 2038–2053.

NADLER, V., BIEGON, A., BEIT-YANNAI, E., ADAMCHIK, J., and SHOHAMI, E. (1995). ^{45}Ca accumulation in rat brain after closed head injury; attenuation by the novel neuroprotective agent HU-211. Brain Res. **685,** 1–11.

NATH, R., RASER, K.J., STAFFORD, D., et al. (1996). Non-erythroid alpha-spectrin breakdown by calpain and interleukin 1 beta-converting-enzyme-like protease(s) in apoptotic cells: contributory roles of both protease families in neuronal apoptosis. Biochem J. **319,** Pt 3, 683–690.

NEUMANN-HAEFELIN, T., KASTRUP, A., DE CRESPIGNY, A., et al. (2000). Serial MRI after transient focal cerebral ischemia in rats: dynamics of tissue injury, blood–brain barrier damage, and edema formation. Stroke **31,** 1965–1973.

NEWCOMB, J.K., KAMPFL, A., POSMANTUR, R.M., et al. (1997). Immunohistochemical study of calpain-mediated breakdown products to alpha-spectrin following controlled cortical impact injury in the rat. J. Neurotrauma **14,** 369–383.

PALMER, G.C., PEELING, J., CORBETT, D., DEL BIGIO, M.R., and HUDZIK, T.J. (2001). T2-weighted MRI correlates with long-term histopathology, neurology scores, and skilled motor behavior in a rat stroke model. Ann. NY Acad. Sci. **939,** 283–296.

PETZOLD, A., KEIR, G., LIM, D., SMITH., M, and THOMPSON, E.J., (2003). Cerebrospinal fluid (CSF) and serum S100B: release and washout pattern. Brain Res. Bull. **61,** 281–285.

PIKE, B.R., FLINT, J., DAVE, J.R., et al. (2004). Accumulation of calpain and caspase-3 proteolytic fragments of brain-derived alphaII-spectrin in cerebral spinal fluid after middle cerebral artery occlusion in rats. J. Cereb. Blood Flow Metab. **24,** 98–106.

PIKE, B.R., FLINT, J., DUTTA, S., JOHNSON, E., WANG, K.K., and HAYES, R.L. (2001). Accumulation of non-erythroid alpha II–spectrin and calpain-cleaved alpha II–spectrin breakdown products in cerebrospinal fluid after traumatic brain injury in rats. J. Neurochem. **78,** 1297–1306.

PIKE, B.R., ZHAO, X., NEWCOMB, J.K., POSMANTUR, R.M., WANG, K.K., and HAYES, R.L. (1998). Regional calpain and caspase-3 proteolysis of alpha-spectrin after traumatic brain injury. Neuroreport **9,** 2437–2442.

RAABE, A., GROLMS, C., KELLER, M., DOHNERT, J., SORGE, O., and SEIFERT, V. (1998). Correlation of computed tomography findings and serum brain damage markers following severe head injury. Acta Neurochir. (Wien) **140,** 787–792.

RAABE, A., and SEIFERT, V. (2000). Protein S-100B as a serum marker of brain damage in severe head injury: preliminary results. Neurosurg. Rev. **23,** 136–138.

REIBER, H. (2003). Proteins in cerebrospinal fluid and blood: barriers, CSF flow rate and source-related dynamics. Restor. Neurol. Neurosci. **21,** 79–96.

REIBER, H., and PETER, J.B. (2001). Cerebrospinal fluid analysis: disease-related data patterns and evaluation programs. J. Neurol. Sci. **184,** 101–122.

ROBERTS-LEWIS, J.M., SAVAGE, M.J., MARCY, V.R., PINSKER, L.R., and SIMAN, R. (1994). Immunolocaliza-

tion of calpain I–mediated spectrin degradation to vulnerable neurons in the ischemic gerbil brain. J. Neurosci. **14,** 3934–3944.

AU2 → RINGGER, N.C., TOLENTINO, P.J., McKINSEY, D.M., PIKE, B.R., WANG, K.K.W., and HAYES, R.L. (2004). Effects of injury severity on regional and temporal mRNA expression levels of calpains and caspases after traumatic brain injury in rats. J. Neurotrauma. (in press).

ROTHOERL, R.D., WOERTGEN, C., and BRAWANSKI, A. (2000). S-100 serum levels and outcome after severe head injury. Acta Neurochir. Suppl. **76,** 97–100.

SAATMAN, K.E., BOZYCZKO-COYNE, D., MARCY, V., SIMAN, R., and McINTOSH, T.K. (1996a). Prolonged calpain-mediated spectrin breakdown occurs regionally following experimental brain injury in the rat. J. Neuropathol. Exp. Neurol. **55,** 850–860.

SAATMAN, K.E., MURAI, H., BARTUS, R.T., et al. (1996b). Calpain inhibitor AK295 attenuates motor and cognitive deficits following experimental brain injury in the rat. Proc. Natl. Acad. Sci. USA **93,** 3428–3433.

SAIDO, T.C., YOKOTA, M., NAGAO, S., et al. (1993). Spatial resolution of fodrin proteolysis in postischemic brain. J. Biol. Chem. **268,** 25239–25243.

SHAW, G.J., JAUCH, E.C., and ZEMLAN, F.P. (2002). Serum cleaved tau protein levels and clinical outcome in adult patients with closed head injury. Ann. Emerg. Med. **39,** 254–257.

VERWEIJ, B.H., MUIZELAAR, J.P., VINAS, F.C., PETERSON, P.L., XIONG, Y., and LEE, C.P. (1997). Mitochondrial dysfunction after experimental and human brain injury and its possible reversal with a selective N-type calcium channel antagonist (SNX-111). Neurol. Res. **19,** 334–339.

WANG, K.K. (2000). Calpain and caspase: can you tell the difference? Trends Neurosci. **23,** 59.

WANG, K.K., POSMANTUR, R., NATH, R., et al. (1998). Simultaneous degradation of alpha-II– and beta-II–spectrin by caspase 3 (CPP32) in apoptotic cells. J. Biol. Chem. **273,** 22490–22497.

WILSON, J.T., HADLEY, D.M., WIEDMANN, K.D., and TEASDALE, G.M. (1995). Neuropsychological consequences of two patterns of brain damage shown by MRI in survivors of severe head injury. J. Neurol. Neurosurg. Psychiatry **59,** 328–331.

XIONG, Y., GU, Q., PETERSON, P.L., MUIZELAAR, J.P., and LEE, C.P. (1997). Mitochondrial dysfunction and calcium perturbation induced by traumatic brain injury. J. Neurotrauma **14,** 23–34.

ZEMLAN, F.P., JAUCH, E.C., MULCHAHEY, J.J., et al. (2002). C-tau biomarker of neuronal damage in severe brain injured patients: association with elevated intracranial pressure and clinical outcome. Brain Res. **947,** 131–139.

ZEMLAN, F.P., ROSENBERG, W.S., LUEBBE, P.A., et al. (1999). Quantification of axonal damage in traumatic brain injury: affinity purification and characterization of cerebrospinal fluid tau proteins. J. Neurochem. **72,** 741–750.

ZINK, B.J. (2001). Traumatic brain injury outcome: concepts for emergency care. Ann. Emerg. Med. **37,** 318–332.

Address reprint requests to:
N.C. Ringger, D.V.M.
Department of Neuroscience
McKnight Brain Institute
University of Florida
100 S. Newell Dr.
L1-100 (P.O. Box 100244)
Gainesville, FL 32610

E-mail: ringger@ufbi.ufl.edu

PROTEOMICS STUDIES OF TRAUMATIC BRAIN INJURY

Kevin K. W. Wang,[*, †, ‡, §] Andrew Ottens,[*, †, §] William Haskins,[*, †, §]
Ming Cheng Liu,[*, †, §] Firas Kobeissy,[*, †, ‡, §] Nancy Denslow,[*, ||]
SuShing Chen,[*, ¶] and Ronald L. Hayes[†, ‡, §]

[*]Center of Neuroproteomics and Biomarkers Research, University of Florida
Gainesville, Florida 32610
[†]Center for Traumatic Brain Injury Studies, University of Florida, Gainesville, Florida 32610
[‡]Department of Psychiatry, University of Florida, Gainesville, Florida 32610
[§]Department of Neuroscience, University of Florida, Gainesville, Florida 32610
[||]Interdisciplinary Center of Biomedical Research, University of Florida
Gainesville, Florida 32610
[¶]Computing and Information Science Engineering, University of Florida
Gainesville, Florida 32610

I. Introduction

With the completion of human and rat genomes, the next major technological challenge facing the biomedical community is the deciphering of the human proteome. Study of the proteome has been aided by recent advances in protein

0074-7742/04 $35.00

separation, protein identification/quantification, and bioinformatics. Although the application of proteomics technologies in brain injury research is still in its infancy, enormous insights can be achieved from such endeavors. There are approximately 30,000–40,000 hypothetical protein products transcribable from the human genome (Aebersold and Watts, 2002; Grant and Blackstock, 2001; Grant and Husi, 2001; Hanash, 2003; Hochstrasser *et al.*, 2002; Service, 2001; Smith, 2000). Yet, the proteome is extremely complex. Even in a single cell type the set of proteins that are expressed, as well as their steady state levels, depend on time and the specific state of the cells in response to environmental stimuli or challenges. In addition, cellular proteins are almost constantly subjected to various forms of post-translational modifications (PTMs), including phosphorylation/dephosphorylation by different kinases and phosphatases, proteolysis, or processing by different protease families, acetylation, glycosylation, and cross-linking by transglutaminases or conjugation to small protein tags such as ubiquitin or SUMO (similar to ubiquitin modifier) (Janssen, 2003; Schäfer *et al.*, 2003; Schwartz and Hochstrasser, 2003). Because of these challenges, one often has to focus on a specific subproteome. The case in point is neuroproteomics, or the study of nervous system proteomes. The importance of neuroproteomics studies is that they will help elucidate the poorly understood biochemical mechanisms or pathways that currently underlie various psychiatric, neurological, and neurodegenerative diseases. The example we will focus on here is traumatic brain injury (TBI), a neurological disorder currently with no Food and Drug Administration (FDA) approved therapeutic treatment.

II. Traumatic Brain Injury

Traumatic brain injury or traumatic head injury is characterized as a direct, physical impact or trauma to the head, causing brain injury (Denslow *et al.*, 2003; Hayes *et al.*, 2001). Annually there are 2 million TBI cases in the United States alone. They result in 500,000 hospitalizations, 100,000 deaths, 70,000–90,000 people with long-term disabilities, and 2000 people who survive but live in a permanent, vegetative state. Medical costs of TBI are estimated to be more than $48 billion annually in the United States. The cause of TBI can be broken down into the following catalogories: Motor vehicle accidents (50%), falls (21%), assault and violence (12%), sports and recreation (10%), and all others (7%) (Fig. 1). Importantly, 30–40% of all battlefield injuries also have a head injury component.

Because of intensive research both in clinical settings and in employing experimental animal models of TBI, there is now a general understanding of the pathology of TBI. Typically there is mechanical, compression-induced direct tissue injury often associated with hemorrhage and contusion at the site of

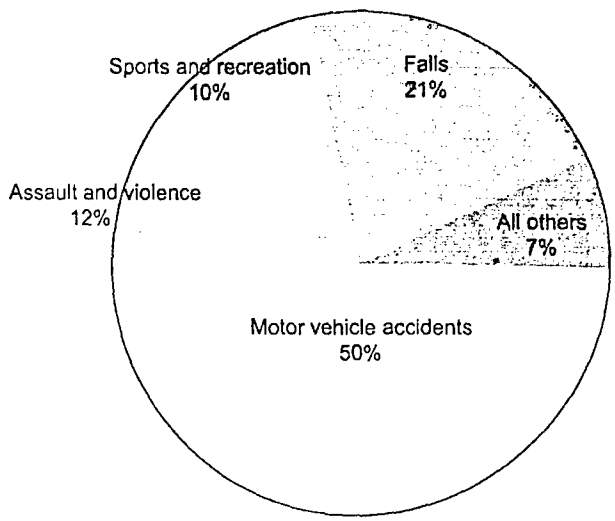

FIG. 1. Different causes of traumatic brain injury in humans.

impact. A significant amount of cell death will occur very rapidly in this zone. More distal to the injury zone, due to the impact of the force, long fiber tracts (axons) are especially at risk to this type of injury. Usually after the first phase of cell injury/death occurs, there is also the secondary injury, which is believed to be mediated by secondary biochemical events such as neurotoxic glutamate release (neurotoxicity) or oxidative damage. Other significant alterations include inflammation responses by microglia cells, astroglia activation, and proliferation. Over time, if the TBI patient survives, these events lead to long-lasting brain tissue remodeling, possibly including stem cells differentiation. Therefore the spatial and temporal levels of biochemical and proteomic changes of TBI can be investigated.

A. Animal Models of TBI

Over the past decades, basic science researchers have developed several animal models of TBI (Finnie, 2001; Raghupathi *et al.*, 2000). There are several well-characterized models of TBI, including controlled cortical impact (CCI), which is controlled by compressed gas; a fluid percussion model that transduces a contusion force by the movement of fluid in the chamber, and vertical weight drop models in which a weight is dropped from a certain height within a hollow chamber for guidance. The weight drop model creates an acceleration force that

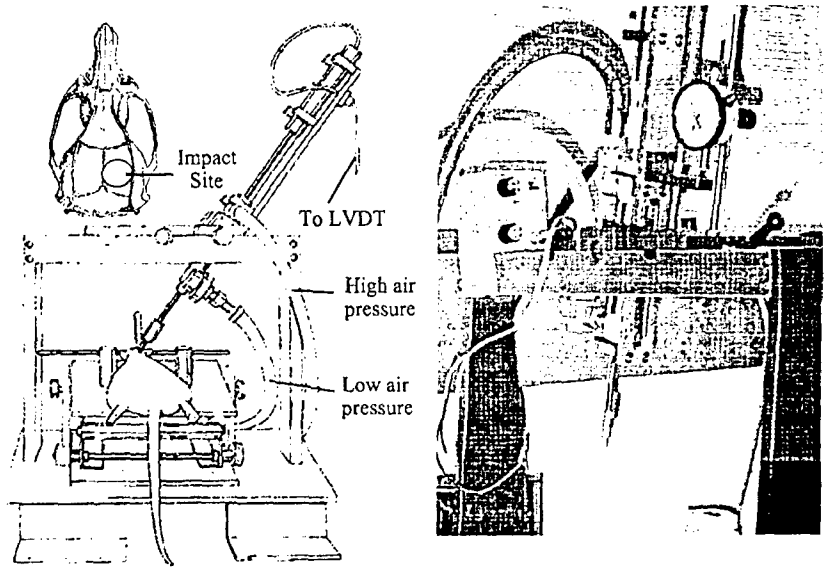

FIG. 2. Rat model of TBI: Controlled cortical impact (CCI). Left panel shows a schematic drawing of the CCI setup. Right panel is a photograph of the CCI device.

is directed to the top of the skull either unilaterally or bilaterally (reviewed by Finnie in 2001). In our work, we employ the rat CCI model of TBI (Dixon *et al.*, 1991; Fig. 2). We have argued that use of proteomics will greatly facilitate the biochemical mechanisms underlying the various phases of TBI pathology (Denslow *et al.*, 2003).

B. Source of Biological Materials

Proteomics studies for TBI generally can be categorized into human studies, animal studies, and cell culture-based studies. For the purposes of this review, cell culture-based studies will not be discussed further. When comparing human versus. animal studies, there are pros and cons in each scenario (Table I). Regarding the sample types that can be exploited for proteomics analysis, they will include brain tissues, cerebrospinal fluid (CSF), and blood (serum and plasma). For human TBI studies, blood samples (which are further fractionated into plasma or serum) are the easiest to obtain. Interestingly, there is increasing interest now focused on using CSF because its status will reflect that status of the central nervous system itself. After severe traumatic brain injury, spinal shunt or spinal tap are routinely performed, thus obtaining CSF is not an issue. One of the major challenges of

Table I
COMPARING HUMAN VERSUS ANIMAL TBI PROTEOMIC STUDIES

	Human studies	Animal studies
Sample heterogeneity	High	Low
Environmental variables	High	Low
Brain tissue samples	Difficult to obtain (postmortem only)	Routine
CSF samples	Routine (large volume available)	Routine (small volume only)
Blood samples	Routine (large volume available)	Routine (sufficient volume available)
Results relevance to human disease	Yes	Likely (confirmation needed)

using clinical, samples-based proteomic studies is that it is extremely difficult to control individual (biological) and environmental variables (see Table I).

1. *Brain Samples*

Brain tissue from human TBI studies would inevitably come from deceased TBI patients. These brain samples could be subjected to postmortem artifacts, compounded by various and significant time delay before samples can be obtained. The biggest advantage of animal neuroproteomics studies over human counterparts is the ability to obtain brain tissues in a controlled laboratory environment. Furthermore, it is possible to harvest samples from defined anatomical regions. For example, for our TBI studies we often focus on cortical and hippocampal samples. This is important because different brain regions might be selectively more vulnerable to traumatic or ischemic insults.

2. *CSF*

CSF can be collected from the cisterna magna from lab animals such as rats and mice. CSF may contain rich brain proteome information that is relevant to disease diagnosis (Davidsson *et al.*, 2002). However, only approximate 50–100 μl can be withdrawn from rats and 25–30 μl from mice. Care must also be taken not to contaminate samples with blood as a result of puncture. Although more than one CSF draw might be possible, in our laboratory we generally withdraw only one CSF sample, followed by sacrifice. In the case of human TBI, CSF can also be collected routinely from ventriculotomy or from spinal tap. Importantly, a relatively large amount (2–5 ml) of CSF can be routinely obtained from human TBI patients from each CSF sampling time point, and repeating samples can often be achieved.

3. *Blood Samples (Serum and Plasma)*

In both human and animal TBI studies, blood can be routinely collected and usually further processed into either serum or plasma fractions before subjecting to proteomics analysis. Like CSF, most proteomics researchers believe there is significant proteomic information in the blood that would reflect the status of the brain, particularly after TBI caused by possible blood-brain barrier compromise (Raabe *et al.*, 1999; Romner, 2000).

C. Sample Collection and Processing Consistency

It needs to be emphasized that for proteomics results to be consistent and reproducible, one needs to use extra caution to ensure the variables can be kept to a minimum. All sample collection procedures should be discussed and finalized and the operators made familiar with the procedures. Some practice runs are highly desirable. For human studies, detailed record keeping is extremely important for future analysis or trouble-shooting purposes. For example, for human studies, CSF or blood samples should be taken at consistent intervals and before food consumption, because it might significantly affect the blood proteomics profile. For animal studies that are conducted in controlled environments, it should be possible to keep brains and biofluid sample collection time and routine as standardized as possible. Also, the animal subjects should be tagged and observed carefully and regularly, with any out-of-the-norm observations recorded. They might become very helpful in enhancing proteomics analysis. Tissue and biofluid samples, once obtained and processed, should be snap frozen and stored at $-85\ ^{\circ}C$ until use.

D. Sample Pooling Considerations

There is also an important decision to be made before the proteomics analysis (i.e., whether to pool samples for analysis or to analyze individual samples). Pooling samples significantly reduces minor individual variability and the amount of workload. Yet, at the same time its disadvantage is that it might miss certain proteomics changes that are present in only a subset of samples. On the other hand, analysis of individual samples has the advantage of being an exhaustive analysis of individual proteomics profiles but can be highly time consuming and cost-prohibitive. Another consideration is that it would be useful to pool samples when protein amount is a limiting factor.

A known biochemical marker that correlates with TBI, such as alphall-spectrin breakdown products, can be used as positive control for quality assurance, and might even be used to guide inclusion criteria for sample pooling (Pike

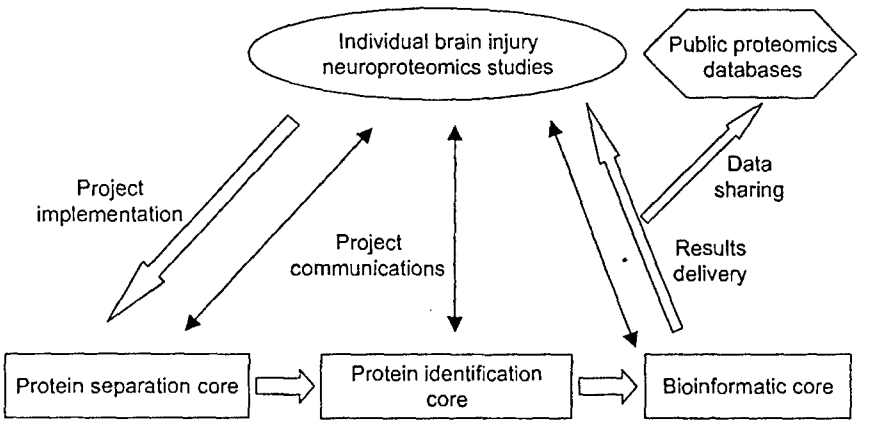

FIG. 3. Flowchart and organization of traumatic brain injury neuroproteomics studies. See text for details.

et al., 2001, 2004). It is also possible to incorporate both pooling and individual proteomics analysis in the same studies. For example, pilot studies or initial proteomics profiling of TBI can be performed with pooled samples while final detailed analysis can be done with individual samples.

III. Proteomics Analysis Overview

Regardless of whether we are dealing with human or animal samples, or whether they are tissue lysate or biofluid (CSF, serum, or plasma), the strategy we developed can be organized into three interacting, scientific disciplines or phases: protein separation, protein identification followed by quantification, and bioinformatics analysis (Fig. 3). By design, any proteomics center should spend two-thirds of its scientific and financial resources to establish a robust and readily usable proteomics platform. However, it is equally important for the center to develop new and improved neuroproteomics technologies on all fronts.

IV. Protein Separation Methods

In TBI neuroproteomics studies, we are less interested in descriptive and exhaustive characterization of the whole neuroproteome; rather we will focus on protein level or post-translational changes that occur in TBI. With this in mind, it

is important to devise methods in comparing and contrasting the two proteomics data sets: control versus TBI. To productively identify all the proteins in a specific system of interest (subproteome) or a subset of proteins that are differentially expressed in TBI, it is essential that complex protein mixtures (e.g., brain samples or biofluids) be first subjected to multidimensional protein separation. Because proteins differ in size, hydrophobicity, surface charges, abundance, and other properties, there is no single protein separation method that can satisfactorily resolve all proteins in a proteome.

To date there are two mainstream protein separation methods used for proteomic analysis: (1) two-dimensional gel isoelectrofocusing/electrophoresis and (2) multidimensional liquid chromatography.

A. Two-Dimensional Gel Electrophoresis Approach

Two-dimensional gel electrophoresis (2DE) is the most established protein separation method for the analysis of a proteome or subproteome (Boguslavsky, 2003). It is achieved by subjecting protein mixtures to two protein separation methods under denaturing condition (in the presence of 6–8 M urea and cationic detergent such as sodium dodecylsulfate [SDS]). Traditionally proteins are first separated based on their isoelectric point (pI) value with a tube gel (polyacrylamide), by isoelectric focusing (IEF) with the aid of mobile ampholytes with different (pI) values. After IEF, the tube gel is placed atop a polyacrylamide gradient gel within which the SDS-bound proteins are separated by size. Because of poor gel consistency, the IEF step (the first dimension) is most variable. However, a recent breakthrough in IEF technology using immobilized pH gradient (IPG) strips, provides improved reproducibility (Bjellqvist *et al.*, 1982; Gorg *et al.*, 1988; Hanash, 2003; Jungblut *et al.*, 1996). Another disadvantage with 2D gels is the inevitable gel-to-gel variability in exact location and patterns of protein spots. This proves problematic when comparing two samples directly (e.g., control versus TBI brain samples).

The recent advance of 2D-differential in-gel electrophoresis (2D-DIGE) has resolved this problem (Patton, 2002; Unlu *et al.*, 1997). The fluorescent cyanine dyes Cy3 and Cy5 are a match in molecular weight and charge but have distinct excitation and emission wavelengths (Yan, 2002). One dye is used to label control samples, and the other to label treated samples, which are then mixed and differentially compared in the same gel (Fig. 4). These advantages are incorporated into our approach, as outlined in Table I. They include in particular the high resolving power for complex mixtures of proteins and the capability of resolving post-translationally modified proteins, including acetylation, phosphorylation, glycosylation, and protein cross-linking (Janssen, 2003; Schäfer *et al.*, 2003). It is possible to annotate each protein of a proteome by pI and molecular

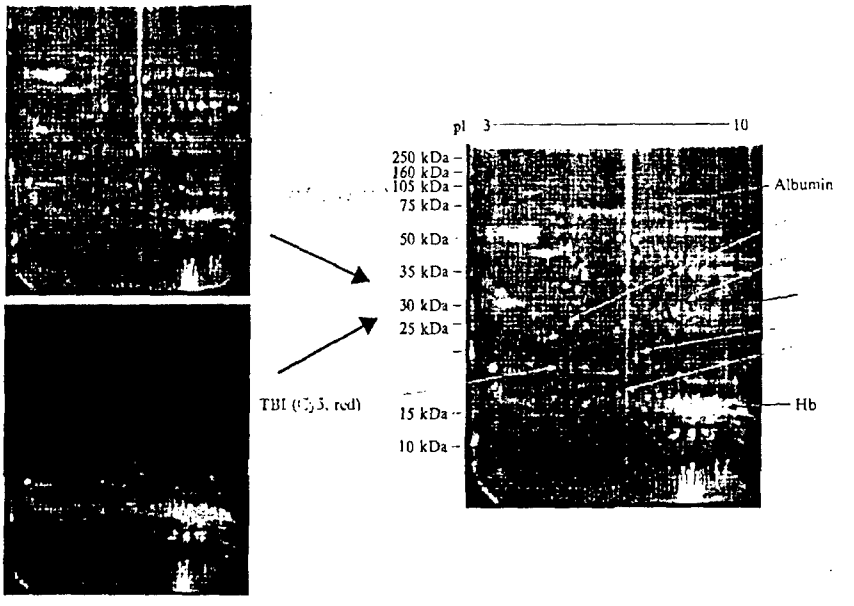

FIG. 4. Rat TBI protein separation by 2D differential in-gel electrophoresis *(DIGE)*. Pooled naïve and TBI rat cortex samples were labeled with Cy3 and Cy5 dyes, respectively (left panels) and co-run and resolved by 2DE. The fluorescence signals were merged, allowing the identification of differentially expressed proteins (right panel). Yellow spots represent proteins common to both samples. Green and orange-red spots are differentially expressed proteins in pooled naive and TBI sample, respectively. Blue arrows point to blood-borne protein contaminants found in TBI sample (e.g., albumin and hemoglobins [Hb]).

weight values in X-Y coordinates to form a 2D protein map, of which publicly accessible and searchable databases already exist (Appel *et al.*, 1999; Fountoulakis *et al.*, 1999, 2000; Lemkin, 1997; Lubec *et al.*, 2003). There are, however, several persistent weaknesses of 2D gels (See Table II). Proteins of extreme pI or minute quantity and proteins that are either very small or very large may be missed. Also, integral membrane proteins, of which many are central nervous system (CNS) disorder drug targets (membrane-bound receptors or neurotransmitter transporters), are lost because of their extreme hydrophobicity.

Regarding protein separation, there is also research in the direction of microfluidic 2D protein separation with miniaturized IEF and electrophoresis. This approach has the advantage of reducing sample usage with less waste and without compromising detection sensitivity (Derra, 2003; Reyes *et al.*, 2002).

B. Two-Dimensional Liquid Chromatography Approach

Alternative protein separation methods are needed to overcome some of the shortcoming of 2D gels. Recently there has been significant movement toward multidimensional liquid chromatography methods to resolve complex protein mixtures (Peng and Gygi, 2001). The general idea draws on classic chromatographic principles including size chromatography (gel filtration), ionic interaction (strong cation exchange [SCX] and strong anion exchange [SAX]), hydrophobic interaction (C4- or phenyl-agarose chromatography), and IEF chromatography. One can envision combining multiple chromatographic approaches in a series to achieve multidimensional separations. In our own work we have also combined the use of a size exclusion column (SEC) and a SAX column (Fig. 5) in series with some success. Challenging this method are: (1) incompatibilities of buffer components (e.g., salt concentration, organic components) and (2) the logistics of configuring fraction elution from one column with loading of a second column. Often, individual fractions are manually loaded onto the second column, but this is extremely labor intensive and may introduce run-to-run variability.

When selecting chromatographic separation methods, considerations must be given to take advantage of the size, pI, and hydrophobicity differences of the proteins of interest. In addition, when dealing with membrane-bound proteins, the chromatographic method must be compatible with the use of the proper

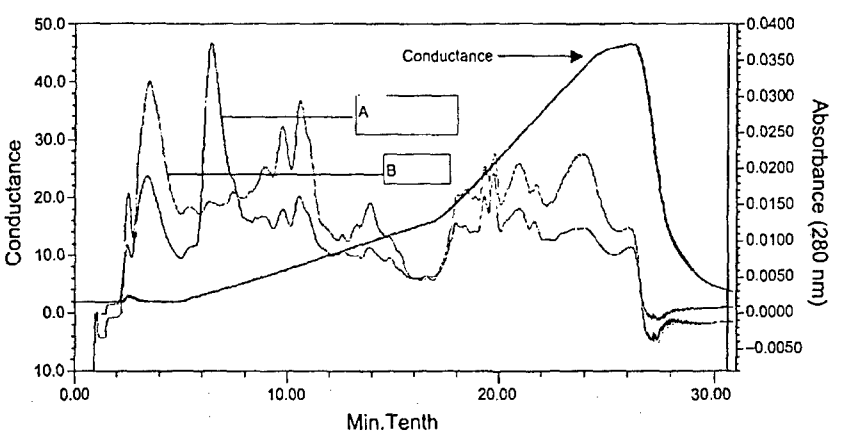

FIG. 5. Example of rat brain protein separation by strong ion exchange chromatography. Protein elution (30 min, 30 fractions) chromatograms (proteins are measured as absorbance at 280 nm). A = pooled rat cerebellum lysate and B = pooled rat cerebrum lysate. Chromatographic differences between A and B are detected readily throughout the elution. The third line is relative conductance measured over the NaCl gradient elution of the column.

neutral detergent (e.g., Triton X-100 or CHAPS). Importantly, minute proteins can be concentrated to enhance their detection. One weakness of this approach is that even with 2D liquid chromatographic (LC) separation, it is often not possible to separate all proteins individually. This problem will be addressed in the next section. In summary, when compared to 2DE, tandem LC is more compatible with membrane-bound proteins and can enrich proteins in minute quantity.

V. Protein Identification and Quantification Methods

The approach we are taking represents an effort to apply systematically the most contemporary proteomics approaches to identify and develop clinically useful biomarkers for brain injury from trauma, disease, or drugs. Classical methods of protein identification involving protein separation by gels or LC (see previous section), coupled with mass spectrometry, provide a potent and novel methodological array never before applied systematically to the detection of biomarkers of CNS injury, either alone or in combination. This integrated strategy makes possible both "targeted" analyses of known potential biomarker candidates as well as "untargeted" searches for novel proteins and protein fragments that could prove even more useful. Each of these technologies has advantages and disadvantages that together complement each other. Thus combining multiple proteomics strategies optimizes the opportunity for successful brain injury proteomics studies. Lastly, protein identification research also benefits from improved bioinformatics tools for protein database searching (Chakravarti *et al.*, 2003). Thus, importantly, research designs must incorporate appropriate bioinformatics support (see next Section).

A. Mass Spectrometry Approach

1. *MALDI-TOF MS*

The most classical method for protein identification in a given protein mixture is to perform 2DE, followed by in-gel digestion of the gel band(s) of interest with protein identification by mass spectrometry. The 2D-gel method has been improved by the use of IPG strips for the first dimension and the ability to label protein samples from control and experimental tissues with cyanine dyes (e.g., Cy3 and Cy5) that form co-migrating labeled samples that are compared in the same gel. Differentially expressed proteins are easily found, cut from the gel, digested in the gel spot with trypsin, and then identified by MALDI-TOF MS (matrix-assisted laser desorption ionization time-of-flight mass spectrometry) approach (Bienvenut *et al.*, 2002). It is important to understand that

MALDI-TOF MS identifies peptides based on the accurate determination of peptide masses. Because each amino acid has a unique mass, any given peptide composed of a unique amino acid sequence will have a unique mass. However, this method of protein identification is not infallible. Peptides can have identical amino acid composition but with a different order, or more often peptides of similar length will have mass-to-charge values that are slightly, but indistinguishably, different from one another within the mass accuracy and resolution limits of the instrumentation. Thus it is common practice to use at least four to nine peptide fragments to positively identify a protein, which can be difficult with complex mixtures. In addition, any significant post-translational modifications that will change the mass-to-charge (m/z) value of multiple peptides will make protein identification extremely difficult (Table II).

By using 2D-gel separation, this method is useful for distinguishing proteins that are either up-regulated or down-regulated because of to injury, but it is suboptimal for finding very basic, very acidic, or hydrophobic proteins, and the identification of smaller peptides can be difficult because of chemical noise from matrix ions. Complementary to this method are direct MS procedures that capture the entire range of proteins and peptides but may not distinguish proteins that are post-translationally modified, and the maximal protein size is limited to approximately 25–30 kDa (kilodaltons). A modified MALDI approach, called surface-enhanced laser desorption ionization (SELDI) (invented by Ciphergen, Fremont, CA), combines an affinity matrix-based protein separation phase with the TOF MS-based protein mass determination (also called Protein Chips) (Wiesner, 2004).

2. *LC-MS/MS Approach*

Protein separations strategies including 1D- and 2D-LC techniques (Adkins *et al.*, 2002) and gel separations are commonly used to resolve complex protein mixtures. Subsequent LC fractions or gel bands are processed by in-solution or in-gel digestion (most often with trypsin) to form peptides small enough to be effectively measured by MS. Complex peptide mixtures of protein digests are typically separated by reverse-phase chromatography placed on-line with electrospray ionization mass spectrometry (ESI MS), which not only resolves peptides from one another but also concentrates them, providing greater sensitivity. LC-MS is most often performed on high-powered tandem mass spectrometers, including the quadrupole ion-traps (QIT), quadrupole time-of-flight (QTOF), and Fourier transform ion cyclotron resonance (FT-ICR) mass spectrometers. Tandem mass spectrometry (MS/MS) allows the advantage of providing peptide sequence information in addition to the parent peptide mass (Gygi *et al.*, 2000). (Figs. 6 and 7). In brief, ions of the peptide of interest are isolated (first stage of mass spectrometry) then fragment along the peptide backbone by colliding with neutrals. Pairs of b- and y-daughter ions, formed by fragmentation from the n- or c-terminal side of each residue, respectively, will predominantly be generated.

Table II
ATTRIBUTES OF VARIOUS PROTEIN IDENTIFICATION APPROACHES

Protein identification method	Strengths	Weaknesses
MALDI-TOF MS	-Can analyze both proteins and peptides	-Ion suppression with complex samples (no peptide separations)
	-High mass accuracy ± 0.01%	
	-Resolution 50 ppm	-Does not provide sequence information
	-Protein ID by mass mapping of peptides from tryptic digests	-Requires detection of multiple peptides for protein identification
	-Sensitive to 50 fmol routine	
	-Rapid analysis for high throughput	
	-Preserves sample for later analysis	
LC-MS/MS	-Provides peptide sequence for protein ID—less reliant on mass accuracy	-Slow sample analysis due to long chromatograms
	-Can reliably identify protein with 1 to 2 peptides	-Consumes entire sample loaded
	-Sensitive in the amol range	-Greater complexity of nano-LC requires dedicated operator
	-Provides precise/reproducible quantitation	
	-Routine analysis of multiprotein digests	
Antibody panels/arrays	-Easy protein ID decoding	-Non exhaustive
	-Easy confirmation	-Uneven sensitivity
	-Can potentially detect PTM	
	-Sensitive to high fmol range	

The b- and y-daughter ions are then mass analyzed to form a daughter ion spectrum (second stage of mass spectrometry). Using MS/MS information, the peptide sequence can be reconstructed, which can be performed rapidly with available bioinformatics software (see Table II). LC-MS/MS systems work extremely well for protein identification by coupling the generated mass and sequence information with database searches, and the technique is sensitive enough to identify pM levels of proteins present in complex mixtures such as tissue lysates.

B. Protein and Peptide Quantification by MS

There are currently no less than half a dozen MS-based protein/peptide quantification methods, which were reviewed recently (Denslow, 2003). We will focus on two prominent quantification methods that are applicable to TBI proteomics.

1. *ICAT*

Isotope-coded affinity tags (ICAT) are a direct chromatographic approach to evaluate differential expression (Gygi *et al.*, 1999). ICAT reagent pairs are cysteine-binding tags that differ in molecular weight by use of hydrogen or carbon isotopes. These reagents are used to differentially label two protein samples, which are then mixed together and digested into peptides. Cysteine-containing fragments labeled with the tags can then be selectively isolated and analyzed by LC-MS/MS with differential expression determined from the peak height ratio of the tagged peptides. MS/MS data on the peptides is then searched against a protein database, providing the identity of the differentially expressed proteins (Peng *et al.*, 2003; Yates *et al.*, 1999).

2. *AQUA*

Another innovative method to quantify differential expression is through the use of *A*bsolute *qua*ntitation (AQUA) probes (Gerber *et al.*, 2003). Unlike ICAT, which can be used to tag any cysteine-containing protein, AQUA is applicable

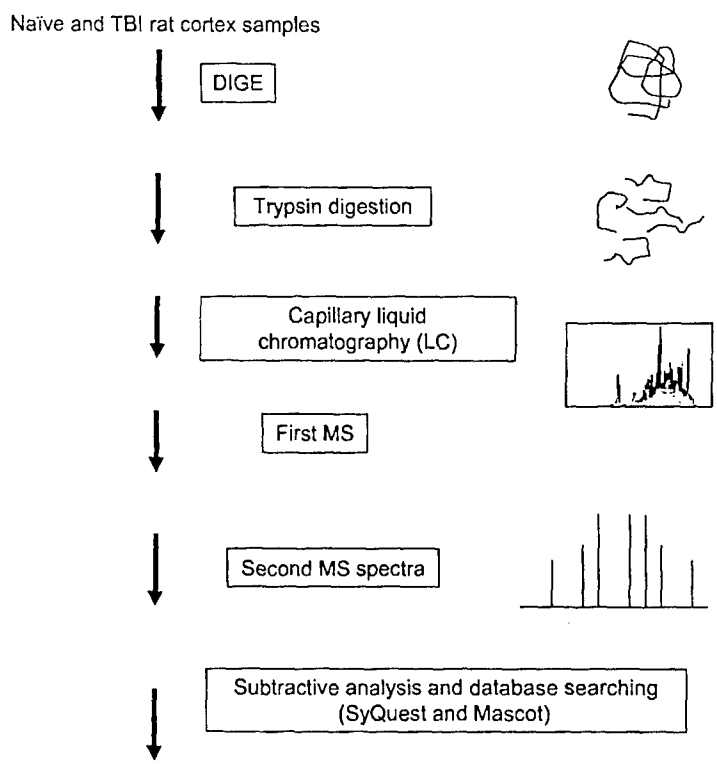

FIG. 6. Schematic sample flow of protein separation/protein identification by LC-MS/MS. See text for details.

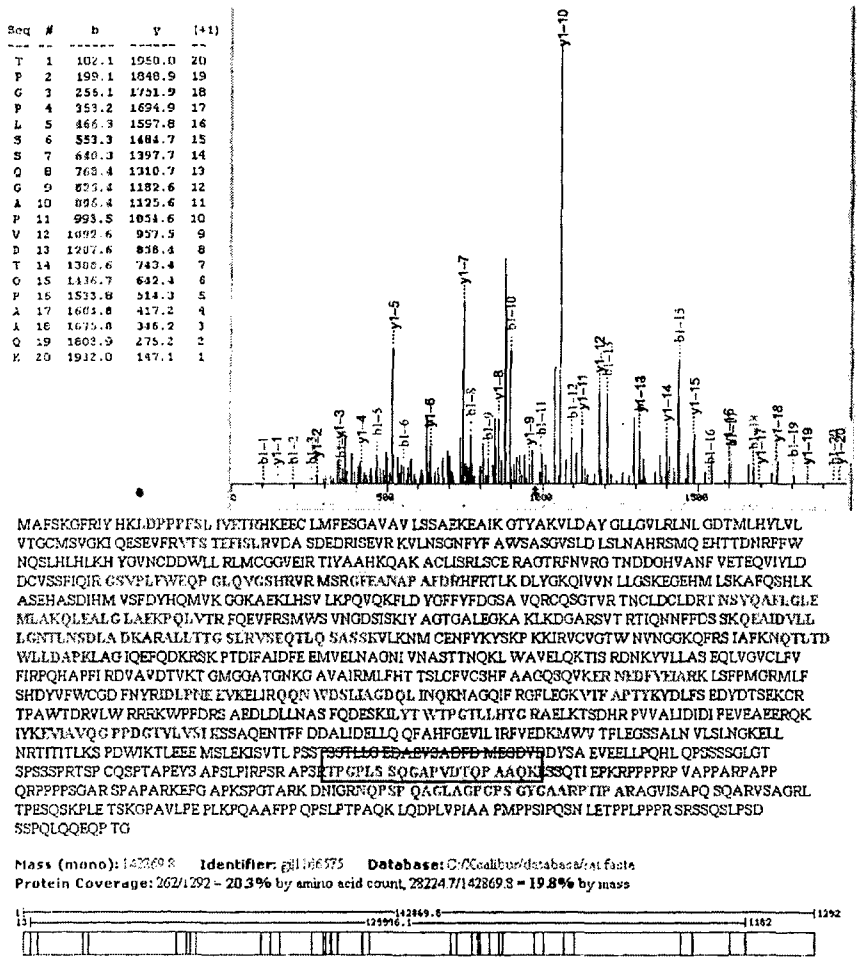

MAFSKGFRIV HKLDPPPFSL IVETRHKEEC LMFESGAVAV LSSAEKEAIK GTYAKVLDAY GLLGVLRLNL GDTMLHVLVL VTGCMSVGKI QESEVFRVTS TEFISLRVDA SDEDRISEVR KVLNSGNFYF AWSASGVSLD LSLNAHRSMQ EHTTDNRFFW NQSLHLHLKH YGVNCDDWLL RLMCGGVEIR TIVAAHKQAK ACLISRLSCE RAGTRFNVRG TNDDQHVANF VETEQVIYLD DCVSSFIQIR GSVPLFWEQP GLQVGSHRVR MSRGFEANAP AFDRHFRTLK DLYGKQIVVN LLGSKEGEHM LSKAFQSHLK ASEHASDIHM VSFDYHQMVK GGKAEKLHSV LKPQVQKFLD YGFFYFDGSA VQRCQSGTVR TNCLDCLDRT NSYQAFLGLE MLAKQLEALG LAEKPQLVTR FQEVFRSMWS VNGDSISKIY AGTGALEGKA KLKDGARSVT RTIQNNFFDS SKQEAIDVLL LGNTLNSDLA DKARALLTTG SLRVSEQTLQ SASSKVLKNM CENFVKYSKP KKIRVCVGTW NVNGGKQFRS IAFKNQTLTD WLLDAPKLAG IQEFQDKRSK PTDIFAIDFE EMVELNAGNI VNASTTNQKL WAVELQKTIS RDNKYVLLAS EQLVGVCLFV FIRPQHAPFI RDVAVDTVKT GMGGATGNKG AVAIRMLFHT TSLCFVCSHF AAGQSQVKER NEDFVEIARK LSFPMGRMLF SHDYVFWCGD FNYRIDLPNE EVKELIRQQN WDSLIAGDQL INQKNAGQIF RGFLEGKVIF APTYKYDLFS EDYDTSEKCR TPAWTDRVLW RRKKWPFDRS AEDLDLLNAS FQDESKILYT WTPGTLLHYG RAELKTSDHR PVVALIDIDI FEVEAEERQK IYKFVIAVQG FPDGTVLVSI ESSAQENTFF DDALIDELLQ QFAHFGEVIL IRFVEDKMWV TFLEGSSALN VLSLNGKELL NRTITITLKS PDWIKTLEEE MSLEKISVTL PSS~~TSTLLQ EDAEVSADFD MESDVD~~DYSA EVEELLPQHL QPSSSSGLGT SPSSSPRTSP CQSPTAPEV3 APSLPIRPSR APSETTPGPLS SQGAPVDTQP AAQKSSSQTI EPKRPPPPRP VAPPARPAPP QRPPPPSGAR SPAPARKEFG APKSPGTARK DNIGRNQPSF QAGLAGFGPS GYGAARPTIP ARAGVISAPQ SQARVSAGRL TPESQSKPLE TSKGPAVLPE PLKPQAAFPP QPSLPTPAQK LQDPLVPIAA PMPPSIPQSN LETPPLPPPR SRSSQSLPSD SSPQLQQEQP TG

Tryptic peptide ID: TPGPLSSQGAPVDTQPAAQK

FIG. 7. Example of LC-coupled MS-MS identification of a protein differentially expressed in rat brain hippocampus after TBI. A protein band (in an SDS-PAGE gel) that is uniquely expressed in TBI-48 hr was cut out and digested with trypsin, and a distinct tryptic peptide was sequenced based on MS-MS data (top panel) and identified to be originated from a brain protein synaptojanin, based on proteomics database searching results (lower panel).

only to target proteins. A peptide of the selected protein is synthesized with an isotopically labeled amino acid. A known amount of the probe is then added to the digested sample, which is analyzed by LC-MS/MS. Because the probe exactly matches the endogenous peptide of interest except for a modest mass difference,

the two will coelute with reverse-phase chromatography and have identical ionization properties, which minimizes variation in ion signal intensities. The tandem mass spectrometer then resolves the two peptides by the small m/z difference, allowing the ion signal of the two to be compared across the chromatographic peak. This method is very precise and can be applied to nearly any protein (with or without cysteine). By accurately measuring the amount of probe added, the absolute amount of a protein can also be determined, though relative protein amounts can also be determined without having to know the exact amount of probe added. In practice this method would follow a nontargeted differential method such as 2D-DIGE or ICAT, which produces a list of potential differentially expressed proteins. This method can then be used to quickly and precisely validate the differential expression of the targeted proteins across many samples. In comparison to the more traditional targeted quantitation of western analysis, AQUA is a much quicker way of validating differential expression than waiting for a specific antibody to be developed.

C. Antibody Panel/Array Approach

Protein identification is also assisted by the availability of various platforms of antibody arrays or panels (e.g., Zyomyx protein biochips, BD Powerblot, and BD antibody arrays) (Graslund *et al.*, 2002; James 2002; Kusnezow and Hoheisel, 2002; Moody, 2001). These methods all rely on antibody-based capturing of the protein of interest. The quantitation of the captured protein can be performed by prelabeling (including differential labeling) of the protein with fluorescent dye(s) (dye-labeling detection) such as BD antibody arrays, which is similar to the gene chip mRNA quantification method. Alternatively, quantitative detection can be accomplished with a second primary antibody specific to the same protein antigen (sandwich detection), which is similar to the sandwich enzyme-linked immunoabsorbant assay (sandwich ELISA) method (e.g., Zyomyx protein Biochips). A third option is the BD Powerblot, which is a high-throughput Western blotting (immunoblotting) system with two distinct protein samples that are differentially subjected to a set of five blots. Each blot has 39 usable lanes with the use of a manifold system. Each lane is developed with five to six different fluorophore-linked monoclonal antibodies (toward antigen with nonoverlapping molecular weight). With this method samples are probed with a total of 1000 monoclonal antibodies. We have actually conducted several Powerblot experiments with animal TBI studies. Figure 8 gives examples of differential protein changes observed in the rat hippocampus after TBI.

The major advantage of the antibody panel or array approach is that proteins of interest can be readily identified, because all antibodies used have known antigens and their positional assignment on the antibody chip or panel is

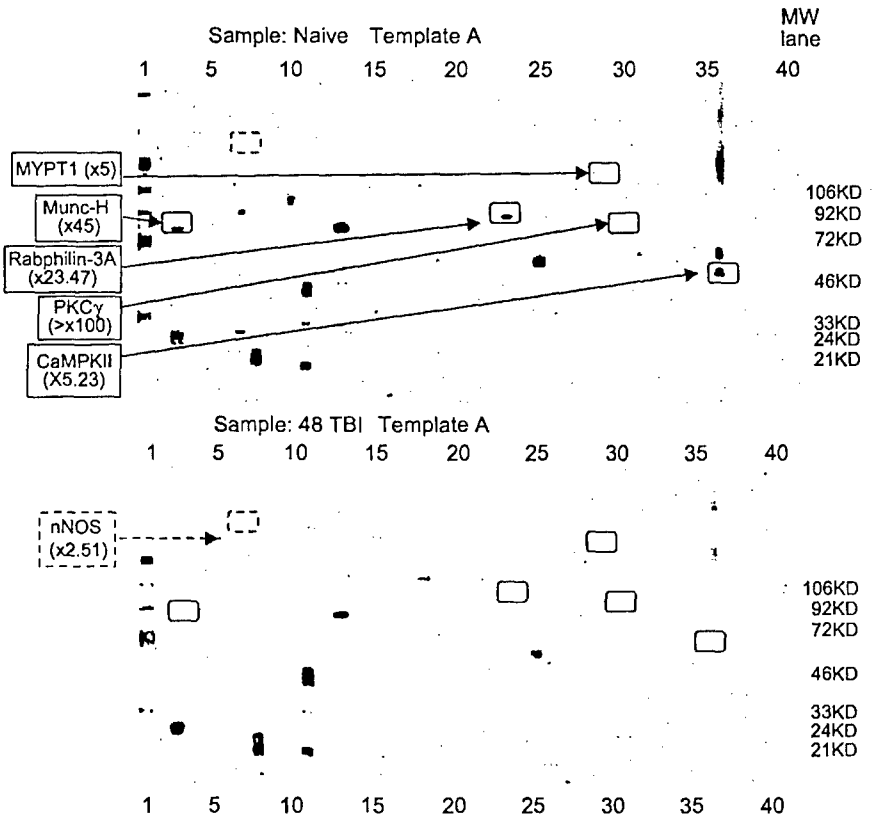

FIG. 8. Example of antibody panel approach-based by indentification of several protein differentially expressed in rat brain hippocampus after TBI. When comparing pooled naïve (top panel) and TBI-48 hr (bottom panel) hippocampal samples, five proteins (MYPT1, Munc-H, Rabphilin-3A, PKCdelta and CaMpKII; solid line) with reduced levels and one protein (nNOS; dotted line) with increased levels after TBI (average fold changes are shown in brackets) were identified.

known (See Table II). Also, quantification is already built into this antibody-based approach without any additional effort. On the other hand, the major disadvantage of this approach is that it is practically impossible to be exhaustive, because one would only have high fidelity antibodies to a subset of proteins. Furthermore, using antibodies collected from many different sources will likely result in uneven sensitivity. As in other immunoassay methods (e.g., Western blotting, immunostaining, or ELISA), it is a given that antibody array methods will likely detect nonspecifically bound proteins or other substances, affecting quantitation with high chemical noise and leading to false positive reactions. Despite its shortcoming,

the antibody array-based protein identification approach is a useful complement to the MS-based approach discussed previously.

VI. TBI Proteomics Bioinformatics

The current advance in databases and web portals has a natural convergence for knowledge and data sharing among local and remote scientists in any National Institutes of Health (NIH) domain. Large databases will be networked, whereas web portals will "federate and access" large databases. Such efforts need to be developed for the neuroproteomics domain. Neuroscience has one of the most complex information structures—concepts, data types, and algorithms—among scientific disciplines. Its richness in organisms, species, cells, genes, and proteins and their signal-transduction pathways provides many challenging issues for biological sciences, computational sciences, and information technology. The advances in neuroscience urgently need developing portal services to access databases for analyzing and managing the following information: sequences, structures, and functions arising from genes, proteins, and peptides (e.g., protein segments and biomarkers) (Chakravarti *et al.*, 2003).

In the bioinformatic phase, two interlinked mandates are: (1) to build a local user-friendly proteomics database, and (2), to develop interoperable proteomics tools and architecture for multiple data integration and to integrate user and public domain-based databases (Fig. 9). Data analysis applications should interoperable with database operations and portal access. The TBI proteomics core technologies will provide an integrative approach to genomic and proteomics information by developing a common portal architecture—the TBI proteomics portal at the University of Florida for data archiving and retrieval among core researchers and end users, and data linking and sharing to national and international neuroproteomics websites (e.g., Human Proteome Organization [HUPO, United States]) (Hanash, 2004) and Human Brain Proteome Project (HBPP, Germany) (Meyer *et al.*, 2003). Lastly, bioinformatic tools and software are also needed to enhance our ability to data mine as well as to study protein-protein interaction, protein pathways and networks, and complex post-translational modification such as protein phosphorylation, processing, cross-linking, and conjugation. This will help us develop knowledge bases about neuroproteomics functions and signal-transduction pathways in terms of dynamic objects and processes (Cattell, 1996; Mendes, 1993, 1997; Reddy, 1993; Somogyi, 1996). In addition, clinical information should be integrated with genomics and proteomics databases. The three major functions of the bioinformatic component of TBI proteomics studies can be further explained in the following section.

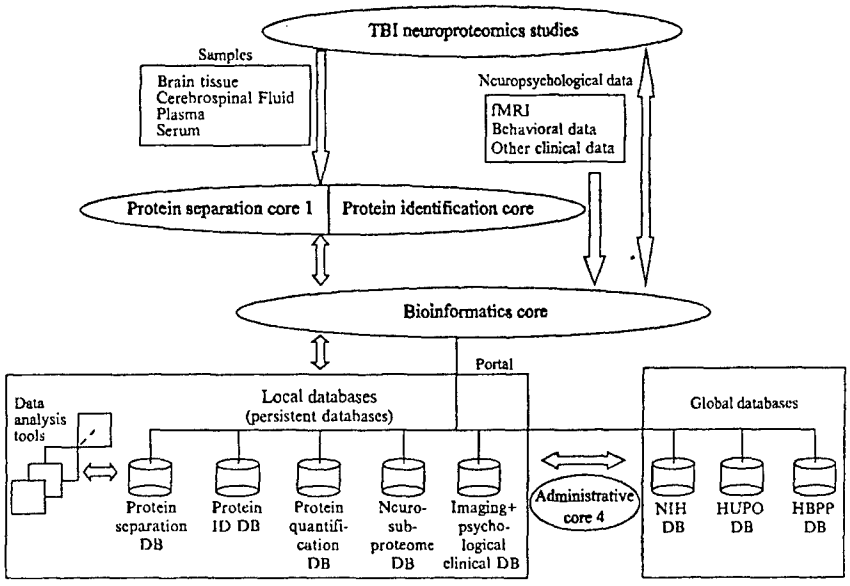

FIG. 9. Schematics of the central role of the bioinformatic core of TBI neuroproteomics studies. The bioinformatics core not only plays a key role in analyzing and archiving protein separation and identification data, but also plays a key role in integrating local TBI databases to global neuroproteome databases. See text for details.

A. PERMANENCE

Permanence is defined here as developing local databases for proteomics separation and identification and linking with national and international data sources. Local databases will include chromatograms, mass spectra, gel images, peptide and protein sequences, and functional magnetic resonance imaging (fMRI) images for control and TBI samples. Data modeling and semantics will be developed by proteomics and computer scientists together, so that semantic equivalence of search attributes and semantic associations can be established.

Our bioinformatics core is in the process of combining different data semantics and knowledge trees in separate genomics, proteomics, and clinical databases. A key requirement is the development of semantics (or ontology) of biological information, which is then captured in two components—semantic indexing and metainformation (i.e., "information about information")—of the intelligent search engines. A book by Chen (1998) has described these two important methods. Furthermore, semantic indexing and metainformation complement each other, reduce the complexity of neural taxonomy and classification, and correlate semantically the proteomics types and phenotypes (e.g., behavior in

drug abuse) at various (e.g., subcellular, cellular, and tissue or fluid) levels of neural activities. Dissemination to national and international data sources (e.g., HUPO and HBPP) will be consistently maintained through our intelligent search engines.

B. Interoperability

Interoperability is defined here as integrating existing data analysis tools with local databases. A proteomics problem-solving environment will be established to provide users with rapid access to TBI neuroproteome center databases and analysis tools. This will include existing tools for proteomics research and drug abuse research. The range of these tools is very broad, from peptide sequencing and protein identification to image processing for fMRI images and data analysis for neuropsychological tests and diagnosis.

A critical component of our bioinformatics core is to conduct research at widely distributed resources of data analysis and multiple levels of proteomic clinical and behavior information. The distributed collections of heterogeneous information resources will be large-scale. The intelligent search engines are beyond the capability of current web search engines and protocols. The TBI neuroproteome center distributed information retrieval component is a set of search engines that extend Emerge. Such an intelligent search engine should allow nomenclature, syntactic, and semantic differences in queries, data, and meta information. It should permit type, format, representation, and model differences as well in databases. In our TBI neuroproteome research, we have to compare information among proteomics and clinical data, such as chromatograms, mass spectra, gel images, peptide and protein sequences, and fMRI images. We will need a set of interoperable search engines to guide users finding information of various domains, formats, types, and levels of granularity (e.g., peptide, protein, cell, and system levels).

In addition, the interoperability of databases and analysis tools will establish a proteomics problem-solving environment. Thus users of the problem-solving environment will also be factored into the interoperability. Whatever users need—small versus large data sets, interactive versus batch computation—will require design and implementation of data and event services. For the current studies we intend to develop a neuroproteomics workbench to gather a collection of data analysis tools for neuroproteomics, as well as TBI neuroproteomics datasets:

1. Peptide sequencing and protein identification by MALDI-TOF MS and LC-MS/MS (Lu and Chen, 2003; Tabb *et al.*, 2002).
2. Protein peak patterns and single protein retention time from 1D or 2D liquid chromatograms.

3. Protein database searching algorithms such as SEQUEST (Yates, 1998).

The integration of databases with proteomic computational algorithms will be based on the object-oriented data modeling and data semantics discussed earlier. The Object Data Management Group (ODMG)-compliant data analysis and databases are highly relevant to the Common Component Architecture. In high-throughput computing, in terms of parallel or multithreaded objects, components (data and algorithms alike) may be distributed over a wide area grid of resources and distributed services.

C. Data Mining

Our neuroproteomics initiative has placed significant effort in new data mining and analysis tools for differential protein expression, protein network and modification analysis, and validation. A unique data-mining workbench will be created to explore protein network and pathways underlying the pathobiology of TBI from a neuroproteomics perspective. Novel data-mining tools will include a differential analysis tool for research on proteins and protein fragments involved in TBI and construction of cognitive maps. Furthermore, the cognitive maps will be used for TBI-induced differential neuroproteome validation and possible brain injury diagnosis.

1. *Creating Cognitive Maps for TBI-Induced Differential Proteome*

New data mining tools for TBI-induced differential proteome analysis and validation are being developed at our center. There are three major zones of neuroproteomics information: (1) pathophysiological stasis (including TBI, other CNS injuries such as ischemic stroke, aging, environmental toxin or substance-abuse induced brain injury, and neurodegenerative diseases such as Alzheimer's or Parkinson's), (2) neuroproteome stasis (pathology-mediated differential protein expression, protein synthesis and metabolism, alternative mRNA splicing and RNA editing, protein-protein interaction, enzymatic activity, or protein functions), post-translational modifications (e.g., protein cross-linking, acetylation, glycosylation protein proteolysis and processing, phosphorylation), and protein-protein interaction and networks and signal-transduction pathways, and (3) sources of neuroproteomics data (Fig. 10). These sources include brain tissue (from different areas or anatomical regions of the brain, such as hippocampus and cerebral cortex), biological fluids such as CSF, and blood samples (including plasma and serum) in which brain proteins stasis might be reflected upon via diffusion-based equilibrium or blood-brain barrier compromise (e.g., from brain to CSF to blood).

Collection of data from these three components will enable the construction of multiple cognitive maps (Axelrod, 1976; Kohn and Letzkus, 1983; Kosko,

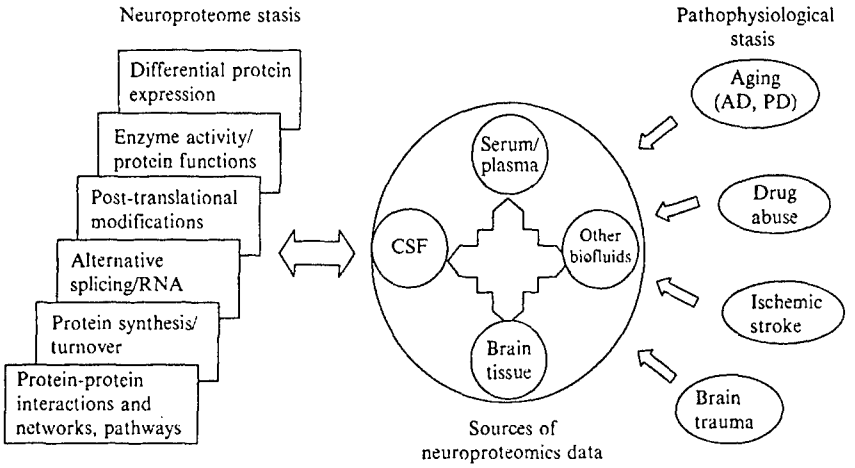

FIG. 10. Putative cognitive maps for the brain injury neuroproteome. The brain injury cognitive maps encompass three major areas (pathophysiological stasis, neuroproteome stasis, and sources of neuroproteomic data).

1986; Shi *et al.*, 2002; Zhang *et al.*, 1989). For instance, cognitive maps will be constructed for the TBI-induced differential proteome, such as the one shown in Fig. 9 for the brain injury neuroproteome. Automated reasoning and knowledge discovery algorithms (Chen, 1986, 1987; Chen and Markowitz, 1995, 1988, 2000a; Kitano, 2000) will distill the information and present the knowledge gained from a systems biology perspective. Thus cognitive maps will enable the brain trauma researchers to gain a greater understanding of the entire TBI-induced differential neuroproteome and hopefully the mechanistic protein-pathways of TBI.

2. *Using Cognitive Maps for TBI-induced Differential Neuroproteome Validation*

A statistical analysis tool is also being developed for TBI-induced differential neuroproteome validation and possible TBI protein-pathways elucidation. For example, up- or down-regulation of multiple proteins and protein fragments in control and injured samples will be quantified by ICAT, AQUA, or ELISA to validate differential TBI neuroproteome. Linear discriminant analysis (LDA) will be used to calculate the probability of a correct diagnosis given the number of injury-specific biomarkers measured the number of samples, etc. Thus statistical analysis tools are expected to provide an important component for all the TBI neuroproteomics research conducted at our neuroproteomics center.

VII. Prospective Utilities of TBI Proteomics Data

In summary, proteomics study of both human and rat traumatic brain injury, if approached systemically, is a very fruitful and powerful analytical technology. To obtain a comprehensive TBI neuroproteome dataset, it is important to integrate multiple protein separation and protein identification technologies. Equally important is the optimization of individual protein separation and identification methods. The bioinformatic platform then becomes the critical adhesive component by serving two purposes: (1) integrating all proteomics datasets and other relevant biological or clinical information, and (2) inferring and elucidating the protein-based pathways and biochemical mechanisms underlying the pathobiology of TBI and identifying and validating biomarkers for the diagnosis and monitoring of TBI (Goldknopf *et al.*, 2003). Ultimately, if we are to be successful, the TBI proteomics approach outlined here must be further integrated with genomics, cytomics, as well as systems biology approaches (Kitano, 2002a,b).

References

Adkins, J. N., Varnum, S. M., Auberry, K. J., Moore, R. J., Angell, N. H., Smith, R. D., Springer, D. L., and Pounds, J. G. (2002). Toward a human blood serum proteome: Analysis by multidimensional separation coupled with mass spectrometry. *Mol. Cell Proteomics* **1,** 947–955.

Aebersold, R., and Watts, J. D. (2002). The need for national centers for proteomics. *Nature Biotech.* **20**(7), 651.

Appel, R. D., Bairoch, A., and Hochstrasser, D. F. (1999). 2-D databases on the World Wide Web in methods in molecular biology. *In* "2-D Proteome Analysis Protocols" (A. J. Link, Ed.), vol. 112, pp. 383–391. Humana Press, Totowa, N.J.

Axelrod, R. (1976). "Structure of Decision." Princeton University Press, Princeton, NJ.

Bienvenut, W. V., Deon, C., Pasquarello, C., Campbell, J. M., Sanchez, J. C., Vestal, M. L., and Hochstrasser, D. F. (2002). Matrix-assisted laser desorption/ionization-tandem mass spectrometry with high resolution and sensitivity for identification and characterization of proteins. *Proteomics* **2,** 868–876.

Bjellqvist, B., Ek, K., Righetti, P. G., Gianazza, E., Gorg, A., and Westermeier, R. (1982). Isoelectric focusing in immobilized pH gradients: Principle, methodology and some applications. *J. Biochem. Biophys. Methods* **6,** 317–339.

Boguslavsky, J. (2003). Resolving the proteome by relying on 2DE methods. *Drug Discovery Develop.* **6**(7), 57–60.

Cattell, R. G. G. (Ed.) (1996). "The Object Database Standard: ODMG-93." Morgan Kaufmann, San Mateo, CA.

Chakravarti, D. N., Chakrarti, B., and Moutsatsos, I. (2003). Informatic tools for proteome profiling. High throughput proteomics; protein arrays. *BioTechniques* **3**(Suppl.), 4–15.

Chen, S. (1988). Knowledge acquisition on neural networks, uncertainty and intelligent systems. *In* "Lecture Notes in Computer Science" (B. Bouchon, L. Saitta, and R. R. Yager, Eds.), vol. 313, pp. 281–289. Springer-Verlag.

Chen, I. A., and Markowitz, V. M. (1995). An overview of the object protocol model (OPM) and the OPM data management tools. *Information Systems* **20,** 393–418.

Chen, S., (1986). Some extensions of probabilistic logic, Proc. AAAI Workshop on Uncertainty in Artificial Intelligence, Philadelphia, August 8–10, 1986, pp. 43–48, an extended version appeared in "Uncertainty in Artificial Intelligence," vol. 2, (L. N. Kanal, and J. F. Lemmer Eds.), North-Holland, Amsterdam, Holland.

Chen, S. (1987). Automated reasoning on neural networks: A probabilistic approach. IEEE First International Conference on Neural Networks, San Diego, June 21-24, 1987.

Chen, S. (2000a). Knowledge discovery of gene functions and metabolic pathways. IEEE BioInformatic and Biomedical Engineering Conference, Washington, November 2000.

Chen, S. (1998). "Digital Libraries: The Life Cycle of Information." BE Publisher, Columbus, OH.

Davidsson, P., Westman-Brinkmalm, A., Nilsson, C. L., Lindbjer, M., Paulson, L., Andreasen, N., Sjogren, M., and Blennow, K. (2002). Proteome analysis of cerebrospinal fluid proteins in Alzheimer patients. *Neuroreport* **13**(5), 611–615.

Denslow, N. D., Michel, M. E., Temple, M. D., Hsu, C., Saatman, K., and Hayes, R. L. (2003). Application of proteomics technology to the field of neurotrauma. *J. Neurotrauma* **20,** 401–407.

Derra, S. (2003). Lab-on-a-chip technologies emerging from infancy. *Drug Disc. Develop.* **6**(5), 40 45.

Dixon, C. E., Clifton, G. L., Lighthall, J. W., Yaghmai, A. A., and Hayes, R. L. (1991). A controlled cortical impact model of traumatic brain injury in the rat. *J. Neurosci. Methods* **39**(3), 253–262.

Fang, Z., Polacco, M., Chen, S., Schroeder, S., Hancock, D., Sanchez, H., and Coe, E. (2003). cMap: The comparative genetic map viewer. *Bioinformatics* **19,** 416–417.

Finnie, J. (2001). Animal models of traumatic brain injury: A review. *Aust. Vet. J.* **79**(9), 628–633.

Fountoulakis, M., Hardmaier, R., Schuller, E., and Lubec, G. (2000). Differences in protein level between neonatal and adult brain. *Electrophoresis* **21**(3), 673–678.

Fountoulakis, M., Schuller, E., Hardmeier, R., Berndt, P., and Lubec, G. (1999). Rat brain proteins: Two-dimensional protein database and variations in the expression level. *Electrophoresis* **20**(18), 3572–3579.

Gerber, S. A., Rush, J., Stemman, O., Kirschner, M. W., and Gygi, S. P. (2003). Absolute quantification of proteins and phosphoproteins from cell lysates by tandem MS. *Proc. Natl. Acad. Sci. USA* **100,** 6940–6945.

Goldknopf, I., Park, H. R., and Kuerer, H. M. (2003). Merging diagnostics with therapeutic proteomics. *IVD Technology* **9**(1), 1 6.

Gorg, A., Postel, W., and Gunther, S. (1988). The current state of two-dimensional electrophoresis with immobilized pH gradients. *Electrophoresis* **9,** 531 -546.

Grant, S. G., and Blackstock, W. P. (2001). Proteomics in neuroscience: From protein to network. *J. Neurosci.* **21**(21), 8315 8318.

Grant, S. G. N., and Husi, H. (2001). Proteomics of multiprotein complexes: Answering fundamental questions in neuroscience. *Trends Biotechnol.* (Suppl. 10), S49–S54.

Graslund, S., Falk, R., Brundell, E., Hoog, C., and Stahl, S. (2002). A high-stringency proteomics concept aimed for generation of antibodies specific for cDNA-encoded proteins. *Biotechnol. Appl. Biochem.* **35**(Pt 2), 75–82.

Gygi, S. P., Rist, B., Gerber, S. A., Turecek, F., Gelb, M. H., and Aebersold, R. (1999). Quantitative analysis of complex protein mixtures using isotope-coded affinity tags. *Nat. Biotechnol.* **17,** 994–999.

Gygi, S. P., *et al.* (2000). Mass spectrometry and proteomics. *Analytical Techniques* **4,** 489–494.

Hanash, S. (2004). HUPO initiatives relevant to clinical proteomics. *Mol. Cell Proteomics.* 298–301.

Hanash, S. M. (2003). Disease proteomics. *Nature* **422**(6928), 226–232.

Hayes, R. L., Newcomb, J. K., Pike, B. R., and DeFord, S. M. (2001). Contributions of calpains and caspases to cell death following traumatic brain injury. *In* "Head Trauma: Basic, Preclinical and Clinical Aspects" (L. P. Miller and R. L. Hayes, Eds.), vol. 10, pp. 219–237. Wiley & Sons, New York, NY.

Hochstrasser, D. F., Sanchez, J. C., and Appel, R. D. (2002). Proteomics and its trends facing nature's complexity. *Proteomics* **2**(7), 807–812.

James, P. (2002). Chips for proteomics; a new tool or just hype? High throughput proteomics; protein arrays *BioTechniques* **12**(Suppl.), 14–23.

Janssen, D. (2003). Major approaches to identifying key PTMs. *Genomics and Proteomics* **3**(1), 38–41.

Jungblut, P., Thiede, B., Zimny-Arndt, U., Muller, E. C., Scheler, C., and Wittmann-Liebold, B. (1996). Resolution power of two-dimensional electrophoresis and identification of proteins from gels. *Electrophoresis* **17,** 839–847.

Kitano, H. (2000). Perspectives on systems biology, "New Generation Computing," Vol. 18, No. 3. Ohm-sha, Springer-Verlag, New York Inc.

Kitano, H. (2002a). Systems biology: A brief overview. *Science* **295**(5560), 1662–1664.

Kitano, H. (2002b). Computational systems biology. *Nature* **420**(6912), 206–210 (review).

Kohn, M. C., and Letzkus, W. J. (1983). A graph theoretical analysis of metabolic regulation. *J. Theoretical Biology* **100,** 293–304.

Kosko, B. (1986). Fuzzy cognitive maps. *Int. J. Man-Machine Studies* **24,** 65–75.

Kusnezow, W., and Hoheisel, J. D. (2002). Antibody microarrays: Promises and problems. High throughput proteomics: protein arrays. *Bio Tech.* **12**(Suppl.), 14–23.

Lemkin, P. F. (1997). Comparing two-dimensional electrophoretic gel images across the Internet. *Electrophoresis* **18,** 2759–2773.

Lu, B., and Chen, T. (2003). A suffix tree approach to the interpretation of tandem mass spectra: Applications to peptides of non-specific digestion and post-translational modifications. *Bioinformatics* **19**(Suppl. 2), II113–II121.

Lubec, G., Krapfenbauer, K., and Fountoulakis, M. (2003). Proteomics in brain research: Potentials and limitations. *Prog. Neurobiol.* **69**(3), 193–211.

Mendes, P. (1993). GEPASI: A software package for modelling the dynamics, steady, states and control of biochemical and other systems. *Comput. Appli. Biosci.* **9,** 563–571.

Mendes, P. (1997). Biochemistry by numbers: Simulation of biochemical pathways with Gepasi 3. *Trends Biochem. Sci.* **22,** 361–363.

Meyer, H. E., Klose, J., and Hamacher, M. (2003). HBPP and the pursuit of standardisation. *Lancet Neurol.* **2**(11), 657–658.

Moody, M. D. (2001). Array-based ELISAs for high-throughput analysis of human cytokines. *Bio Tech.* **31,** 186–194.

Patton, W. F. (2002). Detection technologies in proteome analysis. *J. Chromatogr. B. Analyt. Technol. Biomed. Life Sci.* **771**(1–2), 3–31.

Peng, J., Elias, J. E., Thoreen, C. C., Licklider, L. J., and Gygi, S. P. (2003). Evaluation of multidimensional chromatography coupled with tandem mass spectrometry (LC/LC-MS/MS) for large scale protein analysis: The yeast proteome. *J. Proteome Res.* **2,** 43–50.

Peng, J., and Gygi, S. P. (2001). Proteomics: The move to mixtures. *J. Mass. Spectrom.* **36**(10), 1083–1091.

Pike, B. R., Flint, J., Dave, J. R., Lu, X.-C. M., Wang, K. K. W., Tortella, F. C., and Hayes, R. L. (2004). Accumulation of calpain and caspase-3 proteolytic fragments of brain-derived all-spectrin in CSF after middle cerebral artery occlusion in rats. *J. Cereb. Blood Flow Metab.* **24**(1), 98–106.

Pike, B. R., Flint, J., Dutta, S., Johnson, E., Wang, K. K. W., and Hayes, R. L. (2001). Accumulation of non-erythroid all-spectrin and calpain-cleaved all-spectrin breakdown products in cerebrospinal fluid after traumatic brain injury in rats. *J. Neurochem.* **78,** 1297–1306.

Raabe, A., Grolms, C., and Seifert, V. (1999). Serum markers of brain damage and outcome prediction in patients after severe head injury. *Br. J. Neurosurg.* **13,** 56–59.

Raghupathi, R., Graham, D. I., and McIntosh, T. K. (2000). Apoptosis after traumatic brain injury. *J. Neurotrauma* **17**(10), 927–938.

Reddy, V. N., Mavrovouniotis, M. L., and Liebman, M. N. (1993). Petri net representations in metabolic pathways. *Proc. ISMB* **1,** 328–336.

Reyes, D. R., Iossifidis, D., Auroux, P. A., and Manz, A. (2002). Micro total analysis systems. I. Introduction, theory, and technology. *Anal. Chem.* **74**(12), 2623–2636.

Romner, B., Ingebrigtsen, T., Kongstad, P., and Borgesen, S. E. (2000). Traumatic brain damage: Serum S-100 protein measurements related to neuroradiological findings. *J. Neurotrauma* **17**(8), 641–647.

Schäfer, H., Marcus, K., Sickmann, A., Herrmann, M., Klose, J., and Meyer, H. E. (2003). Identification of phosphorylation and acetylation sites in alphaA-crystallin of the eye lens (mus musculus) after two-dimensional gel electrophoresis. *Anal. Bioanal. Chem.* **376**(7), 966–972.

Schwartz, D. C., and Hochstrasser, M. (2003). A superfamily of protein tags: Ubiquitin, SUMO and related modifiers. *Trends Biochem. Sci.* **28**(6), 321–328.

Service, R. F. (2001). Gold rush—High-speed biologists search for gold in proteins. *Science* **294**(5549), 2074–2077.

Shi, H., Rodriguez, O., Shang, Y., and Chen, S. (2002). Integrating adaptive and intelligent techniques into a web-based environment for active learning. *In* "Intelligent Systems: Technology and Applications" (C. T. Leondes, Ed.), vol. 4, pp. 229–260. CRC Press, Boca Raton, Fla.

Smith, R. D. (2000). Probing proteomes—seeing the whole picture? *Nat. BioTech.* **18,** 1041–1042.

Somogyi, R., and Sniegoski, C. A. (1996). Modeling the complexity of genetic networks: Understanding multigenic and pleiotropic regulation. *Complexity* **1,** 45–63.

Tabb, D. L., McDonald, W. H., and Yates, J. R. (2002). DTASelect and contrast: Tools for assembling and comparing protein identifications from shotgun proteomics. *J. Proteome Res.* **1,** 21–26.

Unlu, M., Morgan, M. E., and Minden, J. S. (1997). Difference gel electrophoresis: A single gel method for detecting changes in protein extracts. *Electrophoresis* **18**(11), 2071–2077.

Wiesner, A. (2004). Detection of tumor markers with ProteinChip technology. *Curr. Pharm. Biotechnol.* **5**(1), 45–67.

Yan, J. X., Devenish, A. T., Wait, R., Stone, T., Lewis, S., and Fowler, S. (2002). Fluorescence two-dimensional difference gel electrophoresis and mass spectrometry based proteomic analysis of *Escherichia coli*. *Proteomics* **2**(12), 1682–1698.

Yates, J. R., III, Carmack, E., Hays, L., Link, A. J., and Eng, J. K. (1999). Automated protein identification using microcolumn liquid chromatography-tandem mass spectrometry. *In* "Methods in Molecular Biology" (A. J. Link, Ed.), vol. 112, pp. 553–569. Human Press, Totowa, N. J.

Yates, J. R., Morgan, S. F., Gatlin, C. L., Griffin, P. R., and Eng, J. K. (1998). Method to compare collision-induced dissociation spectra of peptides: Potential for library searching and subtractive analysis. *Anal. Chem.* **70,** 3557–3565.

Zhang, W. R., Chen, S., and Bezdek, J. C. (1989). Pool2: A generic system for cognitive map development and decision analysis. *IEEE Trans. SMC* **19,** 31–39.

Rapid Discovery of Putative Protein Biomarkers of Traumatic Brain Injury by SDS-PAGE-Capillary Liquid Chromatography-Tandem Mass Spectrometry

William E Haskins[1,2,4,6] ; Firas H Kobeissy[1,2,3]; Regina A Wolper[1,2,4]; Andrew K Ottens[1,2,4]; Jason W Kitlen[2,4]; Scott H McClung[5]; Barbara E O'Steen[2,4]; Marjorie M Chow[5]; Jose A Pineda[2], Nancy D Denslow[1,5]; Ronald L Hayes[2,3,4]; Kevin KW Wang[1,2,3,4]

Center of Neuroproteomics and Biomarkers Research[1],
Center for Traumatic Brain Injury Studies[2],
Departments of Psychiatry[3] and Neuroscience[4],
Interdisciplinary Center of Biotechnology Research[5]
University of Florida, Gainesville, FL 32610, USA
Current affiliation: Sandia National Laboratory[6], Livermore, CA, 94551, USA

Corresponding author:
Kevin K.W. Wang,
kwang@psychiatry.ufl.edu
McKnight Brain Institute, L4-100F
University of Florida, (P.O. Box 100256)
100 S. Newell Drive
Gainesville, FL 32610, USA

ABSTRACT: We report the rapid discovery of putative protein biomarkers of traumatic brain injury (TBI) by SDS-PAGE-capillary liquid chromatography-tandem mass spectrometry (SDS-PAGE-Capillary LC-MS^2). Ipsilateral hippocampus (IH) samples were collected from naïve rats and rats subjected to controlled cortical impact (a rodent model of TBI). Protein database searching with 15,558 uninterpreted MS^2 spectra, collected in 3 days via data-dependent Capillary LC-MS^2 of pooled samples separated by SDS-PAGE, identified more than 306 unique proteins. Differential proteomic analysis revealed differences in protein sequence coverage for 170 mammalian proteins (57 proteins in naïve only, 74 protein in injured only, and 39 proteins in both), suggesting that some of these proteins are putative biomarkers of TBI. Confidence in our results was obtained by the presence of several known biomarkers of TBI, (including αII-spectrin, brain creatine kinase, and neuron-specific enolase) in our data set. Sequence-specific discovery of putative protein biomarkers (by data-dependent Capillary LC-MS^2) and preliminary validation of selected biomarkers (by targeted Capillary LC-MS^2), show that SDS-PAGE prior to *in vitro* proteolysis and Capillary LC-MS^2 is a promising strategy for the rapid discovery of putative protein biomarkers associated with a specific pathophysiological state (i.e., TBI) without *a priori* knowledge of the molecules involved.

KEYWORDS: Controlled Cortical Impact (CCI), Sodium Dodecyl Sulfate-Polyacrylamide Gel Electrophoresis (SDS-PAGE), Capillary Liquid Chromatography (Capillary LC), Tandem Mass Spectometry (MS^2), Traumatic Brain Injury (TBI), differential in-gel electrophoresis (DIGE)

INTRODUCTION

Traumatic brain injury (TBI) is defined as brain damage due to mechanical force applied to the head. TBI is a leading cause of death and disability among persons in the United States. Each year, an estimated 1.5 million Americans sustain TBI. As a result of these injuries, 50,000 people die, 230,000 people are hospitalized and survive, and an estimated 80,000-90,000 people experience the onset of long-term disability (Thurman et al, 1999). Direct and indirect costs of TBI totaled an estimated $56.3 billion in the U.S. in 1995 (Thurman, 2001). Thus, accurate diagnosis following TBI is crucial for appropriate clinical management of TBI patients and for reducing costs. Current assessment tools of TBI include computed tomography and magnetic resonance imaging. Despite the accuracy of these techniques, TBI survivors suffer long-term impairment due to late diagnosis and unguided clinical management. Therefore, increased interest in the discovery of biomarkers that are indicative of injury severity and anatomical localization has been realized in recent years.

Several laboratories have examined a number of biological molecules in cerebral spinal fluid (CSF) and blood from TBI patients in an effort to discover TBI-specific biomarkers (Pike, 2002; Varma, 2003; Zemlan, 2002; Berger, 2002; Raabe, 2003). For example, our laboratory reported the discovery of non-erythroid αII-spectrin and its protease-specific degradation products as biomarkers of TBI (Pike, 2002). However, a major limitation of most of the currently described biomarkers is a lack of TBI-specificity and a poor

understanding of the biochemical mechanisms of brain trauma. Thus, the discovery of novel protein biomarkers of TBI that serve as reliable indicators of injury severity would be highly beneficial for predicting outcome and managing patients (Denslow, 2003). Moreover, novel biomarkers of TBI, particularly neurodegenerative and neuroprotective proteins, provide insights on pathophysiology and may serve as therapeutic targets for various neurological diseases.

Rapid discovery of protein biomarkers in complex samples by state-of-the-art mass spectrometry methods, capable of identifying thousands of proteins in a single sample by protease-specific peptide sequences, is precluded by several limitations. "Shotgun" capillary liquid chromatography (Capillary LC)-tandem mass spectrometry (MS^2) methods (McDonald, 2002) require extended analysis times for each sample (days) and information about post-translational modifications (PTM's), particularly protein degradation, is often lost during *in vitro* proteolysis (e.g., trypsination). Liquid-phase protein separation (e.g., 2D-SDS-polyacrylamide gel electrophoresis (SDS-PAGE) and LC-LC prior to *in vitro* proteolysis and Capillary LC-MS^2, preserves more information about PTM's, but can require 10-100 fold more sample and even greater analysis times for complete characterization (weeks). Reproducible quantification, required for biomarker validation, and limited resources (e.g., mass spectrometer time) further compound these problems.

Recently, the large dynamic range and high quantum yield of cyanine dye-labeled proteins were combined with 2D gels in order to improve gel-to-gel reproducibility and reduce analysis time via sample multi-plexing (Gharbi, 2002; Leimgruber, 2002; Macdonald, 2001; Tonge, 2001). This technique, differential in-gel electrophoresis (DIGE), provides quantitative information complementary to isotope coded affinity tag (ICAT) - Capillary LC-MS^2 approaches (Gygi, 1999) while preserving more information about PTM's. DIGE also provides a reduction in analysis time because only gel spots with a significant difference in the ratio of their fluorescence signals need to be targeted for protein identification by mass spectrometry (Gharbi, 2002; Kernec, 2001; Shaw, 2003; Tonge, 2001; Yan, 2002). However, poorly resolved proteins elude identification, while well-resolved, multiply-modified, proteins produce redundant identifications. Given our emphasis on rapid analysis, rather than more comprehensive characterization, we selected the limited resolving power of SDS-PAGE as an effective means to reduce redundant identifications and accelerate the discovery of putative protein biomarkers.

In this report, we describe the combination of SDS-PAGE-capillary liquid chromatography-tandem mass spectrometry (SDS-PAGE-Capillary LC-MS^2) with differential proteomic analysis for the discovery of putative protein biomarkers of TBI in hippocampus tissue. Herein, protein database searching of uninterpreted MS^2 spectra, collected via data-dependent capillary LC-MS^2 of pooled cyanine dye-labeled samples separated by SDS-PAGE, was performed. We hypothesized that a subset of putative protein biomarkers of TBI, including some

with PTM's, would be rapidly revealed by comparing the protein sequence coverage of naïve and injured samples.

MATERIALS AND METHODS

Chemicals and reagents. The chemicals and reagents used are described elsewhere (Haskins, 2001). Tryptic digests were purchased from Michrom Bioresources (Auburn, CA) for use as quality control standards. Cyanine dye labeling reagents were purchased from Amersham Biosciences (Piscataway, NJ).

Controlled Cortical Impact. The controlled cortical impact (CCI) device used to model TBI in male Sprague-Dawley rats was described in detail elsewhere (Pike, 2002). Adult rats were anesthetized with 4% isoflurane in a carrier gas of 1:1 O_2/N_2O (4 min) followed by maintenance anesthesia of 2.5% isoflurane in the same carrier gas. Core body temperature was monitored continuously by a rectal thermistor probe and maintained at $37^\circ \pm 1^\circ C$ by placing an adjustable temperature controlled heating pad beneath the rats. Animals were mounted in a stereotactic frame in a prone position and secured by ear and incisor bars. A midline cranial incision was made, the soft tissues were reflected, and a unilateral (ipsilateral to site of impact) craniotomy (7 mm diameter) was performed adjacent to the central suture, midway between bregma and lambda. The dura mater was kept intact over the cortex. Brain trauma was produced by impacting the right cortex (ipsilateral cortex) with a 5 mm diameter aluminum impactor tip (housed in a pneumatic cylinder) at a velocity of 3.5 m/s with a 1.6 mm compression and 150 ms dwell time (compression duration). Velocity was

controlled by adjusting the pressure (compressed N_2) supplied to the pneumatic cylinder. Velocity and dwell time were measured by a linear velocity displacement transducer (Lucas Shaevitz™ model 500 HR, Detroit, MI) that produced an analogue signal that was recorded by a storage-trace oscilloscope (BK Precision, model 2522B, Placentia, CA). At 48 hours post-injury, the animals were anesthetized with 4% isoflurane in a carrier gas of 1:1 O_2/N_2O (4 min.) and subsequently sacrificed by decapitation. Hippocampal samples were rapidly dissected, washed with saline solution, snap-frozen in liquid nitrogen, and stored at -80°C until further processing. Naïve animals neither received a sham surgery, nor an impact injury. Appropriate pre- and post-injury management was maintained to insure compliance with guidelines set forth by the University of Florida Institutional Animal Care and Use Committee and the National Institutes of Health guidelines detailed in the Guide for the Care and use of Laboratory Animals.

Sample preparation. Hippocampal samples were homogenized in a glass tube with a Teflon dounce pestle in 15 volumes of ice-cold detergent-free buffer (50 mM Tris-HCl, pH 7.4, 1 mM EDTA, 2 mM EGTA, 0.33 M sucrose, 1 mM DTT) containing a broad-range protease inhibitor cocktail (Roche Molecular Biochemicals, #1-836-145) and sonicated. Samples were then centrifuged at 9000 g for 5 min at 4°C. The supernatant was stored at -80°C. The protein concentration of each sample was determined by DC protein assay (Biorad, Hercules, CA) with albumin standards. Proteins were diluted to 5 μg/μL in DIGE

lysis buffer containing a 1% protease inhibitor cocktail (P8340, Sigma, St. Louis, MO) to prevent proteolysis during labeling.

SDS-PAGE. The cyanine dye labeling reaction was performed with minimal labeling conditions (50 μg of protein at 5 μg/μL) per the manufacturer's instructions unless stated otherwise (Amersham, Piscataway, NJ). Labeled proteins from pooled and individual naïve control or injured samples were reduced with 5 mM DTT, alkylated with 55 mM iodoacetamide, and heated to 95°C for 2 minutes prior to separation with Tris-tricine SDS-PAGE gels (10-20% polyacrylamide, Invitrogen, Carlsbad, CA) at 4°C. Fluorescence imaging was performed with 1-second exposure times (ProExpress, PerkinElmer, Boston, MA). Alternatively, unlabeled proteins were separated with the same gel system and stained with Coomassie blue. In both cases, image analysis (ImageJ, NIH) was performed to target specific regions of the gel; 1.5 mm x 4 mm gel slices spanning the entire gel lane were excised and stored at -80°C for trypsinization.

***In vitro* proteolysis.** Excised gel bands were destained, reduced with 5 mM DTT and alkylated with 55 mM iodoacetamide prior to overnight digestion with 400 ng of trypsin (Trypsin gold, Promega, Madison, WI) in 100 mM NH_4HCO_3.

Preparation of capillary LC columns with integrated electrospray emitters. The preparation of capillary LC columns with integrated electrospray emitters is described elsewhere (Haskins, 2001); however, 5 cm of 3 μm C18

particles (Alltima C18, Alltech, Deerfield, IL) and 50 μm -i.d. capillary LC columns were used in this work.

Automated 2-pressure capillary LC-MS^2 system. The capillary LC-MS^2 system is described elsewhere (Haskins, 2001). The system utilizes 2 six-port valves to select the pump and flow path for preconcentration, desalting and separation/electrospray steps. During the preconcentration and desalting steps the high flow rate pump was selected without splitting of the sample in order to minimize the sample loading time. During the separation/electrospray step the low flow rate pump was selected with splitting of the gradient in order to maximize the separation and electrospray efficiency and to minimize the delay time of the gradient, respectively.

In this work, 4.5 μL from a 12 μL sample of tryptic peptides was transferred into a 2 μL sample loop with an autosampler and analyzed every 38 min by preconcentrating/desalting at 600 nL/min and separating/electrospraying at 60 nL/min. All measurements were made with the following capillary LC-MS^2 parameters, unless specified otherwise: preconcentration time = 3.3 min (2.0 μL), desalting time = 3.3 min (2.0 μL), separation/electrospray time = 30 min (10 min pump gradient from 5 to 45% mobile phase B; mobile phase A = 2% acetonitrile: 1% acetic acid; mobile phase B = 98% acetonitrile: 1% acetic acid), re-equilibration time = 1.4 min. The mass spectrometer was a QIT (LCQ-Deca XP+, ThermoFinnigan, San Jose, CA) with the following parameters, unless specified otherwise: automatic gain control (AGC) on, max AGC time = 300 msec, q =

0.25, isolation width = 3 *m/z*, normalized collision energy = 35%, activation time = 0.25 msec and the default number of microscans and target count values. Data-dependent MS/MS spectra (MS, 4 x MS/MS) were collected using a precursor ion window of *m/z* 400-1800 and a product ion window calculated for *z* = +2.

Differential proteomic analysis. Protein database searching (RefSeq 785,143 sequences (Pruitt, 2001) with uninterpreted MS^2 spectra and differential proteomic analysis of unmodified proteins were performed with Sequest (Yates, 1998) and DTASelect (Tabb, 2002), respectively. The default precursor and product ion tolerances of 1.5 and 0.0 were selected for Sequest, while only singly-, doubly-, and triply-charged tryptic peptide sequences with Xcorr > 1.8, 2.5, and 3.5 were considered significant for DTASelect. No molecular mass constraints were placed on protein identification by protein database searching. A TBI database containing unmodified peptide and protein sequences that were observed in naïve control only, injured only, or both conditions was constructed in-house (from the DTASelect files via Microsoft Access 2002) as a function of the SDS-PAGE gel position (gel slices were numbered 1-50 from high to low molecular mass). PTM's were investigated with Mascot (Perkins, 1999) using the same protein database as Sequest but with the recommended precursor and product ion tolerances of 2.0 and 0.8, respectively. PTM's were considered significant if the Mascot score indicated homology with greater than 95% probability.

RESULTS

SDS-PAGE-Capillary LC-MS^2. Naïve control and injured hippocampal protein samples were processed and labeled with Cy-3 (green) and Cy-5 (red) dye separately. Proteins from pooled and individual samples were separated side-by-side, and naïve control and injured samples were run on separate lanes (**Figure 1**). Our results show the consistency in protein loading, cyanine dye labeling, and separation efficiency. Alternatively, unlabeled proteins were separated with the same gel system and stained with Coomassie blue (data not shown). Fifty-1.5 mm x 4 mm gel slices spanning each gel lane for the pooled (naïve control or injured) samples were excised, trypsinized, and subjected to data-dependent capillary LC-MS^2 (boxed regions in **Figure 1**). We collected 15,558 uninterpreted MS^2 spectra in 3 days for pooled samples separated by SDS-PAGE. Protein database searching identified more than 306 unique proteins. Overall, we obtained 156 ± 60 MS^2 spectra per gel slice and 1 to 3 tryptic peptide sequences per protein. No effects from cyanine-dye labeling on protein identification were observed. **Figure 2** shows the correlation between the database-derived molecular mass ($M_r$calc) and SDS-PAGE-predicted molecular mass ($M_r$obs). The migration of proteins in the SDS-PAGE gel inversely correlates with $M_r$calc for unmodified proteins identified by capillary LC-MS^2 and database searching (solid line), as expected. Accordingly, $M_r$obs directly correlates with $M_r$calc. In addition, protein sequence coverage shows an inverse correlation with $M_r$calc (dashed line). That is, the higher the molecular mass of the protein, the less sequence coverage is obtained.

Differential proteomic analysis of the gel slices (high to low $M_r$obs) revealed differences in protein sequence coverage for 170 mammalian proteins (57 in naïve only, 74 in injured only, and 39 in both as listed in **Table 1**.) Inspection of the proteins falling into each of the three categories of protein markers shows that several well-studied proteins involved in TBI were observed in both naïve control and injured samples including: brain creatine kinase (CKB), αII-spectrin, neuron-specific enolase (NSE), α-synuclein (α-Syn), microtubule associated protein 2a and 2b (MAP2), neurofilament (NF), proteolipid protein (PLP), and myelin basic protein (MBP).

Classification of putative protein biomarkers of TBI. Stratification of the putative protein biomarkers discovered in this work, based on function and distribution, suggests several classes of proteins that are of interest (**Figures 3 and 4**). Careful examination of the fraction of proteins from each class that were observed in naïve control only, injured only, and both naïve control and injured samples highlights the most promising classes for biomarkers of TBI. For example, **Figure 3** shows that 10% of the putative biomarkers observed only in injured samples were neuronal proteins including: PLP, Syn (α and β), NSE, NF (light and heavy), synapsin (I and II), vesicle associated membrane protein 1, and apolipoprotein E. Other promising classes of biomarkers observed only in injured samples include heat shock proteins (e.g., chaperonin 10) and kinases (e.g., calcium/calmodulin protein kinase II). These observations are reflected by peaks in the line plot shown in **Figure 4**. Thus, neuronal proteins, heat shock proteins, and kinases are a promising class of biomarkers that are up-regulated,

accumulated, or aggregated during TBI. In contrast, the decreased sequence coverage for dehydrogenases (e.g., lactate dehydrogenase) found only in naïve control samples indicates a promising class of biomarkers that are down-regulated, released, or degraded.

Preliminary validation. The relative quantification of several putative protein biomarkers of TBI was investigated by targeted Capillary LC-MS^2 (Haskins, 2001) of selected tryptic peptides (**Figure 5**). A high yield of sequence-specific b- and y-type product ions was observed following isolation and fragmentation of tryptic precursor ions by collision-induced dissociation. Two- to ten-fold changes in tryptic peptide concentration for injured vs. naïve control samples reflect the semi-quantitative differences in protein sequence coverage observed. For example, glutamate dehydrogenase (memory related gene 2), shown in **Figure 5C**, was ~10-fold higher in injured samples than in naïve samples for 3 of 4 sample pairs: corresponding to 2.9% protein sequence coverage in injured samples and 0.0% protein sequence coverage in naïve control samples (i.e., no tryptic peptides were observed in naïve control samples by data-dependent Capillary LC-MS^2).

DISCUSSION

Experimental rationale. We chose to analyze hippocampal tissue rather than the more obvious cortical tissue because the cortex is the impact site, thus containing significant hemorrhage. We did not want to have blood-borne proteins (e.g., hemoglobin) confounding our proteomic analysis. Hippocampus, which is a deep-brain structure significantly injured by the contusion force upon cortical

impact, is therefore an ideal sample site. Similarly, we chose to perform differential proteomic analysis between naïve control and TBI rather than craniotomy as sham control and TBI. This is because our experience tells us that traditionally performed craniotomy itself causes mild brain injury (unpublished data, Liu, Wang and Hayes). Thus, craniotomy samples were not ideal controls for this set of experiments, so there were no "sham controls" being compared.

Discovery. In this study, using SDS-PAGE-Capillary LC-MS^2 and differential proteomic analysis, we revealed differences in protein sequence coverage for 170 mammalian proteins when comparing naïve rat hippocampus versus traumatically injured hippocampus (at 48 h time point). The injured-to-naïve ratio of protein sequence coverage suggests putative biomarkers that may exhibit significant differences in protein concentration between naïve and injured samples. Thus, proteins observed only in naïve samples, or proteins observed with greater sequence coverage in naïve control samples than in injured samples, suggest a subset of putative biomarkers that are down-regulated, released, or degraded during TBI, e.g., αII-spectrin (Pike, 2002), MAP2 (Huh, 2003), NF (Posmantur et al.; 1996; Posmantur et al., 1998) and PLP (Banik et al., 1985; Domanska-Janik et al., 1992). Likewise, proteins observed only in injured samples, or proteins observed with greater sequence coverage in injured samples than in naïve control samples, suggest a subset of putative biomarkers that are up-regulated, accumulated, or aggregated during TBI, e.g., NSE (Varma, 2003), amyloid precursor protein, amyloid β 1-42, tau (Franz, 2003), and α-Syn (Uryu, 2003; Bramlett, 2003; Newell, 1999; Smith, 2003).

Reproducibility. Protein sequence coverage is only a semi-quantitative measure of protein concentration. This is particularly true for protein identifications based on data-dependent MS^2 of complex peptide mixtures separated by Capillary LC (where ions above a threshold are automatically isolated and fragmented on the chromatographic time scale), and it is it is even more pronounced for protein identifications based on single tryptic peptide sequences. While ~ 70% of proteins were reproducibly identified in a triplicate SDS-PAGE-Capillary LC-MS^2 analysis of pooled hippocampal samples with data-dependent scans (data not shown), only 29% of proteins were conserved between naïve control and injured samples. Thus, some ambiguity in our results is expected (e.g., glutamate dehydrogenase was observed only in injured samples while the neuronal protein glial fibrillary acidic protein (GFAP) was observed only in naïve samples). Based on fluorescence line plots of cyanine dye-labeled proteins separated by SDS-PAGE, we hypothesize that this analytical variability will exceed the biological variability of individual samples. However, in order to err on the side of caution, only "putative" protein biomarkers, discovered in pooled samples, are reported in this work.

Validation. Biomarker validation is a significant bottleneck for proteomics methods because the speed of discovery continues to outpace the speed of validation (Bodovitz, 2004). We observed a general agreement between our targeted Capillary LC-MS^2 results (relative quantification) for selected proteins and our data-dependent Capillary LC-MS^2 results (sequence coverage). Absolute quantification (AQUA) of selected proteins, by incorporating an isotopically

labeled tryptic peptide as an internal standard during trypsin digestion (Gerber, 2003), is underway (publication in preparation). However, reproducible quantification of all 170 putative protein biomarkers for multiple injured and naïve control samples (at multiple time points) remains impractical.

Degradomics. Since the fragments of degraded proteins (e.g., breakdown products of αII-spectrin (Pike, 2002) may also be observed, it is important to relate $M_r$calc to $M_r$obs for putative protein biomarkers of TBI. In order to evaluate whether any of our biomarkers were fragments of degraded proteins rather than intact proteins, we performed differential proteomic analysis as a function of $M_r$obs. Degraded protein biomarkers may not be revealed by differences in protein sequence coverage using current differential proteomic analysis tools, even when proteins are separated prior to *in vitro* proteolysis and Capillary LC-MS^2, because $M_r$obs, which is encoded in SDS-PAGE-Capillary LC-MS^2 data, may not be preserved during data reduction. For example, MBP was identified by database searching ($M_r$calc = 27 kDa) in both naïve and injured samples with a sequence coverage of 13.6 %. This information alone would incorrectly suggest that it is not a putative biomarker of TBI. However, incorporating the mass of the protein into the analysis reveals that MBP is cleaved as a consequence of TBI and, in fact is an excellent biomarker. The vertical line in **Figure 2** illustrates that MBP was observed in gel slices 35 to 41 ($M_r$obs ~ 27 kDa to 10 kDa, respectively) in injured (and not naïve) samples, suggesting possible degradation, as confirmed by Western blot (Liu, Wang et al, submitted elsewhere).

Comparison with previous work. Several of the putative protein biomarkers described herein at 48 hours post-injury were accounted for previously by a microarray- and RNA-based gene expression experiment at 24 hours post-injury (Matzilevich, 2002 2026) including: NF (light), MAP2, GFAP, and beta-tubulin. More recently, a proteomics approach using 2D gels and database searching of 2D gel images (Fountoulakis, 1999) at 24 hours post-injury was presented (Jenkins, 2002). In that work, 50 of ~ 1500 protein spots were tentatively identified by matching the experimental molecular mass and isoelectric point with a rat brain database. However, only 6 putative protein biomarkers were discovered by significant changes across 6 of 6 gel pairs (individual samples). Interestingly, an increase in the mitochondrial protein Cu/Zn superoxide dismutase following TBI, and a decrease in the cytoskeletal proteins α- and β-tubulin following TBI were also observed among the 170 putative protein biomarkers discovered in this work (pooled samples). It is also important to note that we have confidently identified, by peptide sequences rather than by peptide masses, more than 20 proteins of high molecular mass (150-300 kDa). In contrast, it is almost impossible to visualize and identify proteins in this molecular mass range by 2D gels (Fountoulakis, 1999).

Future work. This is the first report of SDS-PAGE-Capillary LC-MS^2 for biomarker discovery. Sequence-specific discovery of putative protein biomarkers (by data-dependent Capillary LC-MS^2) and preliminary validation of selected biomarkers (by targeted Capillary LC-MS^2), show that SDS-PAGE prior to *in vitro* proteolysis and Capillary LC-MS^2 is a promising strategy for the rapid discovery

of putative protein biomarkers associated with a specific pathophysiological state (i.e., TBI) without *a priori* knowledge of the molecules involved. Biomarkers of TBI are expected to either accumulate in the CSF and blood, or form aggregates in the extracellular compartment of the brain. However, whether these markers can distinguish TBI from various other brain diseases, and whether the kinetics for their degradation and clearance from tissue to CSF and blood are favorable, must be firmly established in order to obtain reliable indicators of injury severity. A subset of the putative protein biomarkers of TBI, described herein, particularly the neuronal proteins, are expected to meet these criteria for biomarker validation. In the meantime, these biomarkers may also find use in the laboratory setting. For example, β3-tubulin and GFAP are used to distinguish neuronal differentiation in stem cell research (Kornblum, 2001 2019). Lastly, this work provides proof-of-principle for more rapid, more reproducible, and more comprehensive biomarker discovery strategies incorporating protein separation prior to *in vitro* proteolysis and Capillary LC-MS^2.

ACKNOWLEDGEMENTS

This work was supported by DoD grants DAMD17-03-1-0066, DAMD17-01-1-0765, DAMD17-99-1-9565; NIH grants R01 NS39091, R01 NS40182. We thank Professor Steven Gygi (Harvard Medical), Dr David Tabb (Oak Ridge National Laboratory), Dr Anu Waghray, Dr Clair Ringger, and Ms. Alexia Lundberg (University of Florida) for insightful discussion.

FIGURE LEGENDS

Figure 1. Cyanine-dye labeled proteins separated by SDS-PAGE. (A) Fluorescence image of 25 μg of Cy3 (green)- and Cy5 (red)-labeled proteins from naïve control (N) and injured (I) ipsilateral hippocampus (IH) samples separated on a Tris-tricine SDS-PAGE gel (10-20% polyacrylamide).

Figure 2. Correlation between the database-derived molecular mass ($M_r$calc), and SDS-PAGE-predicted molecular mass ($M_r$obs). The migration of proteins in the SDS-PAGE gel inversely correlates with $M_r$calc for unmodified proteins identified by Capillary LC-MS^2 and database searching (solid line), as expected. Accordingly, $M_r$obs directly correlates with $M_r$calc. In addition, protein sequence coverage shows an inverse correlation with $M_r$calc (dashed line).

Figure 3. Stratification of the putative protein biomarkers discovered in injured hippocampus only. Proteins were sorted into classes based on function and localization with increasingly stringent specificity: blood, brain < membrane < nuclear < cytoskeletal < dehydrogenase, enolase, clock, G-protein, heat shock, isomerase, kinase, monooxygenase, phosphatase, reductase < synthase < lysosomal, mitochondrial < neuronal.

Figure 4. Stratification of putative protein biomarkers discovered in naïve control only, injured only, and both naïve control and injured hippocampal samples. The fraction of biomarkers in "Naïve Only" (green columns), "Injured Only" (red) and both "Naïve and Injured" samples (blue) were plotted against each function and localization class. In addition, the difference in the fraction between the "Injured Only" group and the "Naïve Only" group was plotted as a line graph on the same scale. Peaks in the line plot suggest classes of proteins that are elevated, upregulated, aggregated or (e.g. neuronal, heat shock, and kinase) in injured hippocampus. In contrast, the decreased sequence coverage for dehydrogenases (e.g., lactate dehydrogenase) found only in naïve control samples indicates a promising class of biomarkers that are down-regulated, released, or degraded.

Figure 5. Representative targeted MS^2 spectra collected in naïve control (left) and injured (right) hippocampus samples. (A) CKB-rat, (B) α-Syn, (C) memory-related gene 2, and (D) αII-spectrin. The tryptic peptide sequences corresponding to these spectra are (A) LAVEALSSLDGDLSGR, (B) KEGVLYVGSK, (C) HGGTIPVVPTAEFQDR, and (D) DLAALGDKVNSLGETAQR, respectively.

Table 1. Differential proteomic analysis of mammalian proteins. The RefSeq (Pruitt, 2001) accession number, protein description, database-derived molecular mass ($M_r$calc), and SDS-PAGE-predicted molecular mass ($M_r$obs) are shown for putative protein biomarkers of TBI.

RefSeq Accession Number	*Protein Description*	*$M_r$calc* (kDa)	*$M_r$obs* (kDa)
	Protein appears in Naïve animals only		
NM_022007	FXYD domain-containing ion transport regulator 7 [Mus musculus]	8	13 -- 17
NM_181029	casein alpha-S1 [Bos taurus]	25	> 250
NM_012966	heat shock 10 kDa protein 1 (chaperonin 10) [Rattus norvegicus]	11	10 -- 13
NM_017236	phosphatidylethanolamine binding protein [Rattus norvegicus]	21	15 -- 25
NM_018947	cytochrome c [Homo sapiens]	12	< 10
NM_057114	peroxiredoxin 1 [Rattus norvegicus]	22	15 -- 25
NM_022511	profilin [Rattus norvegicus]	15	10 -- 15
NM_174294	casein kappa [Bos taurus]	21	> 250
NM_028207	dual specificity phosphatase 3 [Mus musculus]	20	15 -- 25
NM_016956	hemoglobin, beta adult minor chain; beta min; beta minor globin [Mus musculus]	16	10 -- 15
NM_017169	thioredoxin peroxidase 1 [Rattus norvegicus]	22	15 -- 25
NM_017055	transferrin [Rattus norvegicus]	76	50 -- 75
NM_182839	RIKEN cDNA 2900041A09 [Mus musculus]	23	17 -- 27
NM_010471	hippocalcin [Mus musculus]	22	15 -- 25
NM_023716	tubulin, beta [Mus musculus]	50	35 -- 50
NM_021316	BM88 antigen [Mus musculus]	15	15 -- 25
NM_053511	neural F box protein NFB42 [Rattus norvegicus]	34	30 -- 35
NM_009610	Actin, gamma 2, (smooth muscle) [Mus musculus]	42	40 -- 60
NM_022922	triosephosphate isomerase 1 [Rattus norvegicus]	27	17 -- 27
NM_019131	tropomyosin 1, alpha [Rattus norvegicus]	29	27 -- 33
NM_012498	aldehyde reductase 1[Rattus norvegicus]	36	13 -- 17
NM_000410	hemochromatosis protein 1 [Homo sapiens]	10	35 -- 50
NM_017025	lactate dehydrogenase A [Rattus norvegicus]	36	27 -- 33
NM_008617	malate dehydrogenase, mitochondrial [Mus musculus]	35	27 -- 33
NM_023716	RIKEN cDNA 2410129E14 gene [Mus musculus]	50	35 -- 50

NM_002634	prohibitin [Homo sapiens]	30	17 -- 27
NM_011553	t-complex protein 10b [Mus musculus]	49	> 250
NM_001069	tubulin, beta polypeptide [Homo sapiens]	50	35 -- 50
NM_002301	lactate dehydrogenase C [Homo sapiens]	36	27 -- 33
NM_012949	enolase 3, beta; [Rattus norvegicus]	47	35 -- 50
NM_014364	glyceraldehyde-3-phosphate dehydrogenase, testis-specific [Homo sapiens]	44	27 -- 33
NM_013506	eukaryotic translation initiation factor 4A2 [Mus musculus].	46	35 -- 50
NM_133977	transferrin; hypotransferrinemia with hemochromatosis [Mus musculus]	77	50 -- 75
NM_003026	SH3-domain GRB2-like 2 [Homo sapiens]	40	33 -- 40
NM_139254	tubulin, beta 3 [Rattus norvegicus]	50	35 -- 50
NM_022399	calreticulin [Rattus norvegicus].	48	35 -- 50
NM_031140	vimentin [Rattus norvegicus].	54	35 -- 50
NM_012497	aldolase C, fructose-biphosphate [Rattus norvegicus]	39	33 -- 40
NM_031034	guanine nucleotide binding protein (G protein) alpha 12 [Rattus norvegicus]	44	30 -- 35
XM_236227	protein phosphatase PP2A [Rattus norvegicus].	65	50 -- 75
NM_019225	solute carrier family 1, member 3 [Rattus norvegicus]	60	> 250
NM_017009	glial fibrillary acidic protein [Rattus norvegicus]	50	35 -- 50
NM_025407	ubiquinol-cytochrome c reductase core protein 1 [Mus musculus]	53	35 -- 50
NM_145614	dihydrolipoamide S-acetyltransferase [Mus musculus]	68	50 -- 75
NM_022229	heat shock protein 60 (chaperonin) [Rattus norvegicus]	61	40 -- 60
NM_145518	NADH dehydrogenase (ubiquinone) Fe-S protein 1 [Mus musculus]	80	50 -- 75
NM_175199	heat shock protein 12A [Mus musculus]	75	50 -- 75
NM_008449	kinesin heavy chain 5C,NEURON-SPECIFIC [Mus musculus].	109	80 -- 130
NM_031715	phosphofructokinase, muscle [Rattus norvegicus]	86	60 -- 90
NM_145779	pregnancy-zone protein [Rattus norvegicus]	167	115 -- 205
NM_013559	HSP105[Mus musculus]	97	80 -- 130
NM_031604	H+ transporting ATPase, lysosomal (vacuolar proton pump) [Rattus norvegicus]	96	> 250

NM_021343	spermatogenesis associated factor [Mus musculus]	97	75 -- 105
NM_007804	cut-like 2 [Mus musculus]	155	35 -- 50
NM_152296	ATPase, Na+/K+ transporting, alpha 3 polypeptide [Homo sapiens]	112	80 -- 130
NM_054004	TBP-interacting protein 120A [Rattus norvegicus]	136	105 -- 160
NM_019167	beta-spectrin 3 [Rattus norvegicus]	271	> 250
	Protein appears in Injured animals only		
NM_003509	H2A histone family, member C [Homo sapiens]	14	10 -- 15
NM_080777	synuclein, beta [Rattus norvegicus]	15	10 -- 15
NM_000976	ribosomal protein L12 [Homo sapiens]	18	15 -- 25
NM_025562	RIKEN cDNA 2010003O14 [Mus musculus]	17	13 -- 17
NM_016068	CGI-135 protein [Homo sapiens]	17	13 -- 17
NM_025313	RIKEN cDNA 0610008F14 [Mus musculus]	18	10 -- 15
NM_026369	actin related protein 2/3 complex, subunit 5 [Mus musculus]	16	13 -- 17
NM_012038	visinin-like 1 [Mus musculus].	22	15 -- 25
NM_009923	cyclic nucleotide phosphodiesterase 1 [Mus musculus]	47	35 -- 50
NM_133796	Rho GDP dissociation inhibitor (GDI) alpha [Mus musculus]	23	17 -- 27
NM_014231	VAMP-1A; synaptobrevin [Homo sapiens]	13	10 -- 15
NM_017101	peptidylprolyl isomerase A (cyclophilin A) [Rattus norvegicus]	18	10 -- 15
NM_009001	RAB3A, member RAS oncogene family [Mus musculus].	25	15 -- 25
NM_000518	beta globin [Homo sapiens]	16	10 -- 15
NM_024349	adenylate kinase 1 [Rattus norvegicus].	21	15 -- 25
NM_031603	14-3-3 epsilon [Rattus norvegicus]	29	15 -- 25
NM_017051	superoxide dismutase 2, mitochondrial [Rattus norvegicus]	25	15 -- 25
NM_026267	RIKEN cDNA 1200016B17 [Mus musculus]	30	30 -- 35
NM_008907	peptidylprolyl isomerase A; cyclophilin A [Mus musculus]	18	13 -- 17
NM_053610	peroxiredoxin 5 precursor [Rattus norvegicus]	22	13 -- 17
NM_016131	ras-related GTP-binding protein RAB10 [Homo sapiens]	23	15 -- 25
NM_011670	ubiquitin carboxy-terminal hydrolase L1; gracile axonal dystrophy; protein gene product 9.5 [Mus musculus]	25	15 -- 25
NM_019376	14-3-3 protein gamma [Rattus norvegicus]	28	17 -- 27

NM_011739	14-3-3 theta [Mus musculus]	28	17 -- 27
NM_010312	guanine nucleotide-binding protein, beta-2 subunit [Mus musculus].	37	30 -- 35
NM_023200	protein phosphatase-1 regulatory subunit 7 [Mus musculus]	41	35 -- 50
NM_019632	N-ethylmaleimide sensitive fusion protein attachment protein beta; brain protein I47 [Mus musculus]	34	27 -- 33
NM_017327	GTP-binding protein alpha o; RATBPGTPC [Rattus norvegicus].	40	30 -- 35
NM_026646	RIKEN cDNA 1300006L01 [Mus musculus]	35	30 -- 35
NM_005165	aldolase C, fructose-bisphosphate; Aldolase C, fructose-bisphosphatase [Homo sapiens]	39	33 -- 40
NM_025942	RIKEN cDNA 2810409H07 [Mus musculus]	45	35 -- 50
NM_019291	carbonic anhydrase 2 [Rattus norvegicus]	37	27 -- 33
NM_017215	solute carrier family 1, member 2 [Rattus norvegicus]	62	> 250
NM_005917	cytosolic malate dehydrogenase [Homo sapiens]	36	17 -- 27
NM_006032	copine 6; neuronal copine; N-copine [Homo sapiens]	62	50 -- 75
NM_006136	F-actin capping protein alpha-2 [Homo sapiens]	33	27 -- 33
NM_002074	G protein, beta-1 subunit; transducin beta chain 1l [Homo sapiens]	37	30 -- 35
NM_014203	adaptin, alpha A; [Homo sapiens]	108	80 -- 130
NM_002635	phosphate carrier precursor isoform 1b; mitochondrial [Homo sapiens]	40	> 250
NM_018754	stratifin; 14-3-3 sigm [Mus musculus]	28	17 -- 27
NM_024221	pyruvate dehydrogenase (lipoamide) beta [Mus musculus]	39	30 -- 35
NM_025899	ubiquinol cytochrome c reductase core protein 2 [Mus musculus]	48	35 -- 50
NM_002300	lactate dehydrogenase B [Homo sapiens]	37	27 -- 33
NM_012570	glutamate dehydrogenase 1; memory related gene 2 [Rattus norvegicus]	61	40 -- 60
NM_138828	apolipoprotein E [Rattus norvegicus]	36	27 -- 33
NM_013681	synapsin II [Mus musculus]	52	40 -- 60
NM_033235	malate dehydrogenase 1 [Rattus norvegicus]	36	27 -- 33
NM_011861	protein kinase C and casein kinase substrate in neurons 1 [Mus musculus]	51	40 -- 60
NM_004077	citrate synthase precursor; Citrate synthase, mitochondrial [Homo sapiens]	52	35 -- 50

NM_007505	ATP synthase, H+ transporting, mitochondrial F1 complex, alpha subunit, isoform 1 [Mus musculus]	60	35 -- 50
NM_057118	contactin 1 [Rattus norvegicus].	113	105 -- 160
NM_010481	heat shock protein, A [Mus musculus]	74	50 -- 75
NM_019703	phosphofructokinase [Mus musculus].	86	60 -- 90
NM_012491	adducin 2, beta [Rattus norvegicus].	81	80 -- 130
NM_003178	synapsin IIb [Homo sapiens]	52	40 -- 60
NM_009947	copine VI; copine 6; neuronal copine [Mus musculus]	62	50 -- 75
NM_011393	solute carrier family 1, member 2; glial high affinity glutamate transporter [Mus musculus]	61	> 250
NM_153781	brain glycogen phosphorylase [Mus musculus]	97	75 -- 105
NM_006644	heat shock 105kD [Homo sapiens]	92	80 -- 130
NM_031783	neurofilament, light polypeptide [Rattus norvegicus]	61	50 -- 75
NM_006950	synapsin Ia [Homo sapiens]	74	50 -- 75
NM_013066	microtubule-associated protein 2 [Rattus norvegicus]	199	> 250
NM_021979	heat shock 70kDa protein 2[Homo sapiens]	70	50 -- 75
NM_012607	neurofilament, heavy polypeptide [Rattus norvegicus]	115	115 -- 205
NM_181092	synaptic Ras GTPase activating protein 1 [Rattus norvegicus]	128	105 -- 160
NM_005348	heat shock 90kDa protein 1, alpha [Homo sapiens]	85	75 -- 105
NM_010438	hexokinase 1; downeast anemia [Mus musculus]	106	80 -- 130
NM_000477	albumin precursor [Homo sapiens]	69	10 -- 15
NM_001385	dihydropyrimidinase [Homo sapiens]	57	50 -- 75
NM_001127	Seta-adaptin [Homo sapiens]	105	80 -- 130
NM_003334	ubiquitin-activating enzyme E1 [Homo sapiens]	118	80 -- 130
NM_001835	Clathrin, heavy chain [Homo sapiens]	179	115 -- 205
NM_005657	tumor protein p53 binding protein, 1 [Homo sapiens]	214	15 -- 25
NM_002374	microtubule-associated protein 2a [Homo	199	> 250

	sapiens]		
	Higher sequence coverage in Injured than Naïve (protein appears in both)		
NM_005530	mitochondrial; isocitrate dehydrogenase (NAD+) alpha [Homo sapiens]	40	30 -- 35
NM_024398	mitochondrial aconitase [Rattus norvegicus].	85	60 -- 90
NM_005566	lactate dehydrogenase A [Homo sapiens]	37	27 -- 33
NM_057143	fertility protein SP22 [Rattus norvegicus]	200	15 -- 25
NM_013083	heat shock 70kD protein 5 [Rattus norvegicus].	72	50 -- 75
NM_019169	synuclein, alpha [Rattus norvegicus].	15	10 -- 15
NM_024398	mitochondrial aconitase [Rattus norvegicus]	85	60 -- 90
XM_237718	tubulin alpha 6 [Rattus norvegicus]	50	35 -- 50
NM_171983	alpha-spectrin 2 [Rattus norvegicus]	285	> 250
NM_139325	enolase 2, gamma; neuronal [Rattus norvegicus].	50	35 -- 50
NM_006597	heat shock 70kDa protein 8 isoform 1[Homo sapiens]	71	50 -- 75
NM_015981	CaM kinase II alpha subunit; isoform 1 [Homo sapiens]	55	40 -- 60
NM_011738	14-3-3 eta [Mus musculus]	28	17 -- 27
NM_017042	protein phosphatase 3 (Calcineurin) subunit A beta [Rattus norvegicus].	59	40 -- 60
NM_005507	cofilin 1 (non-muscle) [Homo sapiens]	19	15 -- 25
NM_146100	hypothetical protein MGC25352 [Mus musculus]	55	50 -- 75
XM_217040	tubulin alpha-1 [Rattus norvegicus]	50	35 -- 50
	Same sequence coverage in Naïve and Injured		
NM_006870	destrin[Homo sapiens]	19	15 -- 25
NM_173102	tubulin, beta 5 [Rattus norvegicus]	50	35 -- 50
NM_006000	ubulin, alpha 1; testis-specific [Homo sapiens]	50	35 -- 50
NM_001102	actinin, alpha 1 [Homo sapiens]	103	80 -- 130
NM_008634	microtubule-associated protein 1b[Mus musculus]	270	27 -- 33
NM_008084	glyceraldehyde-3-phosphate dehydrogenase [Mus musculus]	36	30 -- 35
NM_023964	glyceraldehyde-3-phosphate dehydrogenase type 2 [Rattus norvegicus]	47	30 -- 35
NM_153629	(NM_153629) heat shock 70 kDa protein 4 [Rattus norvegicus]	94	80 -- 130

NM_012529	(NM_012529) creatine kinase, brain [Rattus norvegicus]	43	33 -- 40
NM_012734	hexokinase 1 [Rattus norvegicus].	103	75 -- 105
NM_009497	vesicle-associated membrane protein 2; synaptobrevin II [Mus musculus].	13	10 -- 15
NM_016774	ATP synthase, H+ transporting mitochondrial F1 complex, beta subunit [Mus musculus].	58	35 -- 50
NM_010777	(NM_010777) myelin basic protein; myelin deficient [Mus musculus]	27	10 -- 27
NM_031728	synaptosomal-associated protein (AP180) [Rattus norvegicus]	94	80 -- 130
NM_000517	alpha 2 globin [Homo sapiens]	15	10 -- 15
NM_002965	S100 A9; calgranulin B [Homo sapiens]	13	I: > 250, N: 60 -- 90
NM_030873	profilin II [Rattus norvegicus].	15	10 -- 15
NM_012673	thymus cell surface antigen [Rattus norvegicus]	18	15 -- 25
NM_012635	(NM_012635) pancreatic trypsin 1 [Rattus norvegicus]	26	75 -- 105
NM_013177	Glutamate oxaloacetate transaminase 2 mitochondrial [Rattus norvegicus].	27	33 -- 40
NM_012504	ATPase, Na+K+ transporting, alpha 1 [Rattus norvegicus]	113	105 -- 160
NM_010324	glutamate oxaloacetate transaminase 1, cytosolic [Mus musculus].	26	33 -- 40
NM_080583	adaptor-related protein complex 2, beta 1 subunit; beta adaptin [Rattus norvegicus].	105	75 -- 105
NM_026508	(NM_026508) RIKEN cDNA 2410002K23 [Mus musculus]	80	75 -- 105
NM_006310	puromycin-sensitive aminopeptidase; metalloproteinase MP100 [Homo sapiens]	99	75 -- 105
	Higher sequence coverage in Naïve than Injured (protein appears in both)		
NM_030773	beta tubulin 1, class VI [Homo sapiens]	50	35 -- 50
NM_019299	clathrin, heavy polypeptide (Hc) [Rattus norvegicus].	192	160 -- 250
NM_003127	alpha-spectrin 2 (alpha-fodrin) [Homo sapiens]	284	> 250
NM_013096	hemoglobin, alpha 1 [Rattus norvegicus]	15	10 -- 15
NM_018753	14-3-3 protein beta [Mus musculus].	28	17 -- 27
NM_000944	protein phosphatase 3 (calcineurin A alpha) [Homo sapiens]	59	40 -- 60
NM_057213	ATPase, H+ transporting, lysosomal beta 2 [Rattus norvegicus].	57	40 -- 60

NM_138548	nucleoside diphosphate kinase (NM23A) [Rattus norvegicus]	17	10 -- 15
NM_033234	Hemoglobin, beta [Rattus norvegicus]	16	10 -- 15
NM_053543	neurochondrin [Rattus norvegicus].	79	50 -- 75
NM_003406	14-3-3 zeta [Homo sapiens]	28	17 -- 27
NM_031353	voltage-dependent anion channel 1 [Rattus norvegicus]	31	27 -- 33
NM_138597	ATP synthase, H+ transporting, mitochondrial F1 complex, O subunit;[Mus musculus]	23	15 -- 25
NM_053291	phosphoglycerate kinase 1 [Rattus norvegicus]	45	35 -- 50
NM_000034	aldolase A; fructose-bisphosphate aldolase [Homo sapiens]	39	33 -- 40
NM_017245	translation elongation factor 2 [Rattus norvegicus].	95	75 -- 105
NM_023119	enolase 1, alpha non-neuron[Mus musculus].	47	35 -- 50
NM_005918	mitochondrial malate dehydrogenase [Homo sapiens]	36	27 -- 33
NM_053297	\pyruvate kinase, muscle [Rattus norvegicus]	58	40 -- 60
NM_080689	dynamin 1 [Rattus norvegicus]	96	75 -- 105
NM_011123	myelin proteolipid protein [Mus musculus]	30	I, N: 15 -- 30, N: 105 -- 160
NM_134326	albumin [Rattus norvegicus]	69	50 -- 75

REFERENCES

1. Banik NL, McAlhaney WW, Hogan EL. Calcium-stimulated proteolysis in myelin: evidence for a Ca2+-activated neutral proteinase associated with purified myelin of rat CNS. J Neurochem. 1985 Aug;45(2):581-8.
2. Berger RP, Pierce MC, Wisniewski SR, Adelson PD, Clark RS, Ruppel RA, Kochanek PM (2002). Neuron-specific enolase and S100B in

cerebrospinal fluid after severe traumatic brain injury in infants and children. Pediatrics 109:E31.

3. Bodovitz S and Joos T (2004). The proteomics bottleneck: strategies for preliminary validation of potential biomarkers and drug targets. Trends Biotechnol 22:4-7.

4. Bramlett HM and Dietrich WD (2003). Synuclein aggregation: possible role in traumatic brain injury. Exp Neurol 184:27-30.

5. Buki A.; Okonkwo DO; Wang K KW; Povlishock JT (2000). Cytochrome c release and caspase activation in traumatic axonal injury. J. Neuroscience 20(8):2825-2834.

6. Denslow N, Michel ME, Temple MD, Hsu CY, Saatman K, Hayes RL (2003) Application of proteomics technology to the field of neurotrauma. Journal of Neurotrauma 20:401-407.

7. Domanska-Janik K, de Nechaud B, Inomata M, Kawashima S, Zalewska T. Calcium-activated neutral protease (CANP) in normal and dysmyelinating mutant paralytic tremor rabbit myelin. Mol Chem Neuropathol. 1992 Jun;16(3):273-88.

8. Fountoulakis M, Schuller E, Hardmeier R, Berndt P, Lubec G (1999a) Rat brain proteins: two-dimensional protein database and variations in the expression level. Electrophoresis 20:3572-3579.

9. Fountoulakis M, Schuller E, Hardmeier R, Berndt P, Lubec G (1999b). Rat brain proteins: two-dimensional protein database and variations in the expression level. Electrophoresis 20:3572-3579.

10. Franz G, Beer R, Kampfl A, Engelhardt K, Schmutzhard M, Ulmer H, Deisenhammer F (2003). Amyloid beta 1-42, and tau in cerebrospinal fluid after severe traumatic brain injury. Neurology 60:1457-1461.

11. Gerber SA, Rush J, Stemman O, Kirschner MW, Gygi SP (2003). Absolute quantification of proteins and phosphoproteins from cell lysates by tandem MS. Proc Natl Acad Sci U S A 100:6940-6945.

12. Gharbi S, Gaffney P, Yang A, Zvelebil MJ, Cramer R, Waterfield MD, Timms JF (2002). Evaluation of two-dimensional differential gel electrophoresis for proteomic expression analysis of a model breast cancer cell system. Molecular & Cellular Proteomics 1:91-98.

13. Gygi SP, Rist B, Gerber SA, Turecek F, Gelb MH, Aebersold R (1999). Quantitative analysis of complex protein mixtures using isotope-coded affinity tags. Nature Biotechnology 17:994-999.

14. Haskins WE, Wang ZQ, Watson CJ, Rostand RR, Witowski SR, Powell DH, Kennedy RT (2001). Capillary LC-MS2 at the attomole level for monitoring and discovering endogenous peptides in microdialysis samples collected *in vivo*. Analytical Chemistry 73:5005-5014.

15. Huh JW, Raghupathi R, Laurer HL, Helfaer MA, Saatman KE (2003). Transient loss of microtubule-associated protein 2 immunoreactivity after moderate brain injury in mice. J Neurotrauma 20:975-984.

16. Jenkins LW, Peters GW, Dixon CE, Zhang X, Clark RS, Skinner JC, Marion DW, Adelson PD, Kochanek PM (2002). Conventional and functional proteomics using large format two-dimensional gel electrophoresis 24 hours after controlled cortical impact in postnatal day 17 rats. J Neurotrauma 19:715-740.

17. Kernec F, Unlu M, Labeikovsky W, Minden JS, Koretsky AP (2001). Changes in the mitochondrial proteome from mouse hearts deficient in creatine kinase. Physiological Genomics 6:117-128.

18. Kornblum HI, Geschwind DH (2001). Molecular markers in CNS stem cell research: hitting a moving target. Nat Rev Neurosci 2:843-846.

19. Leimgruber RM, Malone JP, Radabaugh MR, LaPorte ML, Violand BN, Monahan JB (2002). Development of improved cell lysis, solubilization and imaging approaches for proteomic analyses. Proteomics 2:135-144.

20. Macdonald N, Chevalier S, Tonge R, Davison N, Rowlinson R, Young J, Rayner S, Roberts R (2001). Quantitative proteomic analysis of mouse liver response to the peroxisome proliferator diethylhexylphthalate (DEHP). Archives of Toxicology 75:415-424.

21. Matzilevich DA, Rall JM, Moore AN, Grill RJ, Dash PK (2002). High-density microarray analysis of hippocampal gene expression following experimental brain injury. J Neurosci Res 67:646-663.

22. McDonald WH, Yates JR. (2002). Shotgun proteomics and biomarker discovery. Disease Markers 18:99-105.

23. Newell KL, Boyer P, Gomez-Tortosa E, Hobbs W, Hedley-Whyte ET, Vonsattel JP, Hyman BT (1999). Alpha-synuclein immunoreactivity is present in axonal swellings in neuroaxonal dystrophy and acute traumatic brain injury. J Neuropathol Exp Neurol 58:1263-1268.

24. Perkins DN, Pappin DJ, Creasy DM, Cottrell JS (1999). Probability-based protein identification by searching sequence databases using mass spectrometry data. Electrophoresis 20:3551-3567.

25. Pike BR, Flint J, Dutta S, Wang DS, Wang KKW, Hayes RL (2002). Accumulation of spectrin and calpain-cleaved spectrin breakdown products in CSF after traumatic brain injury. Journal of Neurochemistry 81:73.

26. Pike BR, Flint J, Johnson E, Glenn CC, Dutta S, Wang KKW and Hayes RL. (2001) Accumulation of Calpain-Cleaved Non-Erythroid αII-Spectrin in Cerebrospinal Fluid after Traumatic Brain Injury in Rats. J. Neurochem. 78, 1297-1306.

27. Posmantur RM, Kampfl A, Liu SJ, Heck K, Taft WC, Clifton GL, Hayes RL. Cytoskeletal derangements of cortical neuronal processes three hours after traumatic brain injury in rats: an immunofluorescence study. J Neuropathol Exp Neurol. 1996 Jan;55(1):68-80.

28. Posmantur RM, Zhao X, Kampfl A, Clifton GL, Hayes RL. Immunoblot analyses of the relative contributions of cysteine and aspartic proteases to neurofilament breakdown products following experimental brain injury in rats. Neurochem Res. 1998 Oct;23(10):1265-76.

29. Pruitt KD, Maglott DR (2001). RefSeq and LocusLink: NCBI gene-centered resources. Nucleic Acids Research 29:137-140.

30. Raabe A, Kopetsch O, Woszczyk A, Lang J, Gerlach R, Zimmermann M, Seifert V (2003). Serum S-100B protein as a molecular marker in severe traumatic brain injury. Restor Neurol Neurosci 21:159-169.

31. Shaw J, Rowlinson R, Nickson J, Stone T, Sweet A, Williams K, Tonge R (2003). Evaluation of saturation labeling two-dimensional difference gel electrophoresis fluorescent dyes. Proteomics 3:1181-1195.

32. Smith DH, Uryu K, Saatman KE, Trojanowski JQ, McIntosh TK (2003). Protein accumulation in traumatic brain injury. Neuromolecular Med 4:59-72.

33. Tabb DL, McDonald WH, Yates JR. (2002). DTASelect and contrast: Tools for assembling and comparing protein identifications from shotgun proteomics. Journal of Proteome Research 1:21-26.

34. Thurman D. (2001) The epidemiology and economics of head trauma. In: Miller L, Hayes R, editors. Head Trauma: Basic, Preclinical, and Clinical Directions. New York (NY): Wiley and Sons.

35. Thurman DJ, Alverson C, Dunn KA, Guerrero J, Sniezek JE. (1999) Traumatic brain injury in the United States: a public health perspective. J Head Trauma Rehabil. Dec;14(6):602-615.

36. Tonge R, Shaw J, Middleton B, Rowlinson R, Rayner S, Young J, Pognan F, Hawkins E, Currie I, Davison M (2001). Validation and development of fluorescence two-dimensional differential gel electrophoresis proteomics technology. Proteomics 1: 377-396.

37. Uryu K, Giasson BI, Longhi L, Martinez D, Murray I, Conte V, Nakamura M, Saatman K, Talbot K, Horiguchi T, McIntosh T, Lee VM, Trojanowski JQ (2003). Age-dependent synuclein pathology following traumatic brain injury in mice. Exp Neurol 184:214-224.

38. Varma S, Janesko KL, Wisniewski SR, Bayir H, Adelson PD, Thomas NJ, Kochanek PM (2003). F-2-isoprostane and neuron-specific enolase in cerebrospinal fluid after severe traumatic brain injury in infants and children. Journal of Neurotrauma 20:781-786.

39. Yan JX, Devenish AT, Wait R, Stone T, Lewis S, Fowler S (2002). Fluorescence two-dimensional difference gel electrophoresis and mass spectrometry based proteomic analysis of Escherichia coli. Proteomics 2:1682-1698.

40. Yates JR, Morgan SF, Gatlin CL, Griffin PR, Eng JK (1998). Method to compare collision-induced dissociation spectra of peptides: Potential for library searching and subtractive analysis. Analytical Chemistry 70:3557-3565.

41. Zemlan FP, Jauch EC, Mulchahey JJ, Gabbita SP, Rosenberg WS, Speciale SG, Zuccarello M (2002). C-tau biomarker of neuronal damage in severe brain injured patients: association with elevated intracranial pressure and clinical outcome. Brain Res 947:131-139.

Figure 1.

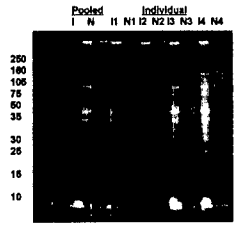

Figure 2.

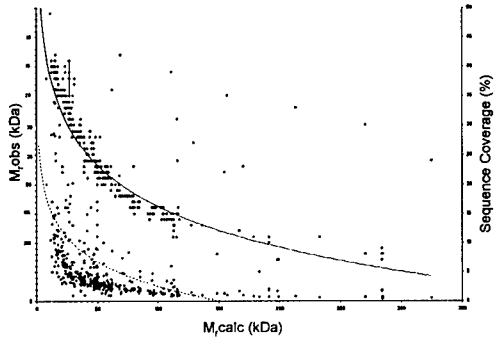

Figure 3.

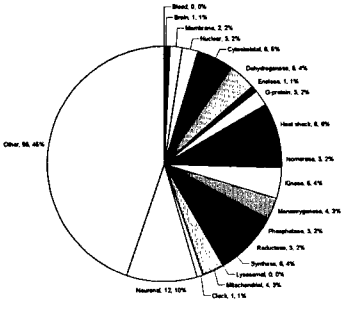

Figure 4.

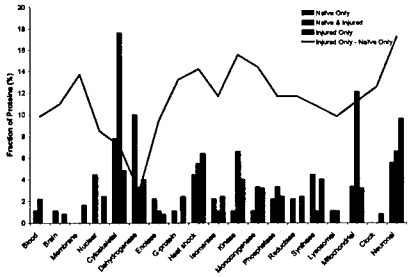

Figure 6.

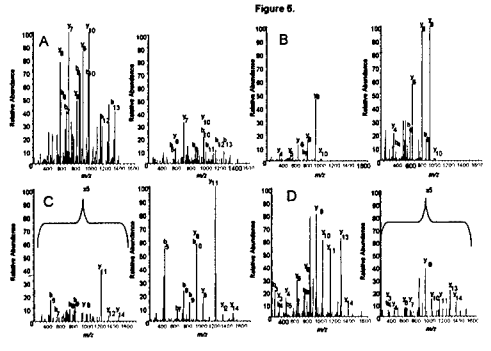

Journal of Neurochemistry, 2004, **88**, 689–697 doi:10.1046/j.1471-4159.2003.02197.x

Cathepsin B mRNA and protein expression following contusion spinal cord injury in rats

Rebecca C. Ellis,* J. Nicole Earnhardt,* Ronald L. Hayes,*,†,§ Kevin K.W. Wang*,‡,§ and Douglas K. Anderson*,¶,**

**Department of Neuroscience, †Department of Neurosurgery, ‡Department of Psychiatry, §Center for Traumatic Brain Injury Studies, and ¶Evelyn F and William L. McKnight Brain Institute of the University of Florida, University of Florida, Gainesville, Florida, USA*
***Malcom Randall VAMC, Gainesville, Florida, USA*

Abstract

We provide the first data that cathepsin B (Cath B), a lysosomal cysteine protease, is up-regulated following contusion-spinal cord injury (SCI). Following T12 laminectomy and moderate contusion, Cath B mRNA and protein expression profiles were examined from 2 to 168 h post-injury in rats using real-time PCR and immunoblots, respectively. Contusion injury significantly increased $[mRNA]_{Cath\ B}$ in the injury site and adjacent segments over sham injury levels. While the largest $[mRNA]_{Cath\ B}$ induction (20-fold over naive) was seen in the injury site, the caudal segment routinely yielded $[mRNA]_{Cath\ B}$ levels greater than 10-fold over naive. Interestingly, sham injury animals also experienced mRNA induction at several time points at the injury site and in segments rostral and caudal to the injury site. Contusion injury also significantly elevated levels of Cath B proenzyme protein (37 kDa) over sham injury in the injury site (48, 72 and 168 h post-injury). Furthermore, significant protein increases of single and double chain Cath B (both active forms) occurred at the injury site at 72 and 168 h post-injury. Similar significant increases in Cath B protein levels were seen in areas adjacent to the injury site. The induction of Cath B mRNA and protein expression following contusion injury is previously undescribed and suggests that Cath B may potentially be involved in the secondary injury cascade, perhaps for as long as 1 week post-injury.

Keywords: cathepsin B, trauma, spinal cord, induction.
J. Neurochem. (2004) **88**, 689–697.

Injury to the spinal cord is typically the result of some type of mechanical insult. This primary injury can be contusive, shearing, stretching or concussive in nature. Primary injury deforms neuronal cell bodies, axons and oligodendrocytes. Disruption of vascular elements and structures within injured tissue leads to petechial hemorrhage, the release of vasoactive molecules and loss of autoregulation by the vascular system (Anderson and Hall 1993; Amar and Levy 1999; Mautes *et al.* 2000). The primary injury also initiates a cascade of pathochemical and pathophysiological events, collectively known as the secondary injury. These events include but are not limited to lipid hydrolysis, eicosanoid production, lipid peroxidation, loss of mitchondrial function and ionic homeostasis, invasion of neutrophils and macrophages, cytokine production, loss of the blood–spinal cord barrier integrity and excitotoxicity (Velardo *et al.* 1999; Demediuk *et al.* 1985, 1987; Anderson and Hall 1993; Amar and Levy 1999; McGrath 1999; Lu *et al.* 2000). Ultimately there is significant loss of neural tissue via apoptotic and necrotic cell death, which frequently results in cavitation around the injury site. As a result, there is a loss of function and sensation distal to the injury site and the prognosis for substantial functional recovery is usually poor.

There has been significant interest in understanding the activation and involvement of enzymatic cascades in the secondary injury response associated with trauma to the spinal cord. Several phospholipases, kinases, endonucleases and proteases are activated by injury-induced increases in intracellular Ca^{2+} levels. Of these proteases, calpain and

Received July 25, 2003; revised manuscript received October 2, 2003; accepted October 3, 2003.

Address correspondence and reprint requests to Douglas K. Anderson, University of Florida, PO Box 100244 Gainesville, FL 32610, USA. E-mail: anderson@mbi.ufl.edu

Abbreviations used: Cath B, cathepsin B; CPV, crossing point value; FON, fold over naive; GAPDH, glyceraldehyde-3-phosphate dehydrogenase; SCI, spinal cord injury; SDS–PAGE, sodium dodecyl sulfate–polyacrylamide gel electrophoresis.

caspase, and now to some extent cathepsin B (Cath B), have been linked to neurodegeneration and cell death in multiple models of central nervous system (CNS) injury. The literature on calpain and caspase involvement in neurodegeneration is quite extensive. Calpain has been associated with tissue destruction and cell death in traumatic brain injury (Kampfl *et al.* 1996, 1997; Saatman *et al.* 1996), ischemia (Rami and Krieglstein 1993; Bartus *et al.* 1994) and spinal cord injury (SCI) (Li *et al.* 1996; Ray *et al.* 1999, 2000; Schumacher *et al.* 1999; Shields *et al.* 2000). In these cases, the increases in calpain activity and immunoreactivity associated with injury are accompanied by increased breakdown of cytoskeletal and myelin proteins (Banik *et al.* 1997; Posmantur *et al.* 1998; Buki *et al.* 1999; Ray *et al.* 1999; Banik and Shields 2000). With more than 40 reported substrates (Stroh and Schulze-Osthoff 1998), caspases (predominantly caspase-3, 9 and -12) have also been linked to tissue loss and cell death in models of traumatic (Crowe *et al.* 1997; Liu *et al.* 1997; Keane *et al.* 2001; Larner *et al.* 2003) brain and spinal cord injury and in ischemic SCI (Sakurai *et al.* 1998; Mackey *et al.* 1997; Hayashi *et al.* 1998; Matsushita *et al.* 2000). Caspases were activated in models of global and focal brain ischemia (Chen *et al.* 1998; Fink *et al.* 1998; Namura *et al.* 1998; Ni *et al.* 1998; Didenko *et al.* 2002). Furthermore, the inhibition of some caspase pathways reduced tissue damage and improved neurological functions (Cheng *et al.* 1998; Mouw *et al.* 2002) in rodent models of focal ischemia (reviewed by Robertson *et al.* 2000).

To date, the role of Cath B in traumatic CNS insults has not been the focus of investigation. Under normal conditions, Cath B is synthesized as an inactive preproenzyme (39 kDa) in the *trans*-golgi, which is processed to the still inactive proenzyme (37 kDa) in the lysosomal compartment (Fig. 1) (Mort and Buttle 1997). Removal of the 63-residue propeptide from its N-terminal converts the inactive proenzyme to a single chain active form (30 kDa) (Fig. 1). This single chain Cath B is further processed within the lysosome into a double chain form consisting of heavy (25 kDa) and light (5 kDa) components held together by a disulfide bond (Fig. 1) (Mort and Buttle 1997). Cath B is involved in protein turnover and digestion of cellular debris (Mort and Buttle 1997; Turk *et al.* 2000) and is capable of hydrolyzing carbohydrates, nucleic acids and lipids. Increased levels of Cath B expression and activity have been reported in several pathologies (Rempel *et al.* 1994; Berquin and Sloane 1996; Bever *et al.* 1997; Mackay *et al.* 1997; Kikuchi *et al.* 2003) including ischemia and oxidative stress (Kohda *et al.* 1996; Seyfried *et al.* 1997; Tsuchiya *et al.* 1999). These changes in Cath B expression and activity are frequently accompanied by its redistribution from the lysosome to the cytosol, and in some cases to the nucleus (Roberts *et al.* 1997) in the injured tissues.

While Cath B has not been characterized following traumatic CNS injury, it has been well studied in a model of cerebral ischemic injury. Yamashima *et al.* (1996) found

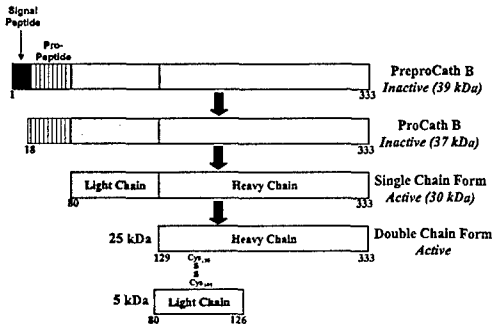

Fig. 1 Schematic of Cath B protein. Preprocathepsin B (333 amino acids) is synthesized on the rough ER where the signal peptide is cleaved cotranslationally. Following transport to the Golgi apparatus, the enzyme is glycosylated and the mannose-6-phosphate signal is assembled. This receptor allows for transport to the *trans*-Golgi network and then onto an acidic compartment where the pro-peptide is removed and enzyme is activated. Within the lysosome, the active single chain form of Cath B (30 kDa) is further modified (loss of a dipeptide) to produce the active double chain form (25 and 5 kDa) held together via disulfide bond.

that the CA1 neuronal population in the hippocampus was completely obliterated five days following transient ischemia. In addition to increased levels of Cath B activity, the protein itself was also redistributed. The administration of two different Cath B inhibitors, CA-074 and E-64c, immediately following ischemia reduced enzyme activity, diminished Cath B immunoreactivity to near negligible levels and spared approximately 67 and 84%, respectively, of CA1 neurons from delayed neuronal death (Tsuchiya *et al.* 1999; Yamashima *et al.* 1998, 1999). These findings suggest that Cath B plays a role in the development of neuropathology following cerebral ischemia and that the inhibition of Cath B may represent a possible avenue for therapeutic intervention.

We propose that Cath B alone, and/or in conjunction with other proteases such as calpain and caspase, could be destructive in spinal cord tissue after injury. However, to date, the effects of contusion injury on Cath B expression levels have not been examined. Thus, the purpose of this study was to examine the effects of sham and contusion injury on expression of Cath B in the spinal cord. Our results demonstrate that contusion injury increased expression of both Cath B mRNA and protein in the injury site and in segments immediately rostral and caudal to the injury site.

Experimental procedures

All experimental procedures were conducted in accordance with the guidelines set forth by the University of Florida's Institute Animal Care and Use Committee (IACUC).

Laminectomy and injury

Female Long–Evans rats weighing approximately 230–300 g (Harlan, Indianapolis, IN, USA) were used in this study. All

surgical procedures were conducted under sterile conditions with supplemental heat. Intraperitoneal administration of nembutal (sodium pentobarbital, 50–60 mg/kg) was used to induce anesthesia. Following a T12, partial T11 laminectomy (intact dura mater), injury to the spinal cord was produced with an NYU impactor device (10 g, 25 mm). The sham injury animals received a laminectomy and were placed in the injury apparatus, but were not injured. The incisions were closed in layers. Animals were recovered in a heated incubator with food and water available *ad libitum*. Bladders were expressed and fluids were administered when required. In the immunoblot analysis ($n = 60$), four animals were used for each treatment group (sham and contusion injury) at each time point (2, 6, 12, 24, 48, 72, and 168 h post-injury). Four naive animals were also utilized. For the real-time PCR experiments (total $n = 44$), both sham and contusion injury ($n = 3$–6 each) were sacrificed at 2, 6, 24, 48, and 168 h post-injury in addition to a group ($n = 5$) of naive animals. Spinal cord tissue was collected after extending the laminectomy to allow three segments of tissue to be removed: (i) rostral to injury site, (ii) injury site, and (iii) caudal to injury site. Each segment was approximately 6–7 mm in length. The fresh tissue was rinsed with cold 1 × phosphate-buffered saline (PBS) and either (i) homogenized with a guanidinum thiocyanate salt solution (500 μL) or (ii) flash frozen with liquid nitrogen. All samples were stored at − 70°C until either (i) RNA isolation or (ii) protein homogenization.

RNA isolation and cDNA synthesis

Total RNA isolation from the spinal cord tissue was achieved using a modified protocol, described by Earnhardt *et al.* (2002), based on the guanidinium thiocyanate/phenol/chloroform extraction developed by Chomczynski and Sacchi (1987). Final RNA concentrations were determined via spectrophotometry and samples were stored at −20°C in diethyl pyrocarbonate water for future cDNA preparation.

For cDNA synthesis, 1 μg of total RNA from all samples was used for enzymatic conversion of mRNA to first strand cDNA using an oligo-dT primer (Invitrogen/Life Technologies, Carlsbad, CA, USA; SuperScript™ First-Strand Synthesis System for RT-PCR). DNA contamination was monitored in our RNA samples by 'no reverse transcriptase' reactions which were performed in conjunction with cDNA synthesis reaction.

Primer design

Base pairs designations for rat GAPDH refer to GeneBank locus AF106860. The primers used for all GAPDH PCR reactions were: sense 5′-ggtga aggtc ggtgt gaac-3′ corresponding to base pairs 852–870 and antisense 5′-ggcat cctgg gctac actg-3′ corresponding to base pairs 1657–1675. Cath B primers were designed using GeneBank locus NM022597. The sense Cath B primer recognized an upstream rat Cath B specific mRNA sequence 5′-tgagg acctg cttac ctgct-3′ corresponding to base pairs 466–485. The antisense Cath B primer recognized a downstream rat Cath B specific mRNA sequence 5′-gcagg gagtg aggca gatag-3′ corresponding to base pairs 1141–1160.

Real-time PCR

The Roche LightCycler and the double-stranded DNA binding dye, SYBR Green I, were used to continuously monitor all PCR reactions. The LightCycler (Roche Biochemicals) is an advanced instrument that conducts rapid thermal cycling of the polymerase chain reaction. SYBR Green I dye™ preferentially binds to double stranded DNA and emits a fluorescent signal proportional to the DNA concentration. The reaction kinetics of this PCR reaction are represented by an amplification curve. Each amplification curve (fluorescence versus cycle number) is assigned a crossing point value (CPV), which is defined as the point of intersection between the amplification curve and the noise band. A lower CPV indicates a more rapid increase in the level of fluorescence and, thus a larger initial concentration of message. When comparing templates, those with lower CPVs contain more amplified message for the gene of interest than those with higher CPVs.

For each PCR reaction the LightCycler FastStart DNA Master^{PLUS} SYBR Green I (Roche) reagent was used according to manufacturer's instructions in combination with primers, cDNA template, dimethyl sulfoxide and $MgCl_2$ at final concentrations of 0.5 μM, 10 ng, 6%, and 2 mM, respectively. After an initial 300 s, 95°C denaturation step, 40 cycles of amplification were performed (95°C for 5 s; denaturation, 65°C for 10 s; annealing, 72°C for 40 s; extension). SYBR Green I fluorescent detection of double stranded PCR products occurred at the end of each 72°C extension within each of the 40 amplification cycles. The specificity of the amplified product was confirmed by (i) the melting curve analysis and (ii) gel electrophoresis. To generate standard curves for the Cath B primer set, contusion injury templates were subjected to serial dilution. Linear regression analysis of the logarithm of the dilution factor versus the CPV generated a standard curve for each specific template. All standard curves were run concomitant with segment- and time-matched unknowns (naive, sham). The relative amount of RNA in the unknown sample was extrapolated from its CPV in relation to the standard curve. Results are reported as relative concentrations.

Northern blot analysis

Northern blot analysis was used to confirm the validity of the real-time PCR technique that we employed to examine mRNA expression. A northern blot prepared as described by Earnhardt *et al.* (2002) was probed with ^{32}P-labeled rat Cath B cDNA (gift from S. Chan, University of Chicago, IL, USA). Autoradiographic films were analyzed using Scion image analysis software. Any differences resulting from loading variability were controlled by normalizing the intensity of the Cath B mRNA signal in each sample to its mRNA signal for cyclophilin.

Tissue lysis and protein purification

Lysis buffer (1 mM EDTA, 2 mM EGTA, 1 small Protease Cocktail Pill™ (Roche Molecular Biochemicals), 0.1% SDS, 1.0% IGEPAL, 0.5% deoxycholic acid, 150 mM NaCl, 20 mM Hepes, ddH_2O, pH = 7.5) was added to each sample based on the mass of the tissue (15 μL/1 mg). The tissue was homogenized on ice with a rotary pestle, returned to Eppendorf tubes and placed at 4°C for at least 30 min Samples were sonicated and spun at 800 *g* for 5 min at 4°C before the supernatant was collected and stored at −70°C.

Immunoblotting

Protein concentrations of the tissue homogenates were determined by bichinchoninic acid (BCA) assay (Pierce Inc., Rockford, IL, USA). Unless otherwise noted, all procedures were performed at room temperature. Eighteen micrograms of total protein were mixed

with 2 × loading buffer (1 × = 125 mM Tris-HCl, 100 mM dithiothreitol, 4.0% sodium dodecyl sulfate (SDS), 0.01% bromophenol blue and 10.0% glycerol) and were resolved by SDS–polyacrylamide gel electrophoresis (PAGE) on 10% Tris/HCl gels (Bio-Rad, Hercules, CA). The fractionated proteins were subsequently transferred to a 0.20-μM nylon membrane (Bio-Rad) in transfer buffer (192 mM glycine, 25 mM Tris/HCl, 10.0% methanol). Staining with ponceau red (Sigma, St. Louis, MO, USA) confirmed transfer of the proteins. Blots were blocked in 5.0% non-fat milk/Tris-buffered saline-Tween (TBS-T) 20 mM Tris/HCl, 150 mM NaCl, 0.005% Tween 20, pH 7.5. Membranes were washed with TBS-T and incubated overnight with a polyclonal anti-Cath B antibody (1 : 1000) (Upstate Biotechnology Inc.). Membranes were washed and then incubated in 3.0% non-fat milk/TBS-T with an anti-rabbit IgG horseradish peroxidase conjugated antibody (1 : 3000) (Bio-Rad). After additional washing, bound antibodies were visualized using the chemiluminescent developing reagent ECL$^+$ (Amersham Pharmacia Biotech, UK). The Cath B antibody recognized three bands: the inactive proenzyme (37 kDa), the active single chain form (30 kDa) and the heavy component of the double chain form (25 kDa). Representative blots were stripped and reprobed with a monoclonal anti-GAPDH antibody (gift of Dr Gerry Shaw, University of Florida, FL, USA) for loading control purposes. Data were acquired as integrated densitometry values (IDVs) by computer-assisted densitometric scanning (Alpha Imager 2000 Digital Imaging System, San Leandro, CA, USA).

Statistical analyses

In these experiments, the levels of Cath B mRNA and protein in the sham and contusion injury animals were normalized to naive levels (or control, in the case of the northern blot analysis) to generate fold induction values (± SEM) referred to as 'fold over naive' (FON). Within each segment (rostral, injury site and caudal), FON values from both the sham and contusion injury groups were analyzed via a two-way ANOVA. Each of the three different protein species (37, 30 and 25 kDa) in the immunoblot experiments required its own ANOVA. Statistically significant differences between the treatment groups were identified with post hoc tests (Tukey's for real-time PCR, immunoblots; independent *t*-test for northern blot analysis).

Results

Contusion-spinal cord injury increased Cath B mRNA levels

Before examining the gene of interest, Cath B, the samples were tested for template integrity using the housekeeping gene GAPDH. Within each set of reactions, the CPVs for the three groups (naive, and sham and contusion injury) were not significantly different at any of the experimental time points (data not shown). Having confirmed template integrity, standard curves were used to ascertain the $[mRNA]_{Cath\ B}$ of the templates within each group. The increase in Cath B mRNA expression in both the sham and contusion injury groups was normalized against the naive levels and represented as the relative induction of (fold over naive). In all segments and at almost all time points examined, $[mRNA]_{Cath\ B}$ was increased following both sham and contusion injury (Fig. 2a).

Sham injury increased $[mRNA]_{Cath\ B}$ although to a lesser degree than the contusion injury. In both the rostral segment (FON = 4.1) and injury site (FON = 5.6), the sham injury induced increase peaked at 48 h post-injury and returned to near basal levels by the last time point examined (168 h). While the pattern of mRNA induction was similar in the rostral and injury segments, the caudal segment responded differently. Here, sham injury induction of Cath B mRNA expression appeared to be more robust than in the other two segments, i.e. at four of the five time points, the mRNA levels exceeded five FON.

Within the injury site, the expression of Cath B mRNA following contusion injury was significantly elevated over the sham injury values at 168 h post-injury. FON increases of 4.2, 10.7 and 19.2 were seen at 24, 48 and 168 h post-injury, respectively, with the largest recorded increase occurring at 168 h post-injury. An injury-induced elevation of Cath B mRNA expression in the injury site 24 h post-injury was demonstrated by northern analysis (Fig. 2b,c). Northern analysis also confirmed a sham injury induced increase in mRNA expression albeit to a lesser degree than the contusion injury (Fig. 2c).

Contusion injury also induced Cath B mRNA expression in areas beyond the injury site. Within the rostral segment, contusion injury significantly increased $[mRNA]_{Cath\ B}$ over sham injury values at 48 and 168 h post-injury. The maximum contusion injury induced increase occurred at 48 h post-injury (6.4 FON) and remained at this level (6.0 FON) until the last time point examined (168 h post-injury). Caudal to the injury site, contusion injury appeared to induce an expression of Cath B mRNA that, like the sham injury animals, was more robust than that seen in the other two segments. $[mRNA]_{Cath}$ was increased at 24, 48 and 168 h post-injury (10 + FON), although a significant increase over sham injury levels occurred solely at the 48 h time point.

Cath B protein expression is elevated following spinal cord injury

Figure 3 displays representative immunoblots (probed with anti-Cath B antibody) for the rostral (Fig. 3a), injury site (Fig. 3b) and caudal (Fig. 3c) segments at 168 h post-injury. Also shown are the GAPDH loading controls. Naive samples produced faint bands while sham and contusion injury yielded broader and more intense bands for the proenzyme and active forms of Cath B. Although the most robust FON increases occurred in the injury site, increased expression of all Cath B protein species was observed in the three segments examined after both sham and contusion injury (Fig. 4). Sham injury did increase Cath B protein levels, but the increases rarely exceeded two FON. In fact, sham injury

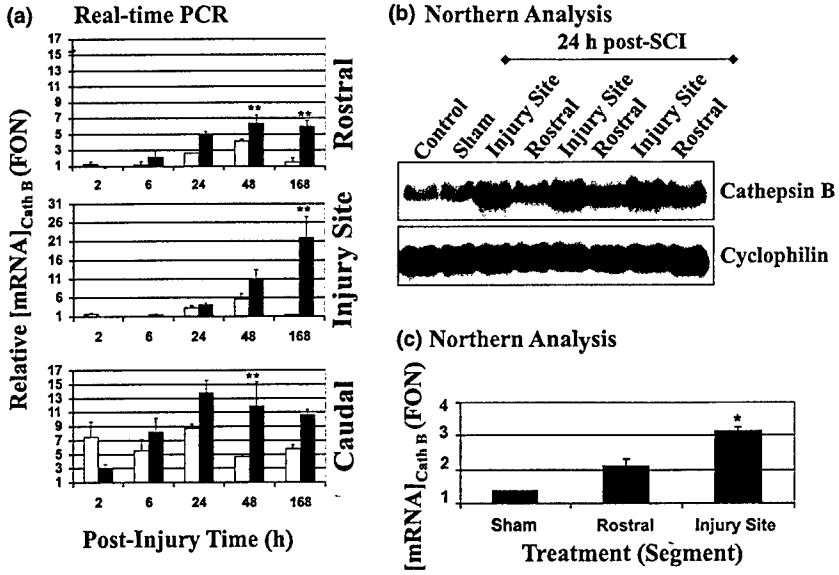

Fig. 2 Sham- and contusion-spinal cord injury (SCI) induced increases in Cath B mRNA. (a) The increases in $[mRNA]_{Cath\ B}$ induced by sham (gray bars) and contusion injury (black bars) are presented here as relative induction of $[mRNA]_{Cath\ B}$ (fold over naive). Cath B mRNA expression was induced following both sham and contusion injury. The post-injury data are presented for the rostral (top panel), injury site (middle panel) and caudal (bottom panel) segments of the spinal cord (Note the different scales for FON values in injury site segment versus the rostral and caudal segments). Following contusion injury, the expression of Cath B mRNA was significantly greater than that of the sham injury in the rostral segment. Similarly, in the injury site, significant differences between the two groups occurred only at 168 h post-injury, where the highest level observed in this study was recorded. In the caudal segment, the $[mRNA]_{Cath\ B}$ peaked at 24 h post-injury but remained elevated at 48 and 168 h post-injury. For this graph and the others, asterisks indicate significant increases ($^*p < 0.05$, $^{**}p < 0.01$) between the sham and contusion injury groups. (b) Northern blot analysis of $[mRNA]_{Cath\ B}$ in both the injury site (vertebral level T13) and rostral (vertebral level T12) segment 24 h following contusion injury. The increases in [mRNA]Cath B in three experimental animals were compared to those observed in control and sham injury animals. Each lane was loaded with 12 μg of total RNA. The signal obtained for the 2.3 kb Cath B message was normalized to the signal previously obtained for cyclophilin (Earnhardt *et al.* 2002). (c) Densitometric analyses of the northern blot shown in (b). Again, contusion injury produced a significant increase in Cath B mRNA. The data represent the mean ± SEM induction (FON) of the three rostral and three injury site samples.

elicited an induction with a two FON or greater at only three of 63 time points (maximum FON value was 2.3).

Contusion injury results in significant increase over sham injury in the 37 kDa proenzyme form of Cath B at 48, 72 and 168 h post-injury at the injury site and at 24, 48, 72 and 168 h post-injury in the caudal segment (Fig. 4). No significant change in the level of proenzyme was seen in the rostral segment. The single chain 30 kDa active form of Cath B was significantly higher following the contusion injury than in sham injury at 168 h post-injury in the rostral segment, and at 72 and 168 h post-injury in both the injury site and in the caudal segment (Fig. 4). The double chain (25 kDa) form of Cath B in contusion injured spinal cord was significantly elevated over sham injury at 168 h post-injury in the injury site and in the rostral (but not caudal) segment (Fig. 4).

In order to examine the relationship between the increases in Cath $B_{[mRNA]}$ and Cath $B_{[protein]}$ following sham and contusion injury, a linear regression analysis was performed for each segment. The FON_{mRNA} (generated in the real-time experiments) was used as the independent factor and the $FON_{protein}$ for the Cath B proenzyme (37 kDa) was the dependent factor. There was a near linear correlation between the increases in $FON_{mRNA\ and}$ $FON_{protein}$ following contusion injury in the rostral ($r^2 = 0.941$, $p < 0.006$), injury site ($r^2 = 0.971$, $p < 0.002$) and caudal ($r^2 = 0.844$, $p < 0.028$) segments, suggesting that the level of Cath B proenzyme increases linearly relative to the increases in Cath B mRNA levels after contusion injury. The same analysis of sham injury samples yielded low r^2 values, suggesting that in the case of sham injury, modest increases of Cath $B_{[mRNA]}$ did not translate into increases in Cath $B_{[protein]}$.

Discussion

Mechanical trauma to the spinal cord initiates a complex cascade of biochemical processes that collectively contribute to neuronal and glial cell death, tissue cavitation, functional deficits and, to date, limited opportunity for restoration and/or functional improvement. Despite the suggestion that

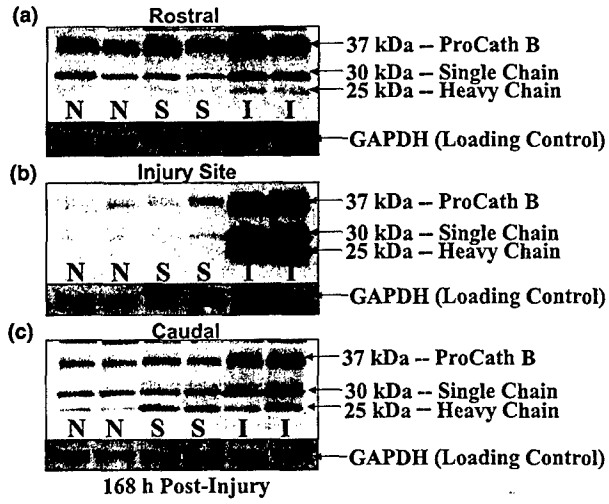

Fig. 3 Sham and contusion injury increase levels of Cath B proenzyme and its two active forms. Naive, sham and contusion injury samples are shown from the 168 h post-injury time point. Three bands were detected: the inactive proenzyme at 37 kDa and two active mature forms, 30 kDa (single chain) and 25 kDa (double chain). Naive samples produced very faint bands in all blots examined. In the injury site (b), the sham injury animals yielded only slightly more dense bands. The contusion injury animals, however, had noticeably more intense and broad bands. These increases also extended to areas rostral (a) and caudal (c) to the injury site. The GAPDH loading control blots are also shown for each panel.

lysosomal rupture and/or leakage may possess the greatest mechanistic potential to directly kill cells (Nixon and Cataldo 1993), the reported increases in calpain and caspase expression and activity levels have overshadowed the characterization of lysosomal hydrolyses following contusion-SCI. While the investigation of SCI-induced changes in Cath B expression has lagged, two separate groups have reported Cath B mRNA induction 3 days after hemisection and sciatic nerve crush (Fan *et al.* 2001) or dorsal root avulsion (Hu *et al.* 2002) using microarray analysis. However, these early studies give a highly circumscribed view of the injury process as they provided the differential expression data for several hundred genes at only one post-injury time point. Our study represents the first in depth analysis of contusion injury induced changes on Cath B expression, as it examines the mRNA and protein levels at several post-injury time points and in areas in and surrounding the injury site.

An examination of the expression profiles revealed significant induction following contusion injury in both the levels of Cath B mRNA (Fig. 2) and protein (Figs 3 and 4). Importantly, the increased presence of the single chain and double chain active forms of Cath B protein illustrate that Cath B proenzyme is being processed after contusion injury (Fig. 1). In addition, following sham injury (i.e. laminectomy and placement in the injury device), elevations in $[mRNA]_{Cath\ B}$ were observed in each segment (Fig. 2). Cath B protein levels were also affected, but to a much smaller extent across the experimental time line (Fig. 4). Laminectomy has been reported to decrease spinal cord blood flow, alter energy metabolism and initiate changes in membrane lipid composition (Anderson *et al.* 1978; Anderson and Means 1985; Demediuk *et al.* 1985, 1987). We previously reported that laminectomy alone induced MnSOD mRNA and protein expression (Earnhardt *et al.* 2002). While great care was taken not to perturb the dura mater or the spinal cord during the sham injury, the increases in Cath B mRNA and protein expression confirm that laminectomy itself is an intrusive procedure. The exact mechanism(s) behind laminectomy-induced increases in Cath B mRNA and protein expression is still unknown.

As a powerful hydrolytic enzyme, Cath B likely contributes to necrotic tissue destruction via degradation of several important cellular proteins. Although little is known about

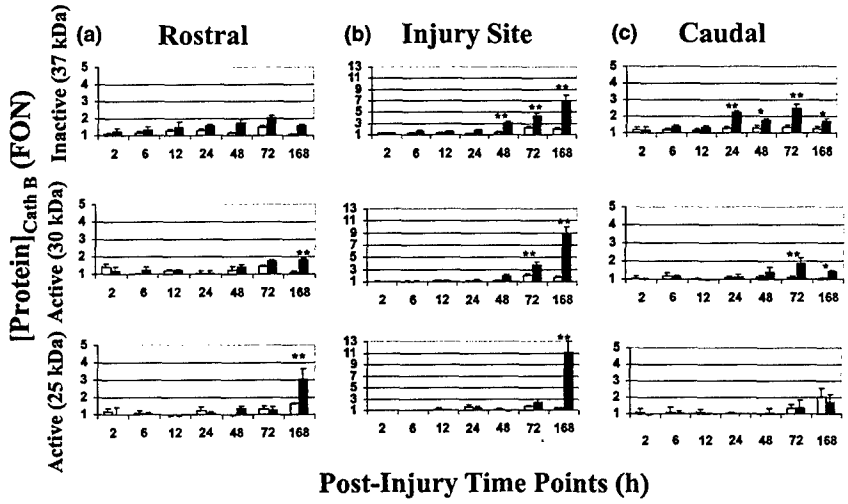

Fig. 4 Increases in levels of the three forms of Cath B following sham and contusion spinal cord injury. The 'fold over naive' (FON) values for the sham injury group (gray bars) were compared to those of the contusion injury (black bars) at seven post-injury time points. The time course of these changes in the proenzyme (37 kDa) and two active forms of Cath B (30 and 25 kDa) are presented for the rostral (a), injury site (b) and caudal (c) segments (Note the different scales for FON values in injury site segment versus the rostral and caudal segments.).

the response of Cath B to traumatic CNS injuries, there is evidence from other models of CNS insults to suggest how sensitive cellular substrates are to Cath B. For example, in one model of transient ischemia, Ca^{2+} influx was accompanied by increased calpain expression and activity (Yamashima *et al.* 1996). These workers characterized the delayed neuronal death that followed the insult in the context of the 'calpain–cathepsin' hypothesis. They noted that activated calpain was localized to vacuolated and disrupted lysosomal membranes, where it acted to degrade the lysosomal membrane. This lysosomal membrane breakdown allowed activated Cath B to escape as showed by a shift of Cath B immunoreactivity from a lysosomal to a cytosolic distribution. Cath B subsequently degraded cellular substrates such as cytoskeletal and myelin proteins contributing to the self-digestion and delayed neuronal death seen in this injury model. The events described by the 'calpain-cathepsin' hypothesis may be applicable to SCI as it has been reported that calpain expression and activity were increased following SCI (Banik *et al.* 1997; Ray *et al.* 1999; Shields *et al.* 2000). However, the specific interaction between these protease systems following SCI is currently unresolved. The concomitant increase in Cath B protein levels we now report may in part reflect this postulated role of calpain, and also contribute to the general degree of protein breakdown, cellular damage and tissue loss seen following SCI.

There is also increasing evidence for Cath B involvement in apoptosis (Leist and Jaattela 2001). While the executioner caspases-3 and -7 are relatively poor substrates for direct Cath B cleavage, the proinflammatory caspases-1 and -11 are readily processed (Schotte *et al.* 1998; Vancompernolle *et al.* 1998). Furthermore, Cath B reportedly participates in several models of apoptosis including nuclear apoptosis (Vancompernolle *et al.* 1998), neuronal apoptosis (Kingham and Pocock 2001), serum deprivation induced apoptosis (Shibata *et al.* 1998), cytokine induced apoptosis (Deiss *et al.* 1996), and tumor necrosis factor-α induced apoptosis (Guicciardi *et al.* 2000; Foghsgaard *et al.* 2001). There is speculation that Cath B acts to induce cytochrome c release and caspase-9 activation (Guicciardi *et al.* 2000). Most likely, a universal mechanism underlying the participation of Cath B in apoptosis does not exist. Rather, several apoptotic pathways may utilize Cath B alone or in conjunction with some other factor (lysosomal, cytosolic, mitchondrial). Whether Cath B is acting upstream or downstream (or perhaps both) of cyto c release and activation of caspases-3 and -9 remains unclear. With time, these questions will be elucidated and help to further explain any role of Cath B may have in apoptotic cell death following SCI.

The impetus driving the induction of Cath B mRNA expression following contusion injury is unknown. Both the human and mouse Cath B genes have been characterized and contain putative promoter regions that exhibit characteristics of housekeeping genes (i.e. absence of TATA or CAAT boxes). However these regions also have high GC content and binding sites for the Sp1 transcription factor (Ferrara *et al.* 1990; Qian *et al.* 1991; Gong *et al.* 1993). Furthermore, Yan *et al.* 2000 reported that the transcription factors Sp1, Sp3 and Ets1 are important factors in the regulation of Cath B transcription. While the presence of a housekeeping-like promoter suggests the constitutive expression of Cath B, the presence of these other regulatory elements coupled with the variations in Cath B mRNA levels in normal and diseased tissues (San Segundo *et al.* 1986) suggest that additional regulators of Cath B transcription may exist. Berquin and Sloane (1996) summarize the results of several studies reporting transcriptional regulation by agents such as phorbol ester, cytokines, interleukins and dexamethasone. At this time, the gene structure of the rat has yet to be resolved. Therefore, the transcriptional regulation of Cath B following contusion injury is outside the scope of this study.

It should be noted that Cath B mRNA expression and levels of the 37 kDa proenzyme form appeared to be greater in the caudal segment than in the rostral segment. However, the increase in the active 30 kDa form was similar in these two segments and the active 25 kDa form was higher in the rostral segment than in the caudal segment. The cause of these differences is unknown but likely reflects a variable spread of the secondary autodestructive cascade over time.

In summary, we report that expression of Cath B, a powerful and ubiquitous protease, is significantly induced by contusion injury and to a lesser extent by laminectomy only. Furthermore, this induction is seen on both the mRNA and protein level and extends beyond the confines of the original injury site. Third, active forms (30 and 25 kDa) of Cath B are also significantly elevated after contusion injury and this elevation is sustained for at least 7 days within the injury site. While its potential substrates and its exact role following contusion injury require further elucidation, by inference of the contributory role of Cath B in the pathobiology of ischemic brain injury and peripheral pathologies, we propose that Cath B is a potentially important mediator of secondary spinal cord injury.

Acknowledgements

This work was supported by (i) the State of Florida's Brain and Spinal Cord Injury Rehabilitation Trust Fund, (ii) the C.M and K.E. Overstreet Family Chair in Spinal Cord Regeneration, and (iii) the Department of Veteran Affairs. The authors thank Wilbur O'Steen for his technical assistance.

References

Amar A. P. and Levy M. L. (1999) Pathogenesis and pharmacological strategies for mitigating secondary damage in acute spinal cord injury. *Neurosurgery* **44**, 1027–1039.

Anderson D. K. and Hall E. D. (1993) Pathophysiology of spinal cord trauma. *Ann. Emerg. Med.* **22**, 987–992.

Anderson D. K. and Means E. D. (1985) The effect of laminectomy on spinal cord blood flow, energy metabolism and ATPase activity. *Paraplegia* **23**, 55.

Anderson D. K., Nicolosi G. R., Means E. D. and Hartley L. E. (1978) Effects of laminectomy on spinal cord blood flow. *J. Neurosurg.* **48**, 232–238.

Banik N. L. and Shields D. C. (2000) The role of calpain in neurofilament protein degradation associated with spinal cord injury. *Methods Mol. Biol.* **144**, 195–201.

Banik N. L., Matzelle D. C., Gantt-Wilford G. and Osborne Hogan E. L. (1997) Increased calpain content and progressive degradation of neurofilament protein in spinal cord injury. *Brain Res.* **752**, 301–306.

Bartus R. T., Baker K. L., Heiser A. D., Sawyer S. D., Dean R. L., Elliott P. J. and Straub J. A. (1994) Postischemic administration of AK275, a calpain inhibitor, provides substantial protection against focal ischemic brain damage. *J. Cereb. Blood Flow Metab.* **14**, 537–544.

Berquin I. M. and Sloane B. F. (1996) Cathepsin-B expression in human tumors, in *Intracellular Protein Catabolism* (Suzuki, K., Bond, J., eds), pp. 281–294. Plenum Press, New York.

Bever C. T. Jr, Panitch H. S. and Johnson K. P. (1994) Increased cathepsin B activity in peripheral blood mononuclear cells of MS patients. *Neurology* **44**, 745–748.

Buki A., Siman R., Trojanowski J. Q. and Povlishock J. T. (1999) The role of calpain-mediated spectrin proteolysis in traumatically induced axon injury. *J. Neuropath. Exp. Neurol.* **58**, 365–375.

Chen J., Nagayama T., Jin K., Stetler R. A., Zhu R. L., Graham S. H. and Simon R. P. (1998) Induction of caspase-3-like protease may mediate delayed neuronal death in hippocampus after transient cerebral ischemia. *J. Neurosci.* **18**, 4914–4928.

Cheng Y., Deshmukh M., D'Costa A., Demaro J. A., Gidday J. M., Shah A., Sun Y., Jacquin M. F., Johnson E. M. and Holtzman D. M. (1998) Caspase inhibitor affords neuroprotection with delayed administration in a rat model of neonatal hypoxic-ischemic brain injury. *J. Clin. Invest.* **101**, 1992–1999.

Chomczynski P. and Sacchi N. (1987) Single-step method of RNA isolation by acid guanidinium thiocyanate–phenol–chloroform extraction. *Anal. Biochem.* **162**, 156–159.

Crowe M. J., Bresnahan J. C., Shuman S. L., Masters J. N., Beattie M. S. (1997) Apoptosis and delayed degeneration after spinal cord injury in rats and monkeys. *Nat. Med.* **3**, 73–76.

Deiss L. P., Galinka H., Berissi H., Cohen O. and Kimchi A. (1996) Cathepsin D protease mediates programmed cell death induced by interferon-gamma, Fas/APO-1 and TNF-alpha. *EMBO J.* **15**, 3861–3870.

Demediuk P., Saunders R. D., Anderson D. K., Means E. D. and Horrocks L. A. (1985) Membrane lipid changes in laminectomized and traumatized cat spinal cord. *Proc. Natl Acad. Sci. USA* **82**, 7071–7075.

Demediuk P., Saunders R. D., Anderson D. K., Means E. D. and Horrocks L. A. (1987) Early membrane lipid changes in laminectomized and traumatized cat spinal cord. *Neurochem. Pathol.* **7**, 79–89.

Didenko W., Ngo H., Minchew C. L., Boudreaux D. J., Widmayer M. A. and Baskin D. S. (2002) Caspase-3-dependent and -independent apoptosis in focal brain ischemia. *Mol. Med.* **8**, 347–352.

Earnhardt J. N., Streit W. J., Anderson D. K., O'Steen W. A. and Nick H. S. (2002) Induction of manganese superoxide dismutase in acute spinal cord injury. *J. Neurotrauma* **19**, 1065–1079.

Fan M., Mi R., Yew D. T. and Chan W. Y. (2001) Analysis of gene expression following sciatic nerve crush and spinal cord hemisection in the mouse by microarray expression profiling. *Cell. Mol. Neurobiol.* **21**, 497–508.

Ferrara M., Wojcik F., Rhaissi H., Mordier S., Roux M. P. and Bechet D. (1990) Gene structure of mouse cathepsin B. *FEBS Lett.* **273**, 195–199.

Fink K., Zhu J., Namura S., Shimizu-Sasamata M., Endres M., Ma J., Dalkara T., Yuan J. and Moskowitz M. A. (1998) Prolonged therapeutic window for ischemic brain damage caused by delayed caspase activation. *J. Cereb. Blood Flow Metab.* **18**, 1071–1076.

Foghsgaard L., Wissing D., Mauch D., Lademann U., Bastholm L., Boes M., Elling F., Leist M. and Jaattela M. (2001) Cathepsin B acts as a dominant execution protease in tumor cell apoptosis induced by tumor necrosis factor. *J. Cell Biol.* **153**, 999–1010.

Gong Q., Chan S. J., Bajkowski A. S., Steiner D. F. and Frankfater A. (1993) Characterization of the cathepsin B gene and multiple mRNAs in human tissues: evidence for alternative splicing of cathepsin B pre-mRNA. *DNA Cell Biol.* **12**, 299–309.

Guicciardi M. E., Deussing J., Miyoshi H., Bronk S. F., Svingen P. A., Peters C., Kaufmann S. H. and Gores G. J. (2000) Cathepsin B contributes to TNF-α-mediated hepatocyte apoptosis by promoting mitochondrial release of cytochrome c. *J. Clin. Invest.* **106**, 1127–1137.

Hayashi T., Sakurai M., Abe K., Sadahiro M., Tabayashi K. and Itoyama Y. (1998) Apoptosis of motor neurons with induction of caspases in the spinal cord after ischemia. *Stroke* **29**, 1007–1012.

Hu J., Fink D. and Mata M. (2002) Microarray analysis suggests the involvement of proteasomes, lysosomes, and matrix metalloproteinases in the response of motor neurons to root avulsion. *Eur. J. Neurosci.* **16**, 1409–1416.

Kampfl A., Posmantur R., Nixon R., Grynspan F., Zhao X., Liu S. J., Newcomb J. K., Clifton G. L. and Hayes R. L. (1996) mu-calpain activation and calpain-mediated cytoskeletal proteolysis following traumatic brain injury. *J. Neurochem.* **67**, 1575–1583.

Kampfl A., Posmantur R. M., Zhao X., Schmutzhard E., Clifton G. L. and Hayes R. L. (1997) Mechanisms of calpain proteolysis following traumatic brain injury: implications for pathology and therapy: a review and update. *J. Neurotrauma* **14**, 121–134.

Keane R. W., Kraydieh S., Lotocki G., Bethea J. R., Krajewski S., Reeds J. C. and Dietrich W. D. (2001) Apoptotic and anti-apoptotic mechanisms following spinal cord injury. *J. Neuropathol. Exp. Neurol.* **60**, 422–429.

Kikuchi H., Yamada T., Furuya H., Doh-ura K., Ohyagi Y., Iwaki T. and Kira J. (2003) Involvement of cathepsin B in the motor neuron degeneration of amyotrophic lateral sclerosis. *Acta Neuropathol. (Berl.)* **105**, 462–468.

Kingham P. J. and Pocock J. M. (2001) Microglial secreted cathepsin B induces neuronal apoptosis. *J. Neurochem.* **76**, 1475–1784.

Kohda Y., Yamashima T., Sakuda K., Yamashita J., Ueno T., Kominami E. and Yoshioka T. (1996) Dynamic changes of cathepsins B and L expression in monkey hippocampus after transient ischemia. *Biochem. Biophys. Res. Commun.* **228**, 616–622.

Larner S. F., Hayes R. L., McKinsey D. M., Pike B. R. and Wang K. K. W. (2003) Increased expression and processing of caspase-12 after traumatic brain injury in rats. *J. Neurochem.* in press.

Leist M. and Jaattela M. (2001) Triggering of apoptosis by cathepsins. *Cell Death Differ.* **8**, 324–326.

Li Z., Hogan E. L. and Banik N. L. (1996) Role of calpain in spinal cord injury: increased calpain immunoreactivity in rat spinal cord after impact trauma. *Neurochem. Res.* **21**, 441–448.

Liu X. Z., Xu X. M., Du Hu R. C., Zhang S. X., McDonald J. W., Dong H. X., Wu Y. J., Fan G. S., Jacquin M. F., Hsu C. Y. *et al.* (1997) Neuronal and glial apoptosis after traumatic spinal cord injury. *J. Neurosci.* **17**, 5395–5406.

Lu J., Ashwell K. W. and Waite P. (2000) Advances in secondary spinal cord injury: role of apoptosis. *Spine* **25**, 1859–1866.

Mackay E. A., Ehrhard A., Moniatte M., Guenet C., Tardif C., Tarnus C., Sorokine O., Heintzelmann B., Nay C., Remy J. M. *et al.* (1997) A possible role for cathepsins D, E, and B in the processing of beta-amyloid precursor protein in Alzheimer's disease. *Eur. J. Biochem.* **244**, 414–425.

Mackey M. E., Wu Y., Hu R., DeMaro J. A., Jacquin M. F., Kanellopoulos G. K., Hsu C. Y. and Kouchoukos N. T. (1997) Cell death suggestive of apoptosis after spinal cord ischemia in rabbits. *Stroke* **28**, 2012–2017.

Matsushita K., Wu Y., Qiu J., Lang-Lzdunski L., Hirt L., Waeber C., Hyman B. T., Yuan J. and Moskowitz M. A. (2000) Fas receptor and neuronal cell death after ischemia. *J. Neurosci.* **20**, 6879–6887.

Mautes A. E., Weinzierl M. R., Donovan F. and Noble L. J. (2000) Vascular events after spinal cord injury: contribution to secondary pathogenesis. *Phys. Ther.* **80**, 673–687.

McGrath M. E. (1999) The lysosomal cysteine proteases. *Annu. Rev. Biophys. Biomol. Struct.* **28**, 181–204.

Mort J. S. and Buttle D. J. (1997) Cathepsin B. *Int. J. Biochem. Cell Biol.* **29**, 715–720.

Mouw G., Zechel J. L., Zhou Y., Lust W. D., Selman W. R. and Ratcheson R. A. (2002) Caspase-9 inhibition after focal cerebral ischemia improves outcome following reversible focal ischemia. *Metab. Brain Dis.* **17**, 143–151.

Namura S., Zhu J., Fink K., Endres M., Srinivasan A., Tomaselli K. J., Yuan J. and Moskowitz M. A. (1998) Activation and cleavage of caspase-3 in apoptosis induced by experimental cerebral ischemia. *J. Neurosci.* **18**, 3659–3668.

Ni B., Wu X., Su Y., Stephenson D., Smalstig E. B., Clemens J. and Paul S. M. (1998) Transient global forebrain ischemia induces prolonged expression of caspase-3 mRNA in rat hippocampal CA1 pyramidal neurons. *J. Cereb. Blow Flow Metab.* **18**, 248–256.

Nixon P. A. and Cataldo A. M. (1993) The lysosomal system in neuronal cell death: a review. *Ann. NY Acad. Sci.* **679**, 87–109.

Posmantur R. M., Zhao X., Kampfl A., Clifton G. L. and Hayes R. L. (1998) Immunoblot analyses of the relative contributions of cysteine and aspartic proteases to neurofilament breakdown products following experimental brain injury in rats. *Neurochem. Res.* **23**, 1265–1276.

Qian F., Frankfater A., Chan S. J. and Steiner D. F. (1991) The structure of the mouse cathepsin B gene and its putative promoter. *DNA Cell Biol.* **10**, 159–168.

Rami A. and Krieglstein J. (1993) Protective effects of calpain inhibitors against neuronal damage caused by cytotoxic hypoxia in vitro and ischemia in vivo. *Brain Res.* **609**, 67–70.

Ray S. K., Matzelle D. D., Wilford G. G., Hogan E. L. and Banik N. L. (2000) Increased calpain expression is associated with apoptosis in rat spinal cord injury: calpain inhibitor provides neuroprotection. *Neurochem. Res.* **25**, 1191–1198.

Ray S. K., Shields D. C., Saido T. C., Matzelle D. C., Wilford G. G., Hogan E. L. and Banik N. L. (1999) Calpain activity and translational expression increased in spinal cord injury. *Brain Res.* **816**, 375–380.

Rempel S. A., Rosenblum M. L., Mikkelsen T., Yan P. S., Ellis K. D., Golembieski W. A., Sameni M., Rozhin J., Ziegler G. and Sloane B. F. (1994) Cathepsin B expression and localization in glioma progression and invasion. *Cancer Res.* **54**, 6027–6031.

Roberts L. R., Kurosawa H., Bronk S. F., Fesmier P. J., Agellon L. B., Leung W. Y., Mao F. and Gores G. J. (1997) Cathepsin B contributes to bile salt-induced apoptosis of rat hepatocytes. *Gastroenterology* **113**, 1714–1726.

Robertson G. S., Crocker S. J., Nicholson D. W. and Schulz J. B. (2000) Neuroprotection by inhibition of apoptosis. *Brain Pathol.* **10**, 283–292.

Saatman K. E., Murai H., Bartus R. T., Smith D. H., Hayward N. J., Perri B. R. and McIntosh T. K. (1996) Calpain inhibitor AK295 attenuates motor and cognitive deficits following experimental brain injury in the rat. *Proc. Natl Acad. Sci. USA* **93**, 3428–3433.

Sakurai M., Hayashi T., Abe K., Sadahiro M. and Tabayashi K. (1998) Delayed selective motor neuron death after transient spinal cord ischemia: a role of apoptosis? *J. Thorac. Cardiovasc. Surg.* **115**, 1310–1315.

San Segundo B., Chan S. J. and Steiner D. F. (1986) Differences in cathepsin B mRNA levels in rat tissues suggest specialized functions. *FEBS Lett.* **201**, 251–256.

Schotte P., Van Criekinge W., Van de Craen M., Van Loo G., Desmedt M., Grooten J., Cornelissen M., De Ridder L., Vandekerckhove J., Fiers W. *et al.* (1998) Cathepsin B-mediated activation of the proinflammatory caspase-11. *Biochem. Biophys. Res. Commun.* **251**, 379–387.

Schumacher P. A., Eubanks J. H. and Fehlings M. G. (1999) Increased calpain I-mediated proteolysis, and preferential loss of dephosphorylated NF200, following traumatic spinal cord injury. *Neuroscience* **91**, 733–744.

Seyfried D., Han Y., Zheng Z., Day N., Moin K., Rempel S., Sloane B. and Chopp M. (1997) Cathepsin B and middle cerebral artery occlusion in the rat. *J. Neurosurg.* **87**, 716–723.

Shields D. C., Schaecher K. E., Hogan E. L. and Banik N. L. (2000) Calpain activity and expression increased in activated glial and inflammatory cells in penumbra of spinal cord injury lesion. *J. Neurosci. Res.* **61**, 146–150.

Shibata M., Kanamori S., Isahara K., Ohsawa Y., Konishi A., Kametaka S., Watanabe T., Ebisu S., Ishido K., Kominami E. and Uchiyama Y. (1998) Participation of cathepsins B and D in apoptosis of PC12 cells following serum deprivation. *Biochem. Biophys. Res. Commun.* **251**, 199–203.

Stroh C. and Schulze-Osthoff K. (1998) Death by a thousand cuts: an ever increasing list of caspase substrates. *Cell Death Differ.* **5**, 997–1000.

Tsuchiya K., Kohda Y., Yoshida M., Zhao L., Ueno T., Yamashita J., Yoshioka T., Kominami E. and Yamashima T. (1999) Postictal blockade of ischemic hippocampal neuronal death in primates using selective cathepsin inhibitors. *Exp. Neurol.* **155**, 187–194.

Turk B., Turk D. and Turk V. (2000) Lysosomal cysteine proteases: more than scavengers. *Biochim. Biophys. Acta.* **1477**, 98–111.

Vancompernolle K., Van Herreweghe F., Pynaert G., Van de Craen M., De Vos K., Totty N., Sterling A., Fiers W., Vandenabeele P. and Grooten J. (1998) Atractyloside-induced release of cathepsin B, a protease with caspase-processing activity. *FEBS Lett.* **438**, 150–158.

Velardo M. J., Reier P. J. and Anderson D. K. (1999) Spinal Cord Injury, in *Neurosurgery: Principles of Basic and Clinical Science* (Hoff, J., Crockard, A., Hayward, R., eds), pp. 499–515. Blackwell Science Publications, Oxford.

Yamashima T. (1999) Postictal blockade of ischemic hippocampal neuronal death in primates using selective cathepsin inhibitors. *Exp. Neurol.* **155**, 187–194.

Yamashima T., Kohda Y., Tsuchiyak K., Ueno T., Yamashita J., Yoshioka T. and Kominami E. (1998) Inhibition of ischaemic hippocamal neuronad death in primates with cathepsin B inhibitor CA-074: a novel strategy for neuroprotection based on 'calpain-cathepsin hypothesis.' *Eur. J. Neuro Sci.* **10**, 1723–1733.

Yamashima T., Saido T. C., Takita M., Miyazawa A., Yamano J., Miyakawa A., Nishijyo H., Yamashita J., Kawashima S., Ono T. *et al.* (1996) Transient brain ischaemia provokes Ca^{+2}, PIP_2 and calpain responses prior to delayed neuronal death in monkeys. *Eur. J. Neurosci.* **9**, 1932–1944.

Yan S., Berquin I. M., Troen B. R. and Sloane B. F. (2000) Transcription of human cathepsin B is mediated by Sp1 and Ets family factors in glioma. *DNA Cell Biol.* **19**, 79–91.